THE DEVELOPMENT OF A FLUID CONSISTENCY TRANSDUCER

by

KASHMIR SINGH MAHIL

Submitted for the Degree of Doctor of Philosophy

at

The University of Aston in Birmingham

November 1975

SUMMARY

A robust fluid consistency transducer suitable for on-line industrial applications has been developed. Its particular application is the monitoring of primary sludge in sewage treatment plants. The transducer uses the effects of fluid loading on a mechanical resonator. This is in the form of a disk (sensor) mounted at the end of a rod about 2.5 m. long. The disk is driven by longitudinal waves in the rod generated by making a section of it of magnetostrictive material.

Three classifications can be given to the liquid loading effects on the vibrating sensor:

(a) inertial or stiffness loading

(b) viscous dissipation of energy stored

(c) acoustic radiation of energy stored.

Of these acoustic radiation has undesired interactions due to back reflections and gas bubbles. It must therefore be minimised. By using low frequencies the radiation efficiency was made sufficiently small for these acoustic effects to be negligible.

In preliminary experiments it was found that viscous dissipation was the more sensitive parameter to measure. Thus the change from sludge to water produced a large change in decrement but only a small frequency shift.

Various forms of sensors were investigated. These included:-

(a) a free edge circular plate vibrating in its fundamental flexural symmetrical mode,

(b) a solid centre circular plate vibrating with one nodal circle,

(c) a rigid circular plate in piston type motion,

(d) a sphere in translational motion,

(e) an 'oyster' shell consisting of two circular plates joined at the periphery with a gap in between, the two plates vibrating in phase in the fundamental mode,

(f) a torsionally resonant rod. This was found to interact sufficiently well without further attachment.

A wide range of sensitivities was achieved. The highest is applicable to light mobile liquids and the lowest to heavy thick fluids of which sludge is the extreme case.

Extensive user trials were carried out at Minworth where the separation of the primary sludge could be monitored. Designs were produced which were impervious to the high speed scrubbing action of sludge. An important economic aspect of the equipment is that the line and electronics is common to the full range of fluids, only the end sensor need be changed.

Patent application is being made for the system.

ACKNOWLEDGEMENTS

First and foremost, I thank Dr. J. F. W. Bell, Reader, for guidance and critical discussions during the entire period.

I thank the Solartron Electronic Group for suggesting the problem and financing this research. I am particularly grateful to Mr. P. Potter, head of the transducer research at Solartron for his keen interest and encouragement.

I also acknowledge the Upper Tame Main Drainage Authority for providing facilities at their Minworth sewage works.

I thank Professor J. E. Flood, Head of the Department of Electrical Engineering for providing facilities. Thanks are also due to the Departments workshop staff and the laboratory staff for their help.

CONTENTS

CHAPTER 1

THE STATEMENT OF THE PROBLEM

1.1. INTRODUCTION

This chapter discusses the problems associated with consistency measurement of primary sludge in waste water treatment plants. The various stages of sewage treatment together with the details of the primary settling tanks and the sludge withdrawal mechanism are described in Chapter 5.

Previous attempts at the measurement of sludge consistency are briefly mentioned. The possibility of correlating consistency with "apparent viscosity" of liquids is discussed; finally, the present transducer design philosophy is given.

1.2. INSTRUMENTATION FOR WATER POLLUTION CONTROL[1-7]

In the past sewage treatment has been based on the manual operation by relatively cheap labour forces using empirically designed equipment. Mechanically and hydraulically the modern sewage plant is efficiently designed; an experienced attendant can judge at what point to close a particular valve or divert flow into another tank on the basis of his past experience, on the appearance of the liquor or by some other process. Because of lack of instrumental information to help him, he cannot be precise but usually makes a valuable judgement. This class of worker is fast disappearing,

consequently there is a need for modern techniques of mechanisation and automation to reduce the labour force required to run a modern sewage treatment plant efficiently. This need for efficiency and automation is enhanced by greater amounts of sewage to be treated with the increase in population.

The automatic remote control of fluid flow is well known and practised in modern sewage works, but the actual sensor or detector by which the need for change in operating conditions is determined presents formidable problems. It has to be decided what parameters indicating the essentials of a process, can be detected reliably and then to design sensors for the appropriate parameter. The need for robustness and minimum maintenance of the sensor is of the utmost importance. In the past this point has often been neglected by instrument manufacturers resulting in the drastic failure of instruments in practice. It has been realised that sewage is an extremely awkward liquid to measure and that the conditions under which these measurements have to be carried out are very adverse.

The sewage works plant have been well supplied with instruments for measuring flow, pressures, temperatures, pH, dissolved oxygen, etc. of sewage effluents. One important gap in this field has been the means to measure sludge density at the bottom of a tank or other point, therefore the automatic removal of settled sludge has not been possible.

The settled sludge on the floor of the primary settling tank is scraped into hoppers where the concentration

of the solid matter occurs. Then the sludge is periodically discharged from the hoppers for further treatment. For efficiency and economy of the subsequent sludge treatment process, sludge of as high a solid concentration as is compatible with mobility must be discharged from the hoppers. In view of this a sensing device is required which will measure the solid content of the sludge as it is withdrawn from the hoppers, so that only sludge of solid content above a predetermined figure is withdrawn. Various forms of sensing devices have been investigated in the past, some of which will be briefly discussed in the following section.

1.3. PRIMARY SLUDGE WITHDRAWAL INSTRUMENTATION

1.3.1. DENSITY MEASUREMENT

(a) The consistency of primary sludge can be determined by measuring the density of the sludge which varies with the solid contents present. An investigation has been made to ascertain whether there was any relationship between the electrical conductivity of sludge and its density. In fact such a correlation was detected; denser sludge gave higher conductivity than thin sludge or liquors, although the variation was quite small. This instrument was found to be impervious to changes in rates of flow and apparently gave consistent results. This system, when installed at the Mogden Works, did not function as had been expected. When used in the manner intended, for periods of up to fourteen

days there had been a marked accumulation of sludge in the sedimentation tanks. It was discovered later that thin stale sludge could have the same conductivity as thick fresh sludge; a sludge of high mineral content could have a high solid content but have a low conductivity, whilst a sewage with a high salt content, as when salt being applied to roads in winter, could settle in a similar manner to sludge and be pumped away as sludge.

(b) An alternative method of determining density is to measure gamma ray absorption of sludge[8]. Essentially this device consists of a radiation source which generates gamma rays into a pipe containing flowing sludge and a radiation detector directly opposite to the source. The detector senses the intensity of gamma rays after being absorbed and scattered by the sludge. This intensity is a measure of sludge density. This device has very serious limitations. Firstly, it needs very careful on-line calibration which needs to be checked regularly; secondly, gamma rays pass through a small portion of the sludge before reaching the detector, therefore the readings may not be representative of actual sludge density. Lastly, the most serious limitation is that this device is very susceptible to the presence of gas bubbles in the sludge.

There is a fairly small difference between the density of sludge and that of water. The specific gravity of the thickest sludge is about 1.1 and that of normal sludge about 1.03. Both of the above instruments mentioned are not suitable for this degree of sensitivity or robustness.

1.3.2. PHOTO-ELECTRIC SLUDGE LEVEL DETECTOR[9]

A different system of automatic sludge withdrawal would be to use the level of sludge in the tank to control the rate of withdrawal. An instrument which measures the top of the sludge deposit in the sedimentation tank, depends on the measurement of the transmission of light between two watertight compartments which are lowered into the tank on a rigid pole. The transmission of light decreases with the increase in the suspended solids. This system has not been used widely because it is affected by changes in the loading on the tank and is suitable for small sewage treatment plants.

1.3.3. CLOSED CIRCUIT T.V. MONITORING SYSTEM[3]

Because of the unreliability of sludge detector instruments available, none of these instruments have been incorporated in the recently commissioned sedimentation plant at Minworth. Instead, visual inspection of sludge withdrawn over an adjustable bellmouth using a closed circuit T.V. was installed. The water breakthrough which is the end point of the emptying process is determined when the appearance of the surface finish of the emerging liquid goes from a matt to highly reflecting as the liquid changes from sludge to water. At this point the valves and penstocks are remotely closed.

In the report of the Director of Water Pollution Research for 1962, in a section on the determination of the solids content of sewage sludge mention was made of

studies carried out using light transmission, gamma ray absorption, electrical conductivity, ultrasonic vibration and viscosity. It was concluded that viscosity and ultrasonics only were worthy of further investigation.

Recently an ultrasonic device has been marketed but no information about its viability is available.

The purpose of the present research has been to design a transducer to measure the consistency of sludge by measuring the "apparent viscosity" or some other related parameter such as density.

1.4.1. INTERDEPENDENCE OF 'VISCOSITY' AND CONSISTENCY OF SLUDGE

It has been mentioned that the importance of consistency measurement lies in its relationship with the mass flow of solids of which precise control is more vital than the actual measurement of solid concentration. Mass flow or consistency cannot be measured directly but the influence of consistency on the rheological properties of sludge may be used as the basis of measurement. The rheological behaviour of sludge is highly complex and does not follow laws applying to homogeneous fluids. Observations of the flow of sludge in the bellmouth suggested that, as well as having the high viscosity, there were rheological properties in which a solid like stiffness is also present.

1.4.2. FLUID FLOW

The rheogram of a Newtonian liquid such as water or

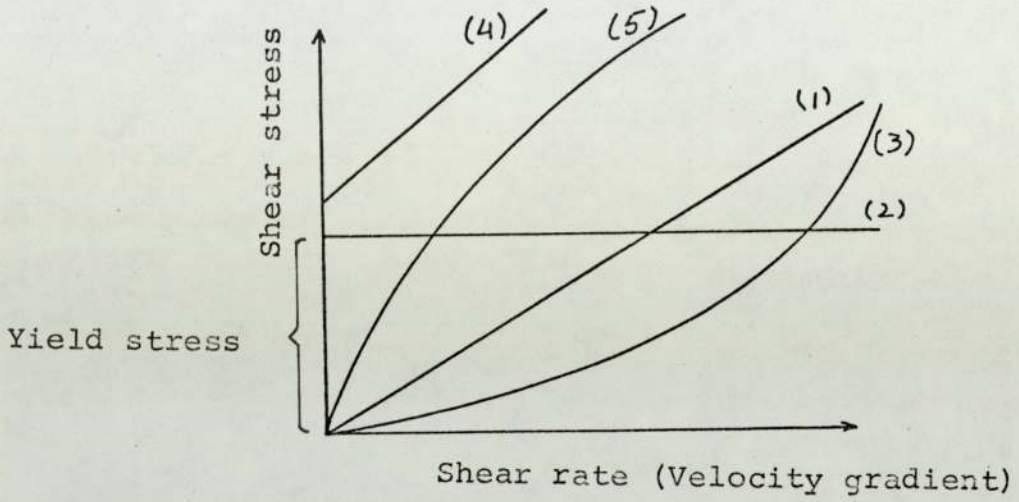

FIGURE 1.4.1.

Rheogram for various fluid flow characteristics.

(1) Newtonian fluids:

water, most mineral oils, salt solutions.

(2) St. Venant body (Pseudoplastic):

paper pulp, catsup, cement.

(3) Dilatant:

starch, quicksand.

(4) Bingham body (Platic solid):

tomato sauce, apple sauce, chewing gum, tar.

(5) Thixotropic:

asphalt, lard, silica gel.

mineral oil is shown in Fig. 1.4.1.

This shows a straight line passing through the origin suggesting that no matter how small the shear stress there is a shear rate. All Newtonian liquids exhibit this characteristic; the slope of this line determines the coefficient of viscosity. Most real liquids show departures from Newtonian flow. The flow characteristic of such non-Newtonian fluids is also shown in Fig. 1.4.1. For instance fluids such as tomato sauce and apple sauce consist of solid phase and liquid phase, in which there is a minimum stress (yield stress) needed before flow occurs. Paper pulp exhibit St. Venant Body characteristics showing that after the yield stress is reached there is no increase in the shear stress with increase in shear rate, giving a "biassed" zero viscosity characteristic.

A variety of consistency measuring instruments, suitable for tomato sauce, paper industry etc., are available." These can be classified according to:-

(a) the property measured, whether pseudo-viscosity or shear force provides the major contribution to the measurement.

(b) the mechanism of measurement, e.g. stock flow passing a fixed sensor, as distinct for a sensor caused to move.

(c) whether on-line or not.

Each have their advantages and disadvantages but do not appear to be feasible for primary sludge measurement.

1.4.3. RHEOLOGICAL PROPERTIES OF SOLID-WATER MIXTURE[10]

No quantitative information about the flow behaviour

of sludge is available up to the present time. But some general comments can be made about the flow properties of solid-water mixture which is relevant to sludge.

The characteristic property of suspension is the amount of interface surface between the solid and the liquid phase of the mixture. The extent of this surface is inversely proportional to the particle size and directly proportional to the solid concentration. Intersurface binding forces and formation of weak chemical bonds etc. increase with specific surface of the mixture. Thus dilution, (decrease in solid concentration) increases the fluidity of the mixture. It is also known that in suspensions finer particles have greater effect on flow characteristics than do the coarser particles. Other factors which may have some bearing on the rheological properties of the sludge are:-

(a) size distribution of solid phase
(b) the shape and deformability of the solid phase
(c) the difference in density between the solid and liquid phase
(d) flocculation of solid particles
(e) chemical interaction between two phases
(f) electrostatic charging of the solid particles.

Considering all these effects, it will be a formidable problem to determine the flow characteristics of sludge. These characteristics will also depend upon the location of the sludge treatment plant, and also vary from day to day over the year for a particular plant.

The correlation of consistency with 'apparent viscosity' may be affected by rate of flow, temperature, amount of entrained air etc. All these factors must be considered when designing a suitable transducer.

1.4.4. TRANSDUCER DESIGN PHILOSOPHY

It must be pointed out here that due to extensive variation in sludge properties, and other factors, the correlation of consistency with 'viscosity' is probably just not good enough to allow for accurate measurement of consistency. Therefore a 'deviation' type of instrument is suggested to detect water breakthrough.

It is proposed to develop a vibrating transducer which, by its resonant frequency and decrement identifies the changes in liquid consistency, e.g. from a fairly thick glycerol to water (laboratory development). The transducer will consist of a robust probe with a sensor at one end. The length of the probe should be about ten feet so that the sensor can be conveniently placed in the "bellmouth" for it to be scrubbed by the outflowing liquid.

The mode of vibration, the geometry and the dimensions, suitable for macroscopic measurement, of the sensor will be discussed in the following chapter.

CHAPTER 2

THE PRESENT APPROACH

2.1 INTRODUCTION

The complex rheological nature of primary sewage sludge has been discussed in the previous chapter. The instruments designed to detect 'water-breakthrough' in the primary sludge withdrawl process have been unreliable due to the nature of the sludge and the adverse environments in which these instruments have to operate. In the present investigation an empirical approach was adopted for the design of an appropriate vibrating transducer to give good resolution of the sludge-water change. This approach was made necessary by the extreme complexity of the physical properties of sludge.

No definite early decision could be made about the most suitable physical parameter of sludge to be measured by the transducer. Therefore a general investigation of the effects of 'fluid-loading' on resonant sensors was commenced, In the laboratory development of the vibrating transducer, particular emphasis was placed on the mass loading and viscous losses due to the surrounding medium. It was realised at an early stage that visco-elastic fluids such as sludge may also introduce stiffness to the transducer thereby counteracting the mass loading effect, since for any vibrating system the resonant frequency ω is proportional to $\left(\frac{S + \Delta S}{m + \Delta m}\right)^{\frac{1}{2}}$, where S is the stiffness and m is the mass of the equivalent lumped circuit of the transducer and ΔS and Δm is the increase

in stiffness and mass due to the presence of sludge.

The suitability and magnitudes of these effects for sludge detection could only be determined experimentally. A detail discussion of the interaction between resonators and surrounding medium will ensue in Chapter 4, but for the sake of clarity these effects are mentioned briefly.

2.2 BASIC DESIGN PHILOSOPHY OF THE TRANSDUCER

The basis of the preliminary investigations is the fluid loading effects on vibrating structures. The loading exerted by this heavy medium on the vibrating structure is of such a magnitude as to modify extensively the dynamic response of the structure. This interaction of the structure in contact with a dense fluid gives rise to problems involving 'fluid-loading' which can be split up into three main effects

(a) inertial loading

(b) radiation of sound

(c) viscous dissipative loading.

(a) Inertial Loading

The motion of the fluid represents an increase in the stored energy of the resonator. This inertial loading lowers the resonant frequency of the system.

(b) Radiation of Sound

Sound represents an energy loss from the resonator, the outcome of which is the damping of the resonator according to

the decrement law. Acoustic radiation is insesitive to fluid composition and can cause spurious effects due to bubble resonance and has been minimised in the application.

The energy radiated from a resonator decreases as the ratio of resonator dimension and the wavelength of sound in the fluid decreases. Therefore this ratio should be made small. A particular transducer of interest is a free edge circular plate vibrating in flexure with one nodal circle. The unloaded resonance frequency is given by:

$$f_r = (K)\ C\ \frac{h}{D^2}$$

where C = rod velocity of sound in disk material.

h = thickness of disk,

D = diameter of disk,

K = 1.66 for fundamental mode.

Let the resonance frequency inside the liquid be f_r' which is given by

$$f_r' = (K')\ C\ \frac{h}{D^2}$$

where K' is effective K for liquid loading situation.

The wavelength in the liquid λ' at this frequency is

$$\lambda' = \frac{C_l}{f_r'} = \frac{1}{(K')}\ \frac{C_l}{C}\ \frac{D^2}{h}$$

where C_l is the sound velocity in the liquid.

Hence

$$\frac{\lambda'}{D} = \frac{1}{(K')}\ \frac{C_l}{C}\ \frac{D}{h}$$

Therefore for minimum acoustic radiation loss the D/h term must be as large as possible;and similarly C_l/C must be

large, therefore a low velocity material for the plate is desirable.

In view of the above comments it was decided to consider resonators of natural frequencies below 5 kHz, the wavelength in the fluid being about 30 cms.

Low frequency also increases the magnitude of the inertial reaction (i.e. lower value of K') mentioned in (a) above. The interpretation given by Junger[12] is that at high frequencies the resonator vibrates with such rapidity that the disturbance does not travel far before the action is reversed; whereas with low frequency the resonator tends to accelerate larger quantities of fluid.

(c) Viscous Dissipation

This is an extremely important phenomenon in the development of the vibrating transducer to measure consistency. The motion of the resonator in the fluid induces circulatory motion of the fluid in the vicinity of the resonator. The viscosity of the fluid results in vibrational energy lost to the resonator and contributes to its decrement. The magnitude of this effect has a dependence on the geometry and mode of vibration of the resonator. Figure. 2.2.1.(a) shows the flow field induced near the surface of a sphere executing translatory motion in the fluid. The fluid 'far' from the sphere flows inwards perpendicular to the axis of oscillations and then outwards along the axis. In the case of an unbaffled circular piston, Figure. 2.2.1.(b), large drag forces are introduced around the periphery of the piston. Figure. 2.2.1.(c) shows the flow-field

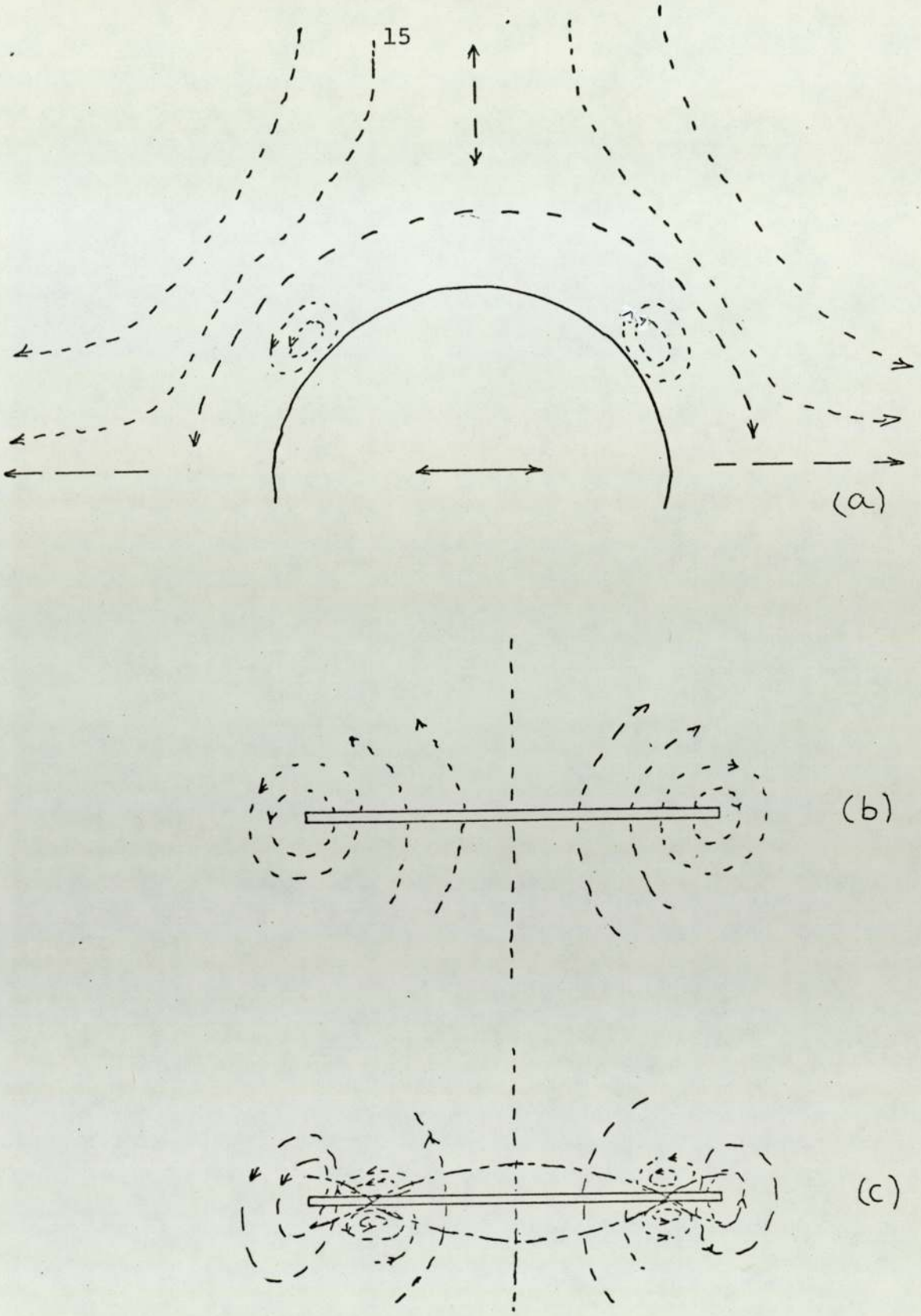

FIGURE 2.2.1.

Stream lines of flow of liquid due to the vibration of

(a) sphere,[50]
(b) piston without baffle,
(c) free-edge disk with one nodal circle.

induced by a free edge circular disk. The mode of vibration of the disk is a nodal circle with the 'flapping' ends. The flow is localised by the antiphase motion of the surface of the disk on either side of the nodal circle. This antiphase motion of the surface generates a high flow close to the nodal circle in addition to the periphery.

Of the three above cases the fluid movement is by far the greatest for the free edge disk. Furthermore the movement is very localised. For these reasons this vibrator was chosen.

Generally the liquid particle velocity decreases with the distance from the surface of the vibrating body. This streaming penetration depth is dependent on the amplitude of motion of the body and the viscosity of the liquid. It may also depend on the frequency of vibrations.[51]

This 'nearfield'viscous flow dissipative effect is a different phenomenon to the undesired sound radiation effect mentioned in (b) above. The electromagnetic analogue is the inductive field and the radiation field of a transmitter. The inductive field is where the energy is stored and corresponds to the mass loading of the resonator; the radiation field, where energy is lost corresponds to acoustic radiation in the liquid.

2.3 VISCOSITY MEASUREMENT TECHNIQUES[13-21]

Mechanical vibration of any elastic system is always accompanied by various processes by which energy stored is dissipated. The sources of energy dissipation can be

subdivided into two principal groups, namely external and internal. The external sources comprise of friction of the vibrating system against the medium in which the vibration is produced, that is the viscous dissipation described above. The internal sources consist of internal friction due to the non-ideal nature of the material and supports of the system.

The relative importance of the external and internal losses depends on the problem considered. In this investigation the external losses are of prime importance, consequently the internal losses are to be minimised. The damping due to the imperfection of the material is small compared to the external damping, e.g. the 'Q' of aluminium in the 6 kHz range is greater than 5000 while that of the transducer in use is typically 100.

Measurement of the external damping of a vibrating system immersed in a fluid will give information about the visco-elastic properties of the fluid. In some laboratory instruments, in order to determine the viscous losses accurately the internal losses, measured separately are subtracted from the total losses. But in the present case total damping is observed.

In the past several methods have been described for measuring the damping of a resonator by the surrounding non-Newtonian medium. In general these methods can be divided into three classes.

(1) Attenuation and Phase Method

This method measures the attenuation and phase of a

travelling wave in a fluid loaded rod. This system has been used by McSkimin. The attenuation and phase of a short torsional pulse travelling along a partly immersed rod is correlated with properties of the material.

(2) Impedence Method

This method employs the fact that the electrical impedence of the driving unit used to set forced vibrations in the system, immersed in a medium, varies with the properties of the medium. Mason used an ADP crystal vibrating torsionally in his apparatus, the electrical impedence of the crystal is calibrated against the medium properties.

(3) Resonance Method

This technique has been used by the author. It consists of measuring the amplitude time decay of the free vibrations of a resonator. A resonance technique has been described by Roth and Rich. This will be considered at length in Capter 7, as their theory can be adopted to the damping of a torsionally resonant rod immersed in a fluid. The instrument of Roth and Rich consists of a thin metal strip, immersed in fluid, excited in its fundamental longitudinal frequency. The strip is excited magnetostrictively and when its amplitude of vibration reaches a certain predetermined level the drive is switched off, and the amplitude decays exponentially to another predetermined level at which the drive is switched on. The time beween 'on' and 'off' is computed to give decrement and hence viscosity.

Irrespective of the nature of the sources of energy loss, the most useful characteristic of the energy dissipation is the 'Q' of the system. The 'Q' is defined as

$$Q = 2\pi \frac{\text{Energy Stored}}{\text{Energy lost/cycle}} = \frac{2\pi E}{\Delta E}$$

The 'Q' can be determined from the decay of natural vibrations of the system. Such a decaying vibration and the envelope curve is shown in Figure.2.3.1.

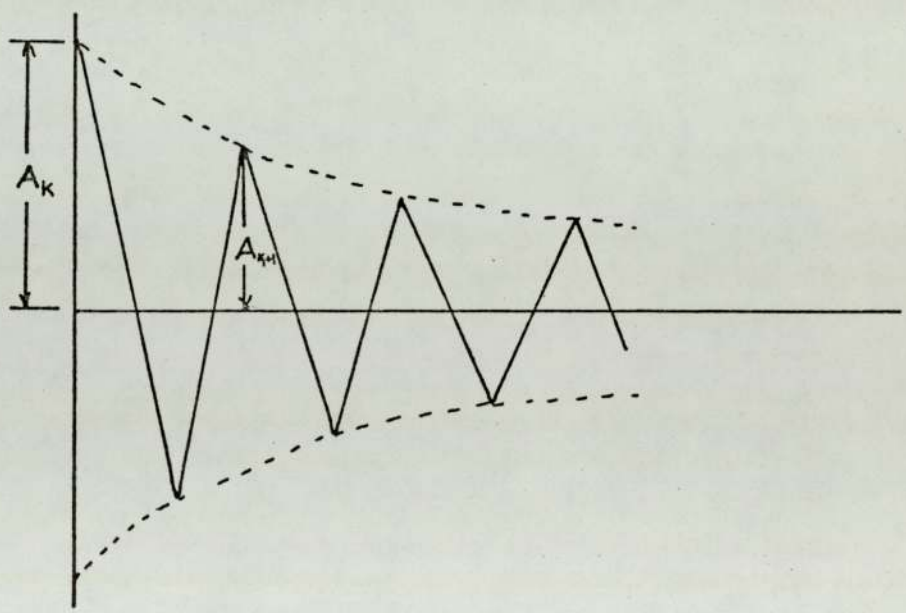

FIGURE 2.3.1.

The logarithmic decrement, δ of the decay of free oscillation is given by

$$\delta = \ln \frac{A_k}{A_{k+1}}$$

where A_k and A_{k+1} are two successive vibration peaks at the beginning and end of the (k+1)th period. The logarithmic

decrement is related to the 'Q' of the system by the relationship

$$\delta = \frac{\pi}{Q}$$

Therefore for n oscillation

$$Q = \frac{\pi n}{\ln A_o/A_n} \qquad \ldots\ldots\ldots\ldots (2.3.1)$$

In using the decrement method attention must be given to the possibility that the losses may be amplitude dependent in which case the exponential law will not be followed. In practice the measurements were carried out at amplitudes below this threshold.

The various instruments cited in the literature being rather fragile are not suitable for on-line sludge consistency measurement. The vibrating plate sensor proposed by the author is large and robust fitting the practical circumstances encountered.

2.4 THE LINE-RESONATOR TECHNIQUE

The functional diagram of the transducer investigated is shown in Figure.2.4.1. It consists of an acoustic transmission line terminated by a resonator which while having a small sensitivity to temperature and pressure is primarily influenced by density and viscosity. The system is driven by a magnetostrictive line, the energy is propagated down the line to set the sensor into vibrations. The decrement is detected by the inverse magnetostrictive effect of the driving element. A burst of pulses is applied to the coil, the

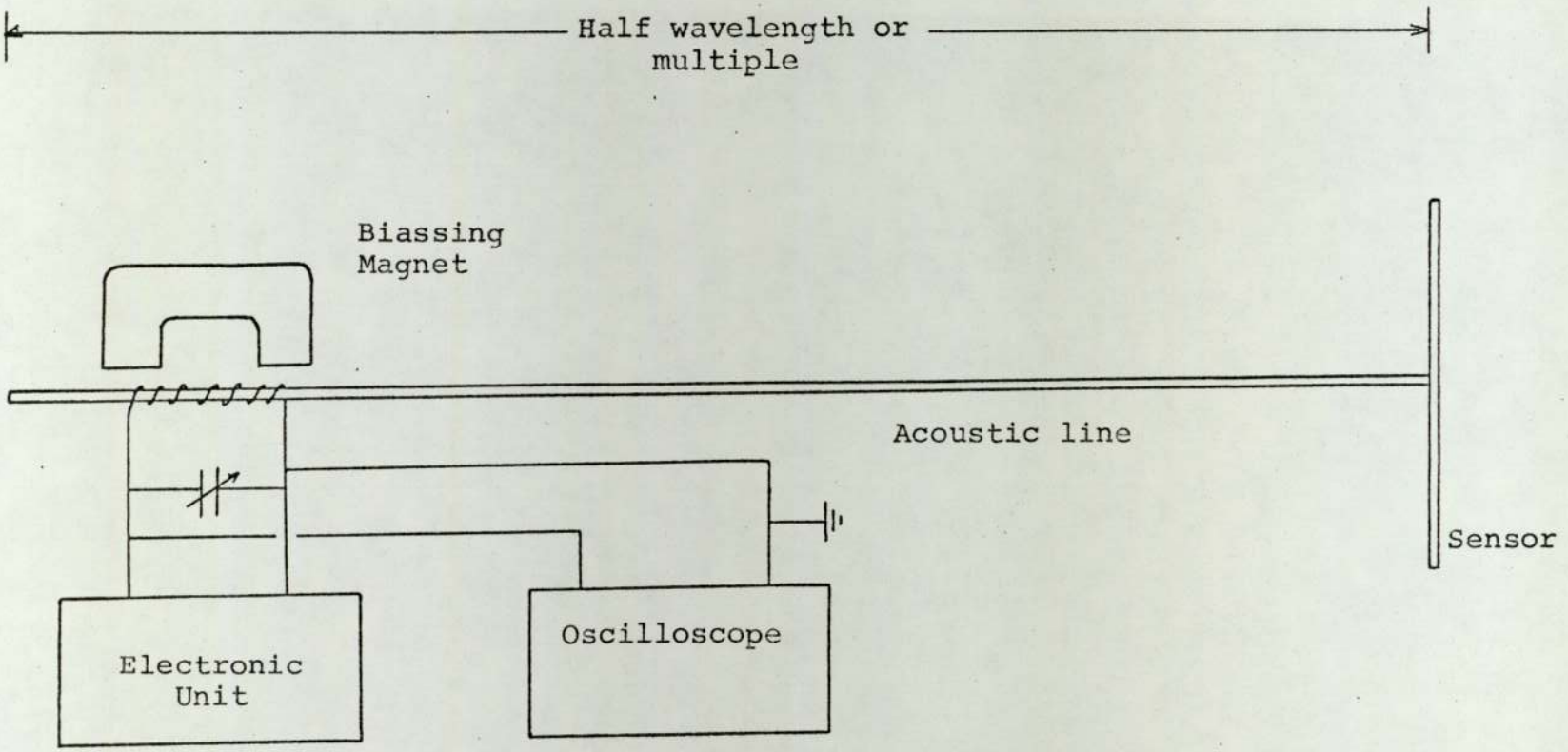

FIGURE 2.4.1.

For maximum efficiency the line must be resonant at the frequency of the mode required.

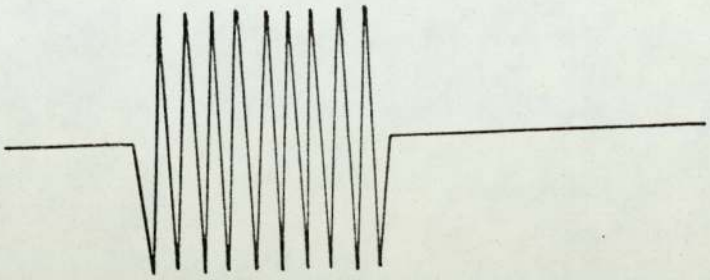

(a) TRANSMITTED SIGNAL

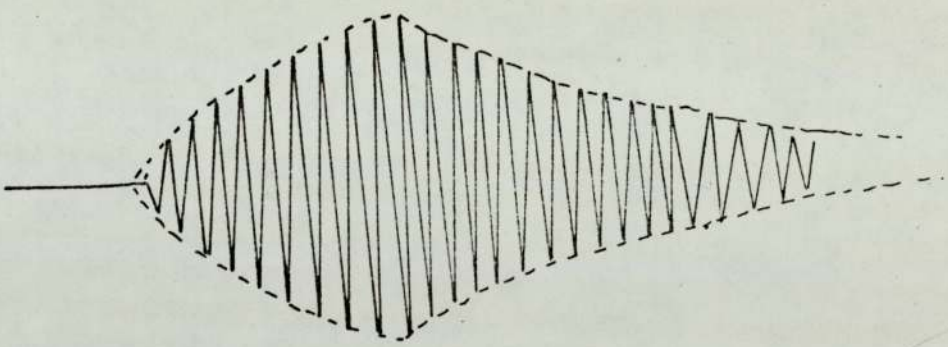

BUILD UP OF STORED ENERGY

DECREMENT USED FOR MEASUREMENT

(b)

FIGURE 2.4.2.

consequence of which is the generation of extensional waves in the magnetostrictive material.[22] This sonic energy propogates down the acoustic line, terminated by a resonator. The resonator takes up energy, stores it and re-radiates it into the line. The magnetostrictive transducer receives this re-radiated energy and induces a voltage in the coil, by the inverse magnetostrictive effect, which is displayed on the oscilloscope.

Figure 2.4.2(a) represents the transmit signal and (b) the build up and decay of the energy in the line-resonator system. The system will give maximum response when the excitation frequency is coincident with resonant frequency of the system, therefore the amplitude of the decrement is a maximum at this frequency. Figure 2.4.3.(a) and (b) show oscillographs for resonance and non-resonance respectively.

(a) Resonance (b) Non-resonance

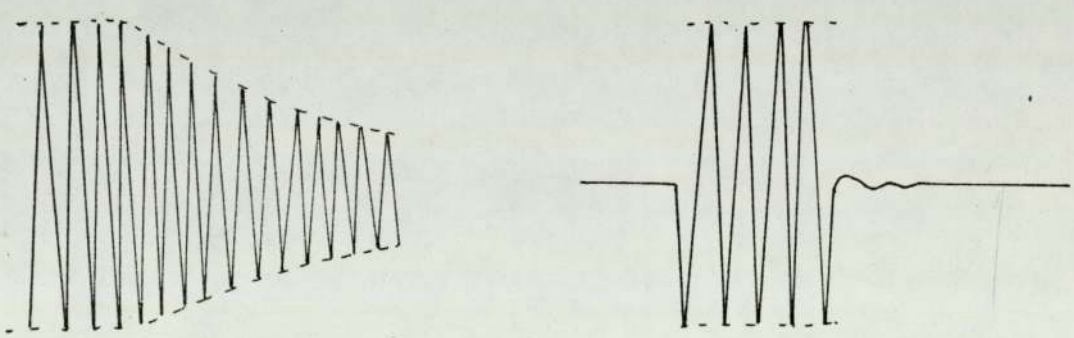

FIGURE 2.4.3.

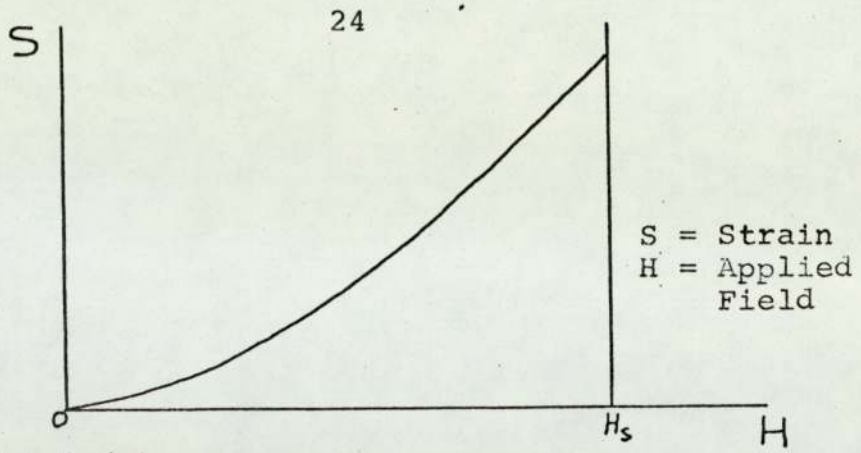

FIGURE 2.4.4.(a)

Magnetostrictive characteristics as a function of static intensity of magnetisation.

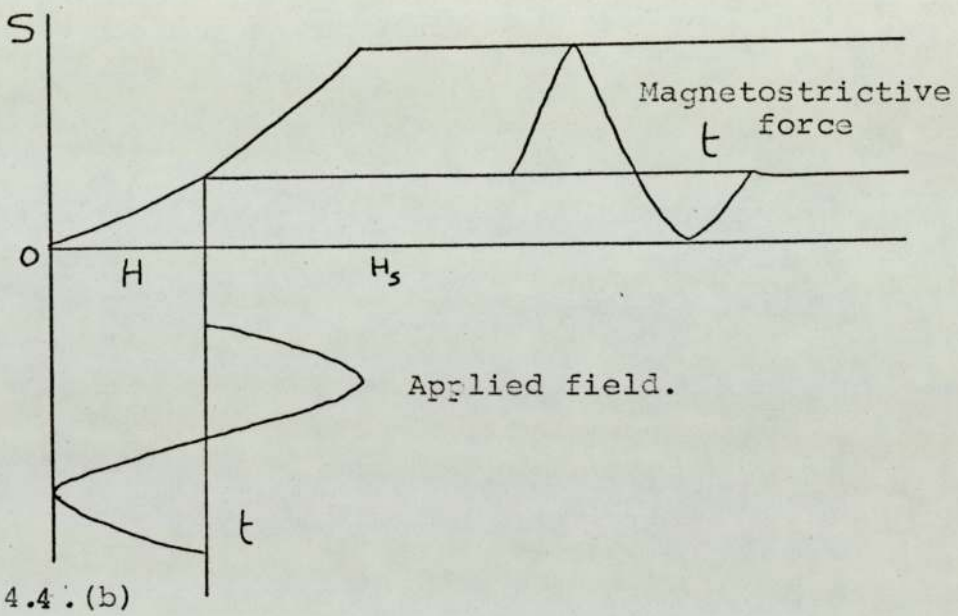

FIGURE 2.4.4.(b)

The force generated in a biassed magnetostrictive material by a sinusoidal applied field.

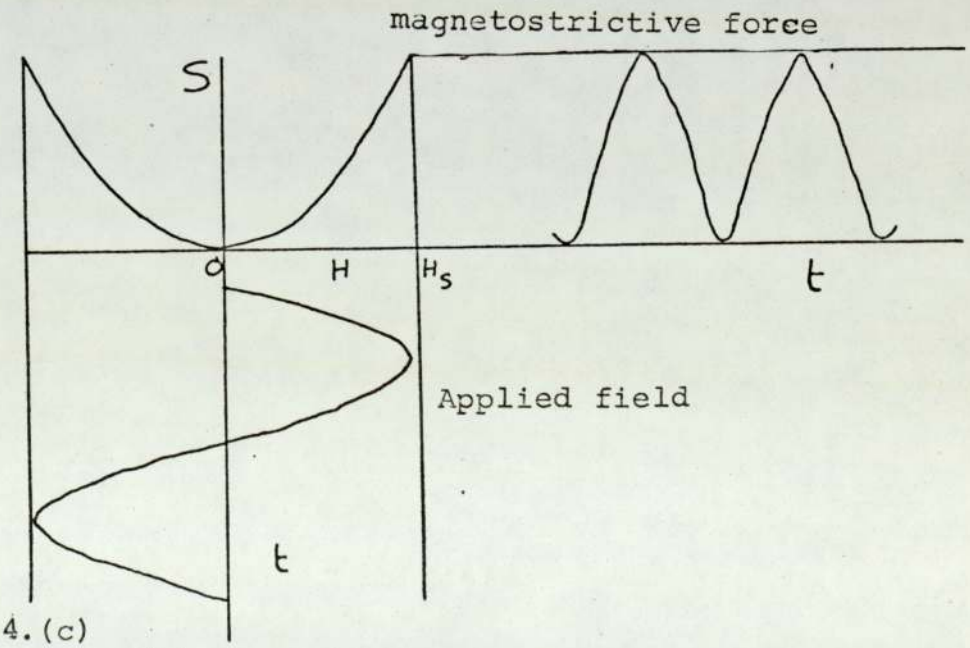

FIGURE 2.4.4.(c)
The force generated in an unbiassed magnetostrictive material by a sinusoidal applied field.

The stored energy will always decay at the resonant frequency of the system.

Static magnetostriction characteristics for a magnetostrictive material is shown in Figure 2.4.4.(a). A steady magnetic bias is necessary to operate in the linear part of the characteristics. This will increase the mechanical strain induced by the field of the magnetostrictive transducer. The mechanical vibration frequency will be twice that of the applied field for an unbiassed case as shown in Figure 2.4.4.(c). This 'frequency doubling' is avoided by the application of a steady magnetic bias.

The length of the launch and receive coil is kept at approximately 10 cms. The number of turns in the coil is so chosen that its impedence is high and it can be conveniently matched to the output stage of the transmitter. On the other hand, it must not be too bulky. The diameter of the former for the coil is such that the magnetostrictive rod is a good fit and also the thickness of the former is small. This gives good flux linkage from the coil to the rod and hence increases efficiency. The coil is tuned with a parallel capacitor to provide a maximum energy transfer from the transmitter to the transducer and back.

Ideally the acoustic line should be resonant at the required frequency, with an anti-node at each end. If this condition is not realised the vibration profile of the sensor will be different; for example, in the case of a free edge disk the position of the nodal circle changes with coupling. Therefore the line length must be chosen

so that its resonant frequency coincides with that of the sensor thereby minimising the coupling.

In the practical case the most important source of internal damping is provided by the supports for the vibrating line. The line is best supported at the nodes where the longitudinal velocity is zero. There is a little damping as the radial vibration coupled by the Poissons ratio is a maximum at the node. A mechanically good support can in fact be achieved without a significicant contribution to the decrement.

CHAPTER 3

LABORATORY DEVELOPMENT OF THE TRANSDUCER

3.1 INTRODUCTION

In this chapter will follow the practical detailed discussion of the laboratory development of the transducer, the basic design philosophy for the sensor having been mentioned previously. The experimental results obtained for sensors of various geometries and modes of vibration and their interaction with 'thick'and 'thin' liquids are given. Since it is known that sludge decomposes into liquids and gases, mostly methane, the effects of the presence of gas bubbles on the transducer performance is investigated.

3.2 FREE-EDGE DISK

A particular sensor of interest at an early stage was a Chladni's plate vibrating in its lowest mode. The most attractive geometry for the plate is a circular disk of uniform thickness undergoing flexural resonance with the anti-nodes at the centre and the free-edge, and a nodal circle. This particular sensor is attractive since the liquid flow field is very localised and therefore the consistency sensor will measure the properties of the liquid in its immediate vicinity only. Any effects due to the external boundaries such as the walls of the container will be absent.

The dynamic deflection curve at resonance of the disk and longitudinally vibrating line is shown in Figure 3.2.1. The position of the magnetostrictive launcher used to generate extensional waves is very critical. The

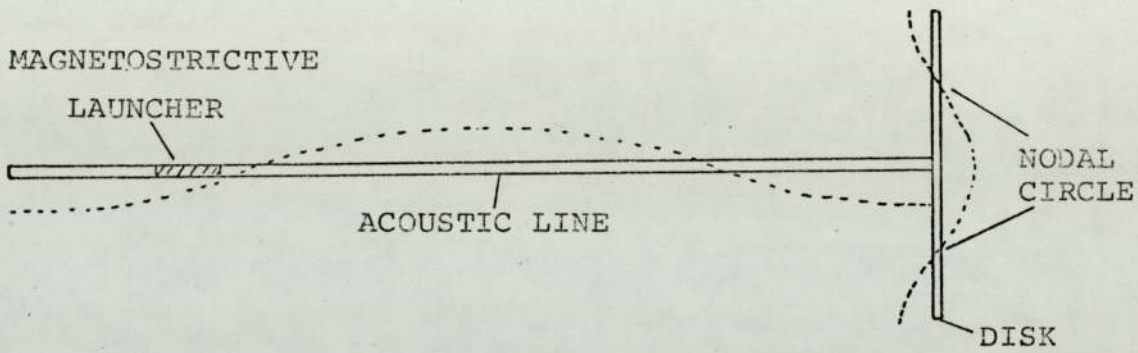

FIGURE 3.2.1

magnetostrictive effect, commonly known as the Joule effect, refers to the phenomena that if a magnetic field is applied to a sample of magnetostrictive material, parallel to its length, it will undergo a change in length. This change in length, or strain, is a maximum at the node, therefore the magnetostrictive launcher must be located at or near the node of a longitudinally vibrating acoustic line. This was verified experimentally by changing the position of the excitation coil on a thin nickel tube. The decrement signal obtained with various positions of the coil is shown in Plate 3.2.1. The decrement signal reduces in amplitude drastically as the coil is moved away from the node. The signal at 0.2λ from

PLATE 3.2.1.

The decrement amplitude of a longitudinally resonant line is dependent on the position of the magnetostrictive launcher:

a) Launcher at the node;

b) Launcher at 0.12λ from node;

c) Launcher at 0.2λ from node.

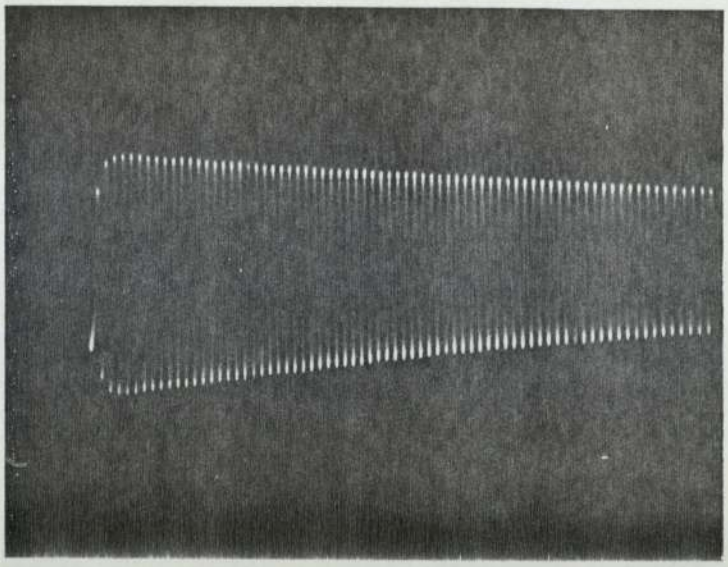

(a)

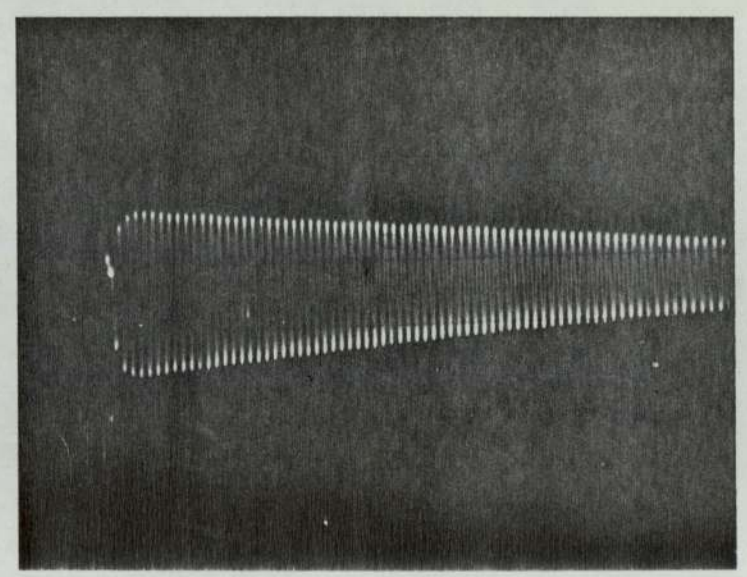

(b)

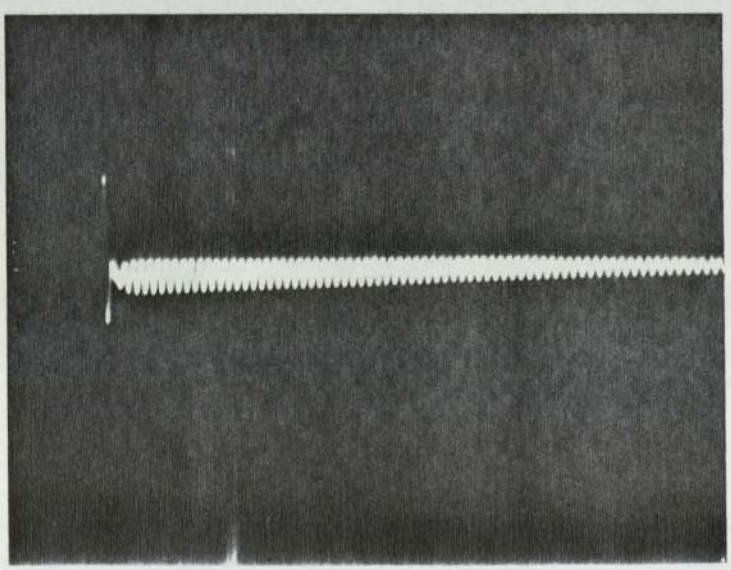

(c)

the node is only about 2% of the signal obtained at the node. With the coil at the anti-node, 0.25λ from the node, the desired mode of vibration can-not be set up but other modes are generated.

The frequencies of resonance of an unloaded free-edge disk undergoing flexural vibration with nodal circles are given by the expression:

$$f = (K)\ C\frac{h}{D^2}$$

where C = rod velocity of sound in disk material.

h = thickness of disk.

D = diameter of disk.

For the fundamental mode with one nodal circle, the value of the constant K is lowest and is 1.66.

To minimise the acoustic radiation from the disk, the wavelength of sound in the medium must be as large as possible in comparison with the disk dimensions. This means that the term $\frac{h}{D^2}$ must be as small as possible and that low velocity material for the plate is desirable for low frequency resonators.

Table 3.2.1. shows the results obtained for various dimensions of disk made of steel and aluminium, excited by a thin Nickel tube of 4 mm diameter used as the line. The line was supported at each of its nodes by three screws to minimise the support losses. It has already been mentioned that to avoid the phenomena of 'frequency pulling' the resonance frequency of the line must coincide with that of the disk. This effect will be further

Disk Number	Disk Material	Diameter D in mms,	Thickness h in mms.	$\frac{h}{D^2} \times 10^{-6}$	Observed Resonant Frequency in KHz	Theoretical Resonant Frequency $0.41\ C\frac{h}{D^2}$ in KHz	Line Length in m.	Q in air
(1)	Aluminium	60	3.0	833	6.989	7.1	0.39	Low
(2)	Aluminium	70	3.0	612	5.01	5.2	1.07	626
(3)	Aluminium	80	3.0	469	4.20	3.8	1.04	1200
(4)	Aluminium	70	1.7	347	2.78	2.95	0.89	140
(5)	Steel	70	1.0	204	2.16	1.74	1.07	1400
(6)	Steel	80	3.0	469	4.10	3.8	1.04	2400
(7)	Steel	60	1.0	278	2.39	2.36	0.94	700
(8)	Steel	70	1.5	306	3.00	2.6	0.65	1650

TABLE 3.2.1.

investigated in a later section.

From the results it is seen that the maximum deviation of the observed resonant frequency from that predicted by equation (3.2.1) is 10%. This may be due to the 'frequency pulling' by the line. Other factors which may cause this disagreement are that in practice the disk is not circular, may be non-uniform in thickness, is not driven by a point source and that it has damping. The 'Q' of the system increases with the mass of the disk. This can easily be explained with the aid of the equivalent electrical analogue circuit of the mechanical system. Such a circuit for the line disk system is shown in Figure 3.2.2. The derivation of the equivalent parameters of the line and the disk is given in the Appendix.

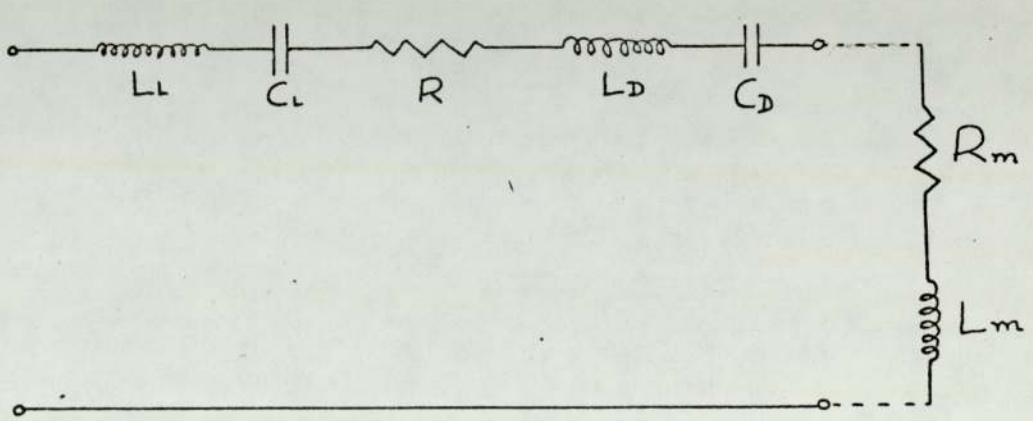

FIGURE 3.2.2.

L_L = equivalent mass of rod,

C_L = eqivalent compliance of rod.

L_D = equivalent mass of disk.

C_D = equivalent compliance of disk.

R = Total internal losses of line and disk, these arise from internal friction and losses to the supports.

R_m= loss due to medium surrounding disk.

L_m= equivalent mass of medium associated with the vibration of disk.

Taking Rm and Lm as zero for an unloaded disk, the 'Q' of the system is given by:

$$Q = \frac{\omega(L_L + L_D)}{R}$$

Assuming that the losses R, L_L and ω are kept constant, increasing the mass of the disk increases equivalent L_D resulting in 'Q', as seen from the results for the disks three and six. The loaded 'Q' is also proportionally higher.

The mode of vibration of the disk can be determined by examining the surface with a probe attached to a condenser microphone. The microphone used was a B & K ½ inch type 4133 attached to a 1 mm diameter probe. The experimental set up is shown in Plate 3.2.2. Photographs 2 and 3 shows the display on the oscilloscope at resonance and with a slight detuning off resonance respectively. The top trace is the acoustical signal, picked up by the probe, from the centre of the disk.

The mode of disk resonance is confirmed by exploring its surface with the microphone probe, the acoustical signal obtained will enable the nodal positions to be found. The signal obtained from either side of a nodal point should be in antiphase with each other since the vibrations on either side of the nodes are in antiphase.

PLATE 3.2.2.

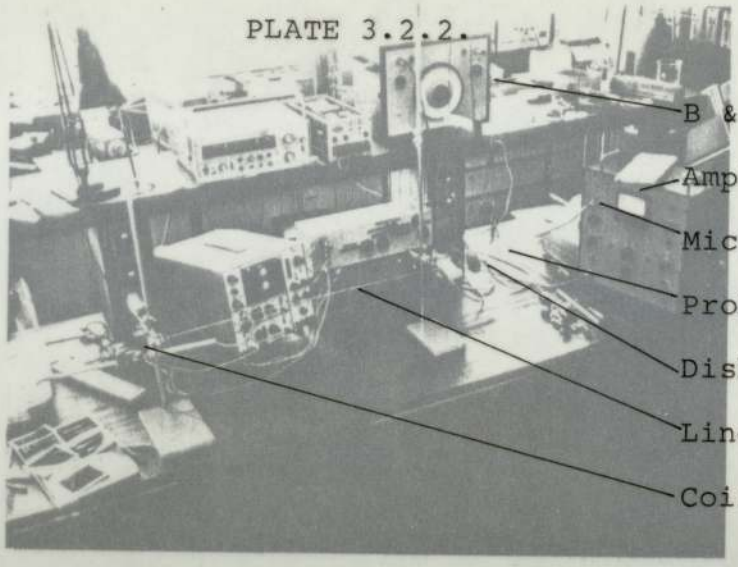

At Resonance

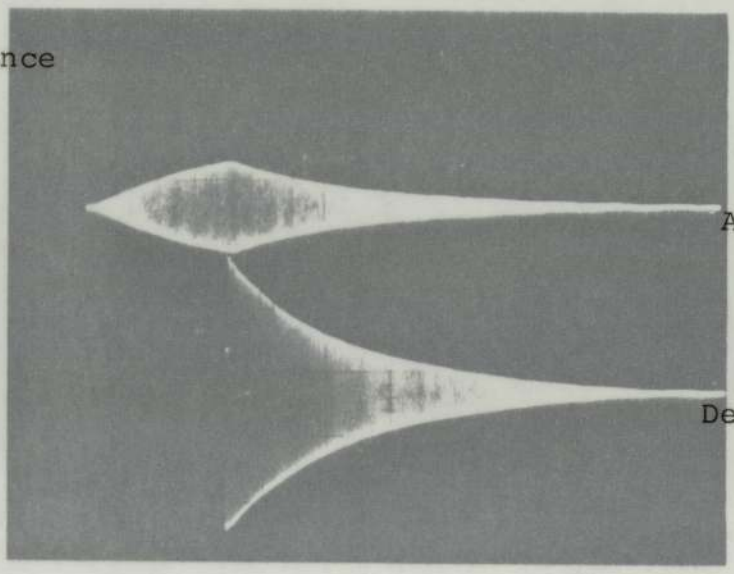

Slight Detuning Off Resonance

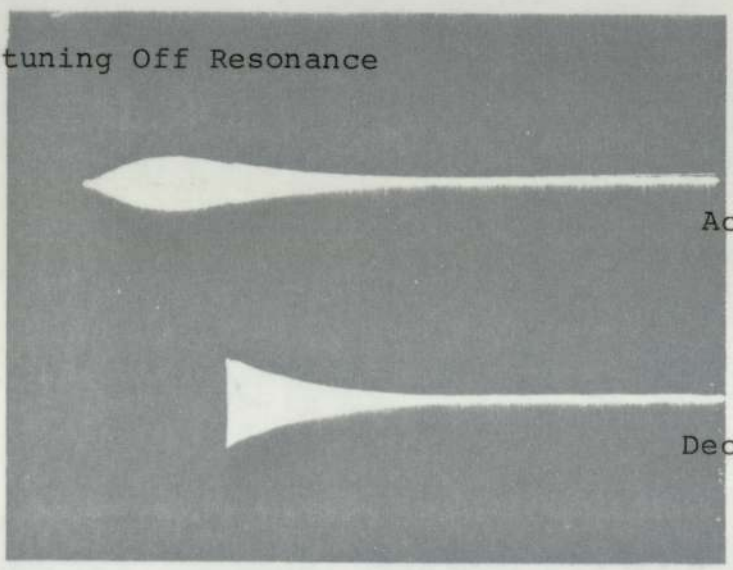

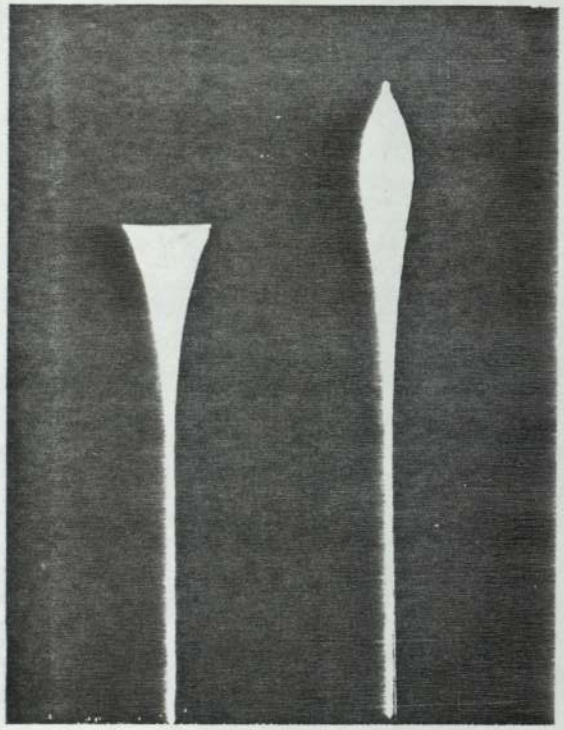

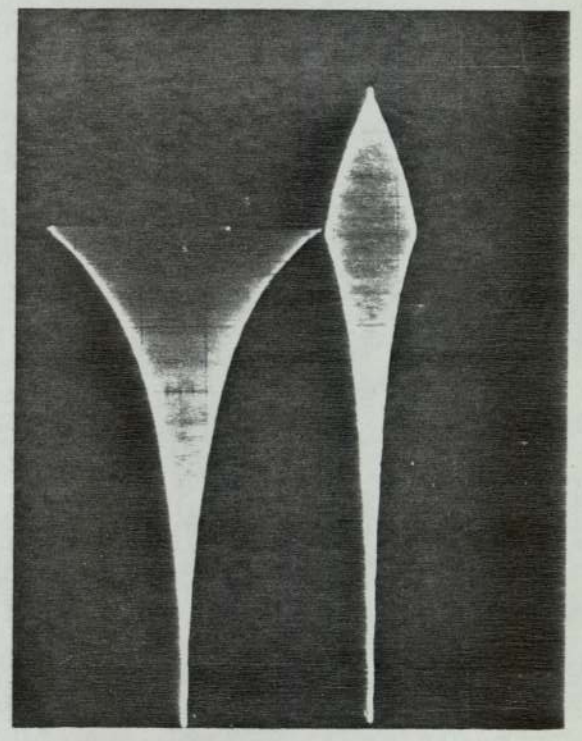

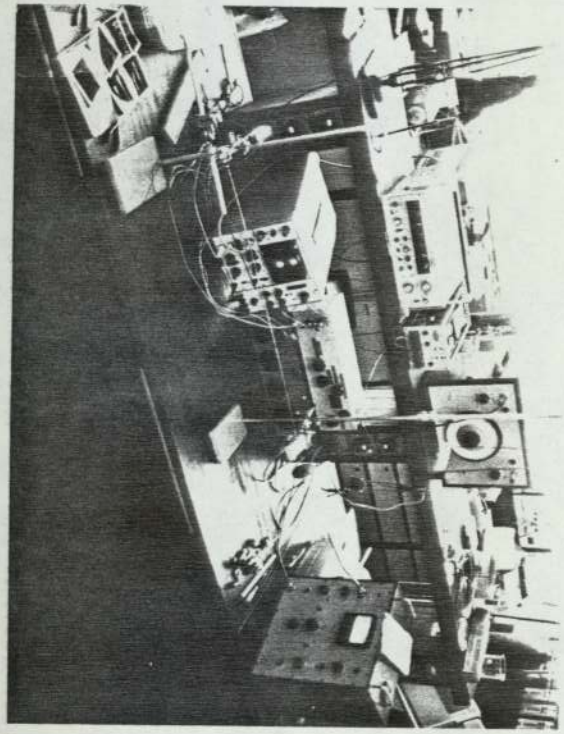

PLATE 3.2.3.

Shows the acoustic signal (top traces), relative to the decrement signal, of a free edge disk.

(a) at the nodal circle

(b) and (c) on either side of the nodal circle; the acoustic signals are 180° out of phase.

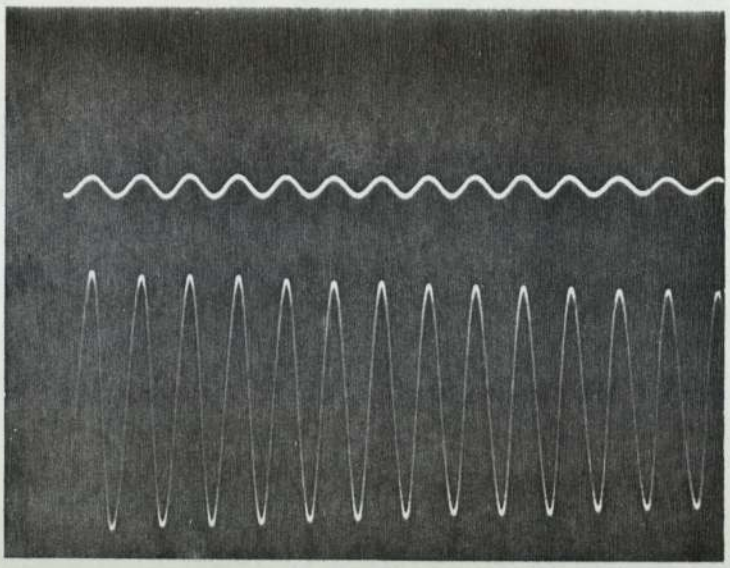

(a)

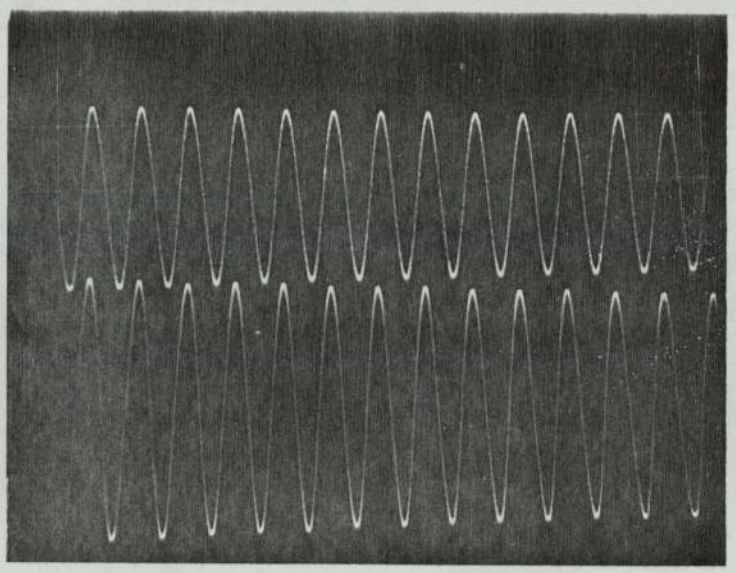

(b)

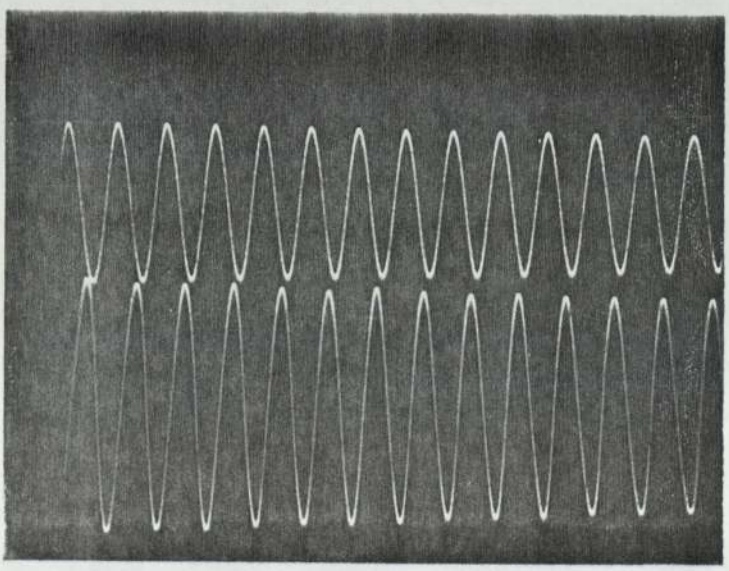

(c)

This is clearly demonstrated in Plate 3.2.3. which shows signals picked up on either side of a nodal circle and at the nodal circle for a disk. The top trace in each of photographs one and three is the acoustical signal on either side of the nodal circle. At resonance the nodal circle of the disk should not radiate any acoustic energy but due to the finite area of the probe signal of small amplitude is obtained (photograph (a)).

The location of nodal points by the microphone probe method becomes unreliable for disks with resonance frequency below 1.5 KHz. Below this range the microphone 'sees' the disk as a piston type source consequently the acoustical signal amplitude does not vary much with the radial positions and also the phase changes associated with the nodal points are undetected.

The microphone probe was used to measure the dynamic deflection curve of a disk at resonance. Such a normalised measured curve is shown in Figure 3.2.3. The measured curve agrees well with that predicted by theory. Figure 3.2.4. shows the variation of the amplitude of deflection, (arbitary units), at the centre of the disk with the number of pulses in the burst exciting the disk.

3.3 'FREQUENCY PULLING' PHENOMENON

It has been pointed out previously that the length of the acoustic line is such that its resonance must coincide with that of the disk so that the resonant frequency of the sensor is not appreciably altered.

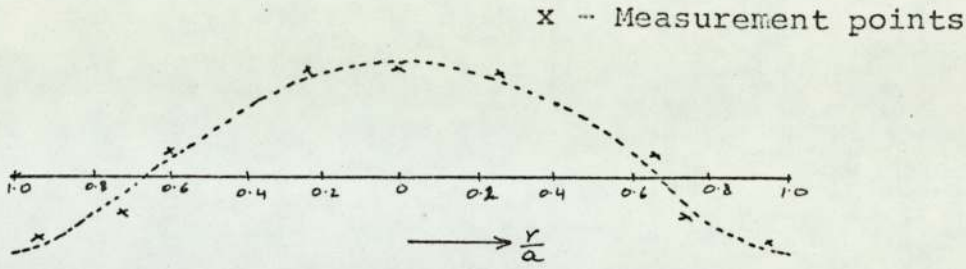

FIGURE 3.2.3.
The normalised dynamic deflection curve of a free edge disk of radius a vibrating with one nodal circle.

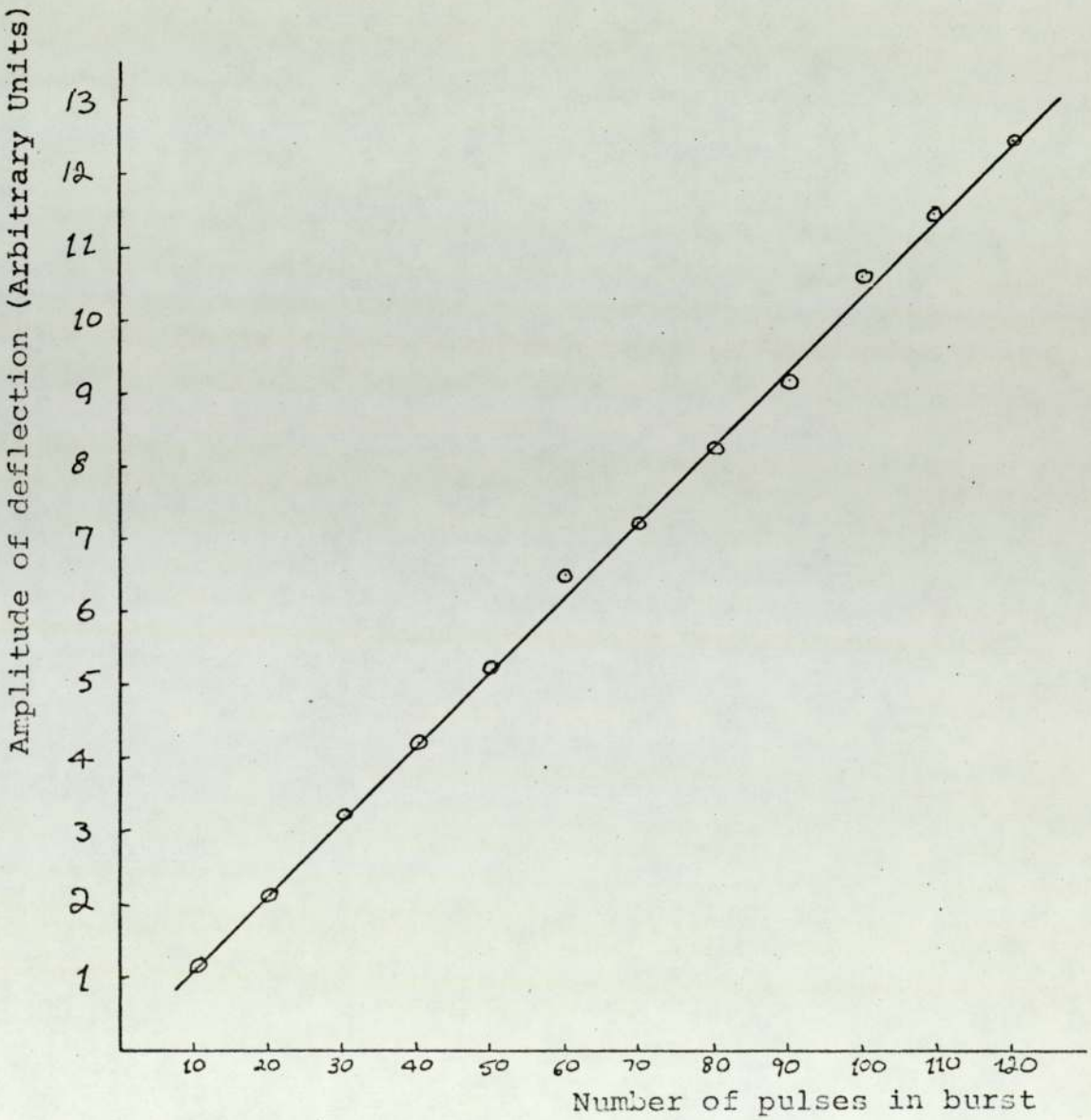

FIGURE 3.2.4.

Variation of amplitude of vibrations with the number of pulses in the burst. This case is in air where the 'Q' is very high,

If these frequencies do not coincide then the coupling between the two systems will produce a frequency shift. Such a frequency shift alters the deflection curve of the disk and the overall Q of the system decreases. The coupling between two or more mechanical oscillators have been extensively analysed in the literature (see Morse[24]), however, here only the experimental results obtained are given.

An aluminium disk of radius 3.8 cms. and thickness 0.16 cms. was excited by a nickel tube. The length of the line was altered and the resonance frequency of the line disk system was measured. Results obtained are plotted in Figure 3.3.1.

The microphone probe was again used to determine the changes in deflection curve of the disk with the resonance frequency of the system. For a frequency of approximately 1.850 KHz the nodal circle was located at the radius of 2.1 cms. as compared to 2.56 cms. predicted from theory. As the true resonance frequency of the disk, 1.940 KHz, was approached the nodal circle radius slowly increased to 2.60 cms. At this frequency a very sharp nodal circle existed and the 'Q' of the system was relatively higher than at 1.850 KHz. With further increase in the resonance frequency above 2.4 KHz no sharp nodal circle was detected. However, the amplitude of vibration of the disk surface was dependent on the radius of the disk with absence of any nodal pattern. The Q of the system was lower than at its true resonance frequency.

FIGURE 3.3.1.

The variation of resonance frequency of a disk with the length of the acoustic line.

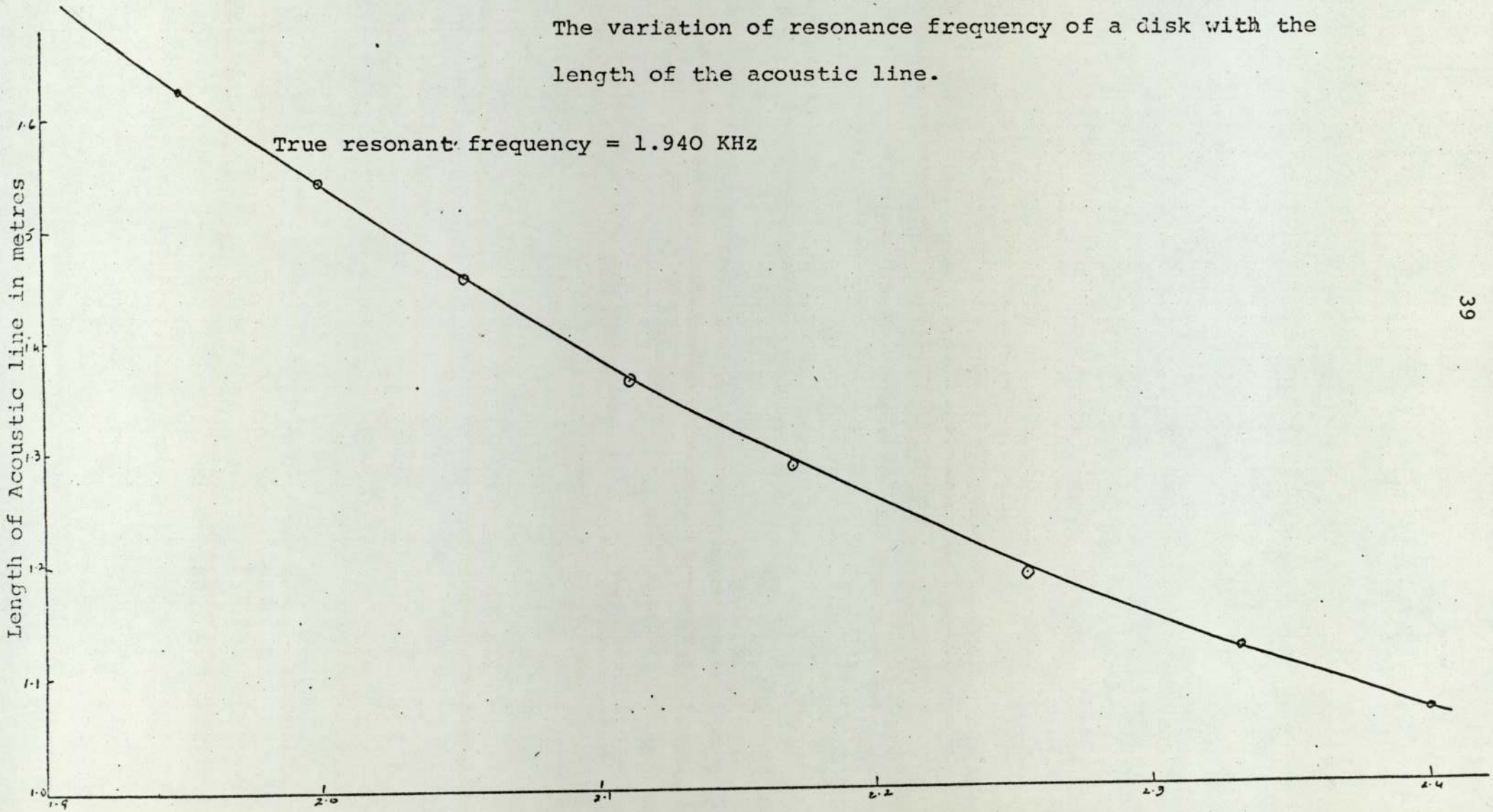

These changes in the 'Q' may be explained by considering the electrical analogue circuit shown in Figure 3.2.2. The component value L_D is calculated from the parameter of the disk and the deflection curve of the disk. It appears that at resonance L_D has a maximum value making the 'Q' of the system highest assuming that all other component values remain constant.

Therefore to avoid the above effects the line length was carefully chosen for all the experiments carried out in this investigation.

3.4 INTERACTION OF FREE EDGE DISK WITH CALIBRATING LIQUIDS

A number of massive disks with resonant frequencies ranging from 1.0 to 4.0 KHz in the flexural mode having one nodal circle were selected. Detailed experiments were carried out to investigate the effects of 'thick' and 'thin' liquids loading on these disks. Table 3.4.1. shows the parameter of the disks under test. The liquids used for these experiments were silicone fluids MS200 which had approximately the same density but a range of values for viscosity; other liquids such as water (ρ = 1.0 gm/cc, η = 1.0 CP), ardox (ρ = 1.3 gm/cc, η = 0.3 CP) and pure glycerol (ρ = 1.26 gm/cc) the viscosity of which is, at room temperature (20°C), 1412 c.P.

The line used in all these experiments was the Nickel tube which has a surface magnetostrictive effect, therefore it is imperative that the line be very lightly supported at the nodes to reduce losses. Similarly the

Disk Number	Disk Material	Thickness h in mms.	Diameter D in mms.	$\frac{h}{D^2} \times 10^{-6}$	Frequency of resonance in air KHz	Q in air
(1)	Steel	3.2	76	554	4.8	very high
(2)	Aluminium	3.2	76	554	4.76	high
(3)	Aluminium	1.6	76	277	2.3	high
(4)	Steel	3.0	89	403	3.7	very high

TABLE 3.4.1.

coil used to launch the longitudinal pulses in the line should not touch the line. Care must be taken to ensure that there are no air bubbles present in the liquids.

Table 3.4.2. shows the results of the effect of fluids on the resonance of the disks studied. Figure 3.4.1 shows the dependence of the resonance frequencies of the disks with the density of the fluid surrounding it. Results for disks 1,2,and 4 show that for any disk the resonance frequency falls linearly with the density of the liquid. The 'Q' of disk 3 (the lightest) was low and no resonances were obtained in liquids of higher viscosity than 50 CP. Although the changes in the frequency with density are quite measureable it is at once apparent that the changes in the Q factor with viscosity is more significant. In view of these results it was anticipated that consistency of materials such as sludge could best be measured by considering their fluidity. With this in mind a special disk shown in Figure 3.4.2.(a) was made. This type of sensor has several advantages:

(a) The solid centre of the disk lowers the resonance frequency without altering the thickness or diameter of the disk.

(b) The Q of the sensor will be higher therefore it can be made to resonate in very thick liquids.

(c) The dynamic deflection curve of the disk was measured with the microphone probe and is shown in Figure 2.(b). The edges of the disk flap with the higher amplitude than at the centre. Therefore larger

Disk Number	Viscosity (η) in C.P.	'Q'	Density in gm/cc	Frequency in KHz
1	(In Kerosene)	230	0.86	3.822
	1.5	175	0.9	3.845
	50	155	0.96	3.790
	100	80	0.97	3.780
	200	75	0.97	3.756
2	0.3	Very high	0.8	3.169
	0.8	Very high	0.86	3.122
	1.5	260	0.96 (η = 50)	3.057
	50	110	0.96 (η = 100)	3.056
	100	97	0.97 (η = 200)	3.080
	200	75	1.0	3.020
	500	52	1.3	2.786
3	0.3	High	0.8	1.175
	1.5	66	0.86	1.154
	5.0	Low	0.9	1.140
4	0.3	Very high	0.8	1.0
	0.8	200	0.86	0.989
	1.0	180	1.0	0.972
	1.5	155	1.3	0.916

TABLE 3.4.2.

FIGURE 3.4.1.

Calibration of the resonance frequency of disks with the density of liquid.

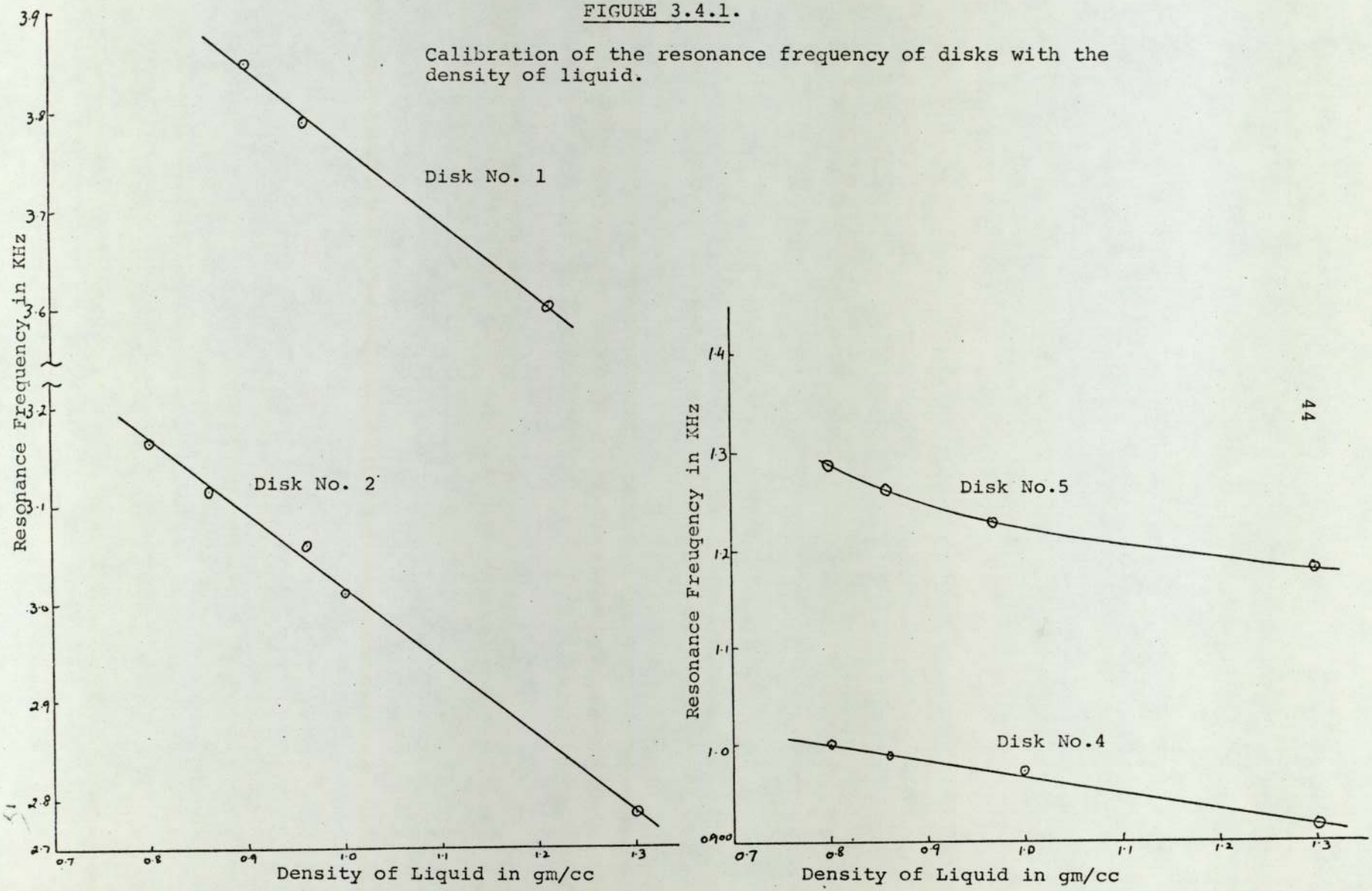

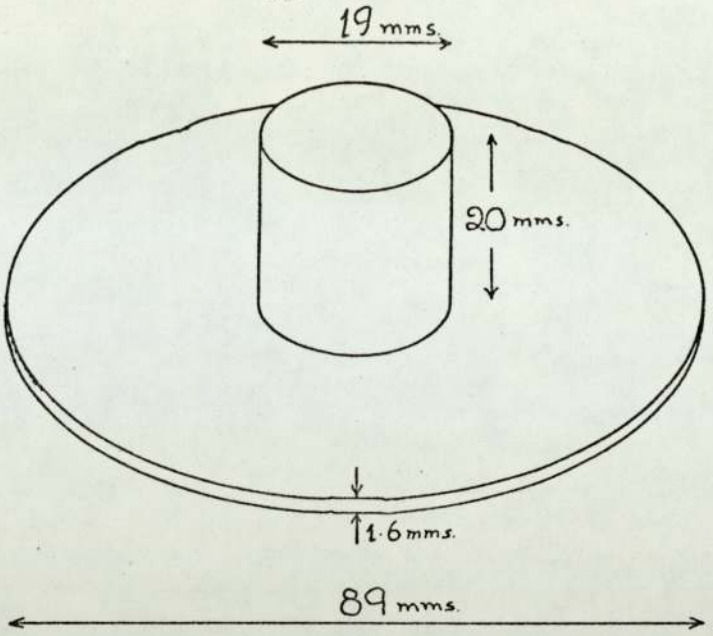

(a)

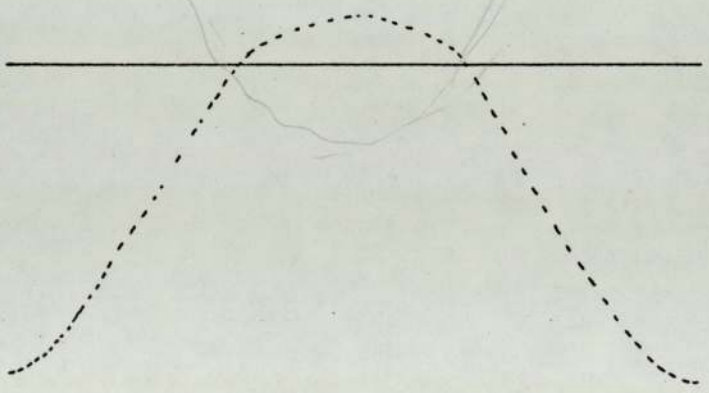

(b)

FIGURE 3.4.2.

The geometry of the solid centre disk (disk No. 5) and the deflection curve at resonance.

amounts of liquid movement will take place at the periphery of the disk making macroscopic measurement on the liquids.

(d) The interfacing of a robust line to the disk is relatively easy.

Some experimental results of this disk (will be known as disk no. 5) with different liquids are shown in Table 3.4.3. The graph in Figure 3.4.1. shows that the variation of resonance frequency with the density of liquid for this disk is no longer linear.

Viscosity (η) in C.P.	Density ρ in gm/cc	Resonance Frequency in KHz	'Q'
0.3	0.8	1.287	Very High
0.8	1.3	1.180	Very High
1.5	0.86	1.260	Very High
100	0.97	1.228	190

TABLE 3.4.3.

3.5 EXPERIMENTS WITH SLUDGE

At this stage it was decided to investigate the effect of the sludge on the free edge disk sensor. A barrel of sludge was obtained from the Mineworth sewage works and its effect on the resonance of disk no. 4 and 5 was determined. Care was taken to stir the sludge thoroughly

so that it had a uniform suspension of solid content throughout the volume of sludge. The results obtained are shown in Table 3.4.4.

DISK NO.	FOR WATER		FOR SLUDGE	
	Frequency in KHz	Q	Frequency in KHz	Q
4	0.972	130	0.947	45
5	1.247	280	1.228	90

TABLE 3.4.4

The decrement obtained for disk 5 in water and sludge is shown in Plate 3.5.1. The 'Q' in the sludge is sufficiently high to give a good resonance. It is realised from the results that although both disk 4 and 5 are suitable transducers for the measurements at hand, disk 5 is preferred because of its higher Q in sludge. The whole experiment was later repeated in a new sample of sludge the results already obtained were verified. Further investigations were carried out to find the effect of the addition of water to the sludge. No quantitative results were taken, but with the thinning of the sludge, the inertia loading decreased, raising the frequency and the 'Q' of the sensor increased as the fluid became more mobile.

Sludge is normally acted up on by anaerobic bacteria to decompose into gases and liquids. It was feared that the presence of gas bubbles in the liquid may interfere

PLATE 3.5.1.

The decrementsignal for Disk no. 5:

a) In Water

f = 1.247 KHz

Q = 280

b) In Sludge

f = 1.228 KHz

Q = 90

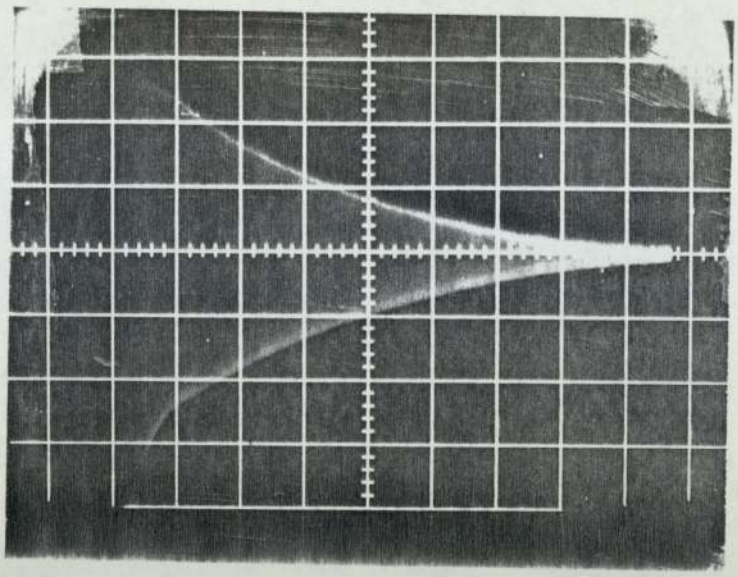

(a)

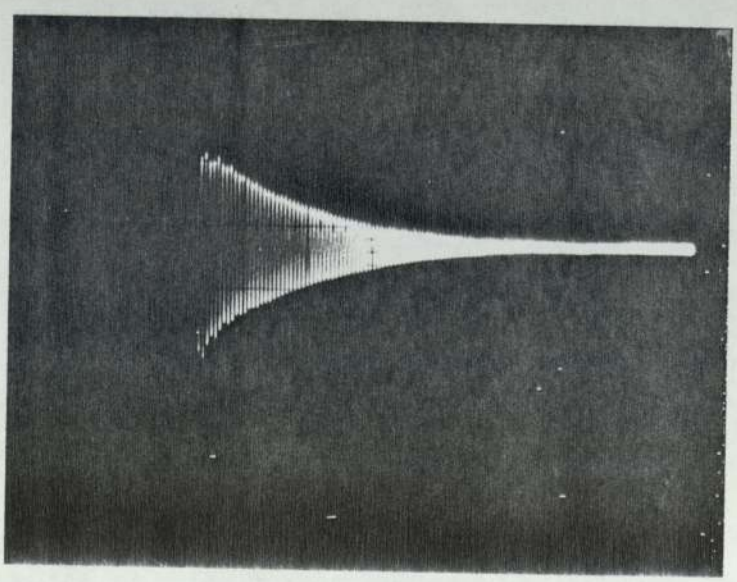

(b)

with the performance of the transducer. It was very difficult to judge the degree of gases present in the sludge under test, however throughout the tests there was no indication of the bubble interaction with the sensor resonance. The bubble problem is further studied at the end of this chapter. It is envisaged that the on-line measurement of the consistency of sludge will not be hindered by the presence of bubbles.

3.6 A BRIEF DISCUSSION OF A ROBUST ACOUSTIC TRANSMISSION LINE[25]

In the present system the transmission of the acoustic energy into the disk resonator takes place through thin wall uniform Nickel tube. But for all practical purposes a much more robust line is required so that the sensor can be held in position as the sludge scrubs it at a high speed.

For rigidness a larger cross-sectional area of the line is required; for magnetostrictive materials the larger the volume the higher the internal losses in the material. As permendur is very lossy and not readily machineable, a composite line using brass or aluminium with a minimum length of the magnertostrictive permendur was used to transmit the acoustic energy into the sensor. Various factors have to be taken into account when lines of different material are terminated together. A brief discussion of such factors follows.

The acoustic transmission lines are analogous to the

electrical transmission lines. Plane acoustic waves are generated in the magnetostrictive launcher and are transmitted down the probe to the disk resonator and back. The probe is a transmission line of acoustic impedence z defined as the ratio of force to particle velocity in the wave. In terms of the parameters of the line, $z = \rho CA$ where ρ is density, A is the cross-sectional area and C is the plane wave velocity in the line material. At the junction of two lengths of line of impedence z_1 and z_2 (Figure 3.6.1) the coefficient of ratios of reflected and transmitted signals, R and T respectively, are given by

$$R = \frac{z_2 - z_1}{z_2 + z_1} \quad \text{and} \quad T = \frac{2\, z_2}{z_1 + z_2}$$

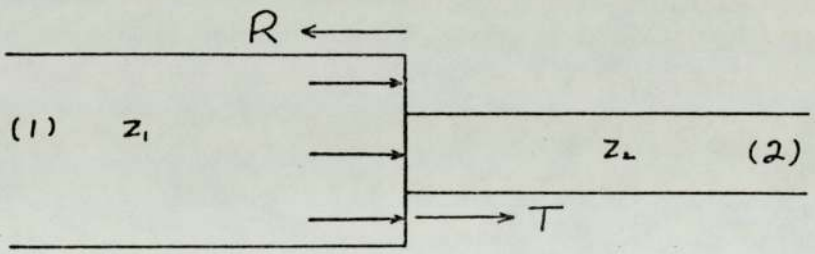

FIGURE 3.6.1.

When $z_1 = z_2$ all the incident signal is transmitted and the lines are perfectly matched. When $z_2 < z_1$ the reflected signal is in reverse phase to the incident, this means that a pulse of compression is returned a pulse of rarefaction at the junction. Similarly for $z_2 > z_1$, the reflected and the incidence pulses are in phase.

The transmitted signal T is always in phase with the incident signal.

Thus for correct matching z_1 must equal z_2 so that there is no reflected signal at the junction of the two lines. When the lines are of the same material they must be of the same area and can be keyed together as convenient. For good acoustic contact they should be brazed together, ideally by a braze of the same acoustic impedence as the material. For different materials the area ratio will be the inverse ratio of the impedence i.e.

$$\frac{A_1}{A_2} = \frac{\rho_2 C_2}{\rho_1 C_1}$$

Hence for rods the diameter ratio will be:

$$\frac{d_1}{d_2} = \left[\frac{\rho_2 C_2}{\rho_1 C_1}\right]^{\frac{1}{2}}$$

3.6.2. EXPERIMENTAL WORK

It was decided to commence the experimental work by investigating a line composed of a permendur rod, used as the magnetostrictive launcher, butt welded to a brass rod. The specific acoustic impedence (ρC) of permendur to brass is 1.4 which gives the diameter ratio of brass to permendur of 1.18 for a good acoustic match.

A butt joint was made between a permendur rod and a brass rod of diameters 8.0 mm and 9.5 mm respectively. The two rods were brazed together and the joint obtained was mechanically strong. The braze forms a section of

lower impedence than that of the permendur causing a mismatch at the junction. The effects of this mismatch become important at high frequency when the length of the section is comparable to the wavelength in the line, but are negligible for low frequency lines.

The length of the permendur is kept low, about 18 cm, to minimise the losses, (permendur is very lossy). The positioning of the magnetostrictive launcher is critical. It must be located at or near a node of the line as shown in Figure 3.6.2. The line shown will resonate in its second harmonic with a frequency of 1.260 KHz.

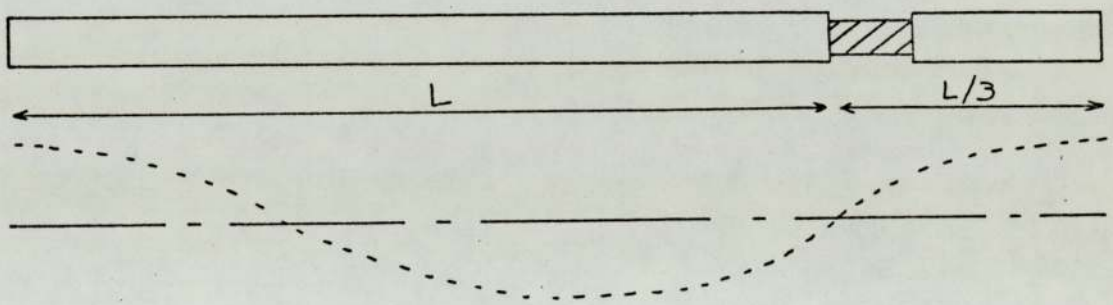

FIGURE 3.6.2.

Typically

L = 2m

Resonance Frequency = 1.260 KHz

Transmitted voltage = 60 V peak to peak.

Burst length = 90

Rep. Rate = 15 Hz

Decrement output = 15 V

Very High Q = (>1000)

3.6.3. INTERFACING THE ROBUST LINE AND THE DISK RESONATOR.

Theoretically a disk will vibrate in the required fundamental mode if it is driven at the centre point .If the robust line discussed in the previous section is directly joined to the centre of the disk which is relatively light the resonance will be modified. Since longitudinal waves are transmitted in the line, the velocity distribution at the rod end will be uniform. Therefore the velocity distribution at the surface of the disk in contact with the rod will also be that of a piston motion. This will render the resonance frequency and the dynamic deflection of the disk to differ vastly from that of the point driven disk.

The second interface problem is the coupling of the line to the disk. The coupling is a maximum when the line drive is at a disk antinode and zero at the node. The more robust the line the closer the drive point must be to the node. In Pollard's[25] paper it is shown that the equivalent mass of a longitudinal resonant line is 0.5 M_L where M_L is the total mass of the line and it will be shown in the Appendix A.1. that the equivalent mass of a centre driven disk is 0.3 M_D where M_D is total mass of disk. For typical dimensions of the robust lines used the equivalent mass of the line will be very much higher than that of a disk, hence most of the energy in the resonant system will be stored in the line and a small amount will be transferred to and stored in the disk.

Figure 3.6.6 . shows the variations of the equivalent

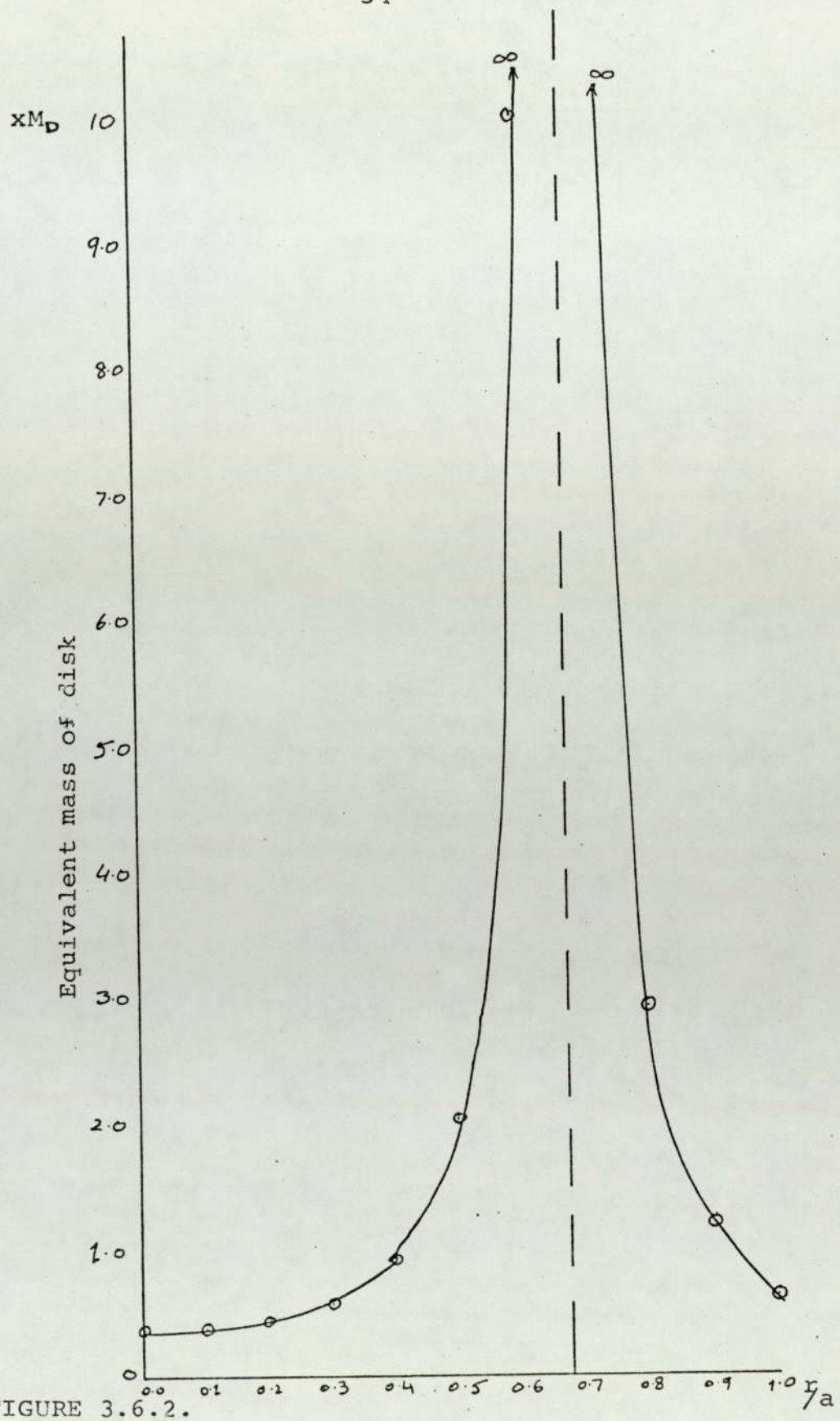

FIGURE 3.6.2.

The variation of the equivalent mass of disk (radius = a) at resonance with the radius r (M_D = total mass of disk)

mass with radius of a resonant disk. The equivalent mass is lowest at the centre of the disk and it increases with the radius, being infinite at the nodal circle. This result indicates that the coupling between the line and the disk will change from a maximum to zero as the coupling point is moved from the antinode at the centre to the nodal circle. Thus the nearer the coupling point to the node the more robust the line can be made.

The brass rod split at the end to drive the disk at two symmetrical points was developed. The end of the line is cut into two prongs as shown in Figure 3.6.3.

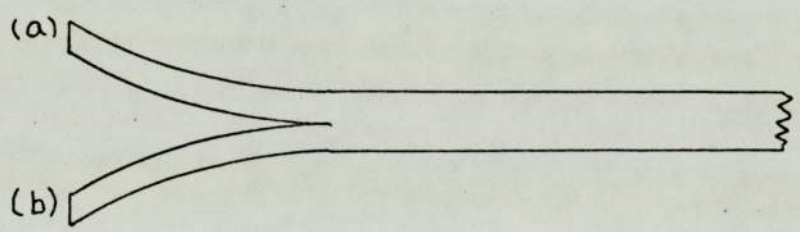

FIGURE 3.6.3.

The end faces (a) and (b) of the line were explored with the microphone probe. It was found that at resonance the acoustic signal in both the prongs is of the same amplitude and phase. Therefore it was possible to terminate the two prongs symmetrically near the nodal circle of a disk resonator, as a nodal circle presents a massive load to the prongs resulting in a better coupling (high 'Q').

Two butt joints were made on the surface of disk No. 4 (table 3.4.1.) at a radius of 12 mm (see photograph 3.6.1.). The disk was found to resonate at the frequency of 1.870 KHz in its correct mode, with the system Q of 700. The two prongs are slightly away from the nodal circle. This is a patentable feature of the transducer.

For disk 5, the robust line is simply butt jointed to the solid centre of the disk Figure 3.6.4. The resonant frequency of this system in air is 1.510 KHz with a 'Q' of 1200.

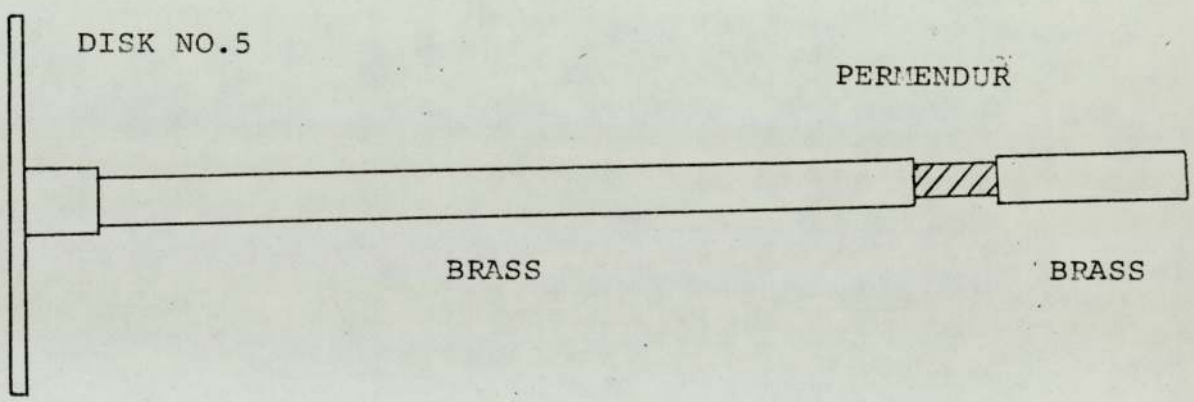

FIGURE 3.6.4

These two plates were prepared for on-line measurement of sludge consistency at Mineworth.

3.7 THE PISTON SYSTEM

The second type of sensor that may be used is a rigid disk undergoing piston type motion. The advantages

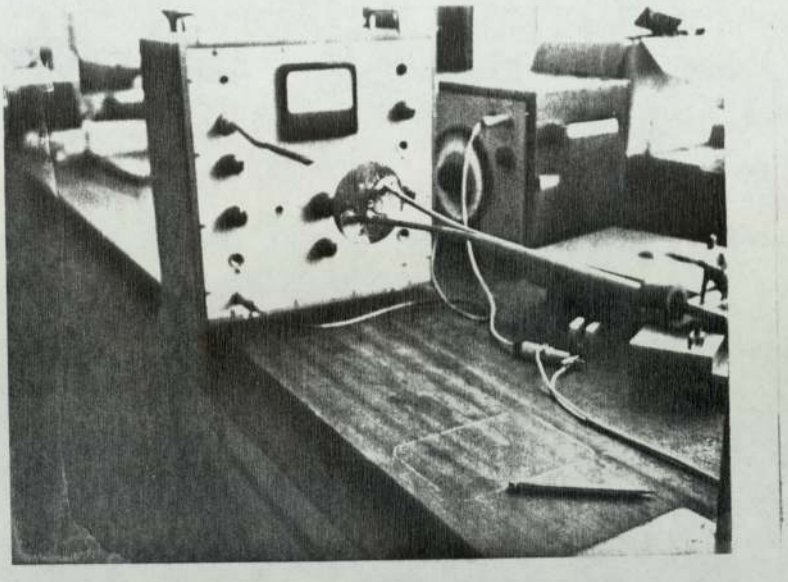

PLATE 3.6.1.

Illustrates the technique used to terminate a robust line to a disk.

of this type of sensor is that, firstly the sensitivity can be easily changed by changing the disk radius, secondly one robust line can be used for different sized disks and lastly there are no interfacing problems discussed in Art 3.6. The parameters of the disk have to be chosen such that the flexural resonant frequencies of the disks are high compared to that of the resonant line.

For this low frequency condition the disk impedence is a pure mass equal to that of the disk mass. Thus attaching a disk to the end of a robust line will decrease the resonant frequency of the line. This is analysed in Chapter 4.

In the experiments carried out the line was a brass rod of length 1.66 m. vibrating in its fundemental mode (½ free-free bar) at a frequency of ·930 KHz with a very high Q in air. Disks of various dimensions were attached to the end of the rod and the experimental results obtained are shown in the Table 3.7.1. Figure 3.7.1. shows the variation of the resonant frequency with the mass of disk attached to the end of the rod. This agrees well with the theoretical results (see Chapter 4).

Figure 3.7.2. shows the variation of Δf(= f_r in water - f_r in glycerol) against the diameter of the disk. It is seen that the smaller the diameter the less the change in Δf, a change of 0.3% for the 30 mm diameter disk, while there is a corresponding change of 60% in the 'Q' of the system. Therefore the transducer could be relatively

Disk Thickness mm	Disk Diameter in mms	$h/D^2 \times 10^{-6}$	Resonance Frequency in air Hz	Resonance Frequency in waterHz	Resonance Frequency in glycerol Hz	Q in water	Q in glycerol
1.7	75	302	852	656	622	350	30
1.6	63	403	889	784	756	400	48
2.2	50	880	901	858	840	400	77
2.2	40	1380	910	896	890	510	170
2.0	30	2220	917	910	907	520	180

TABLE 3.7.1.

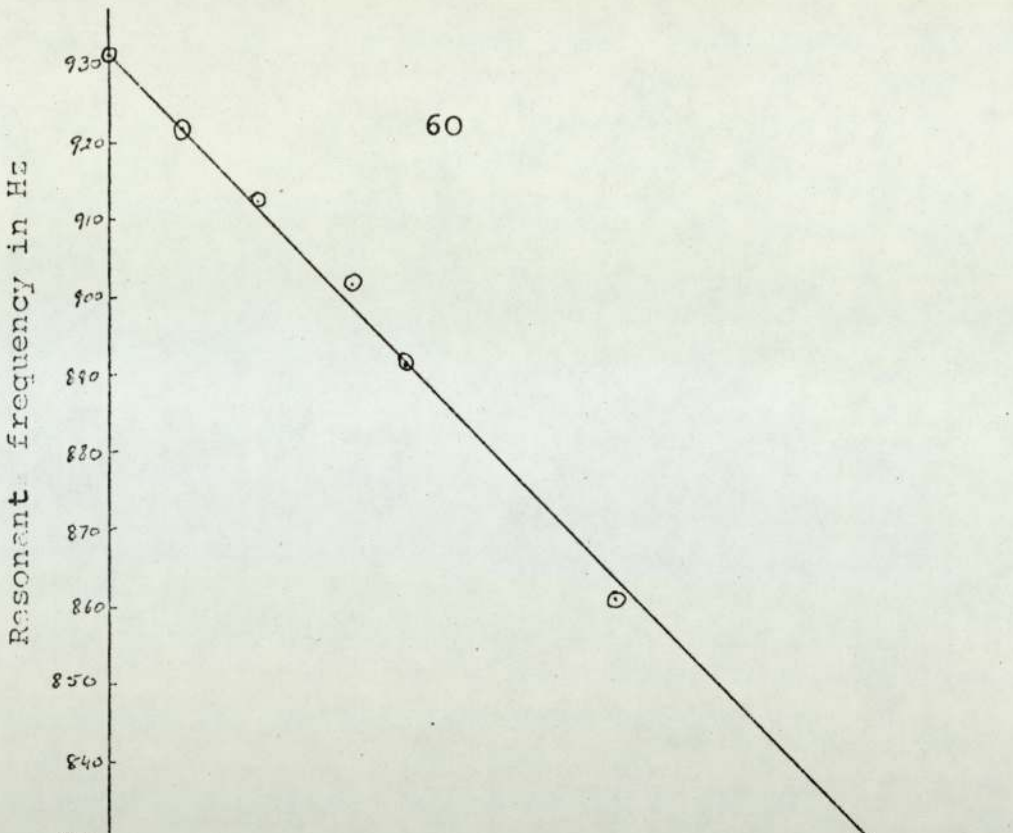

FIGURE 3.7.1. The resonance frequency of a ($\frac{\lambda}{2}$ free-free) brass rod with mass loading at one end.

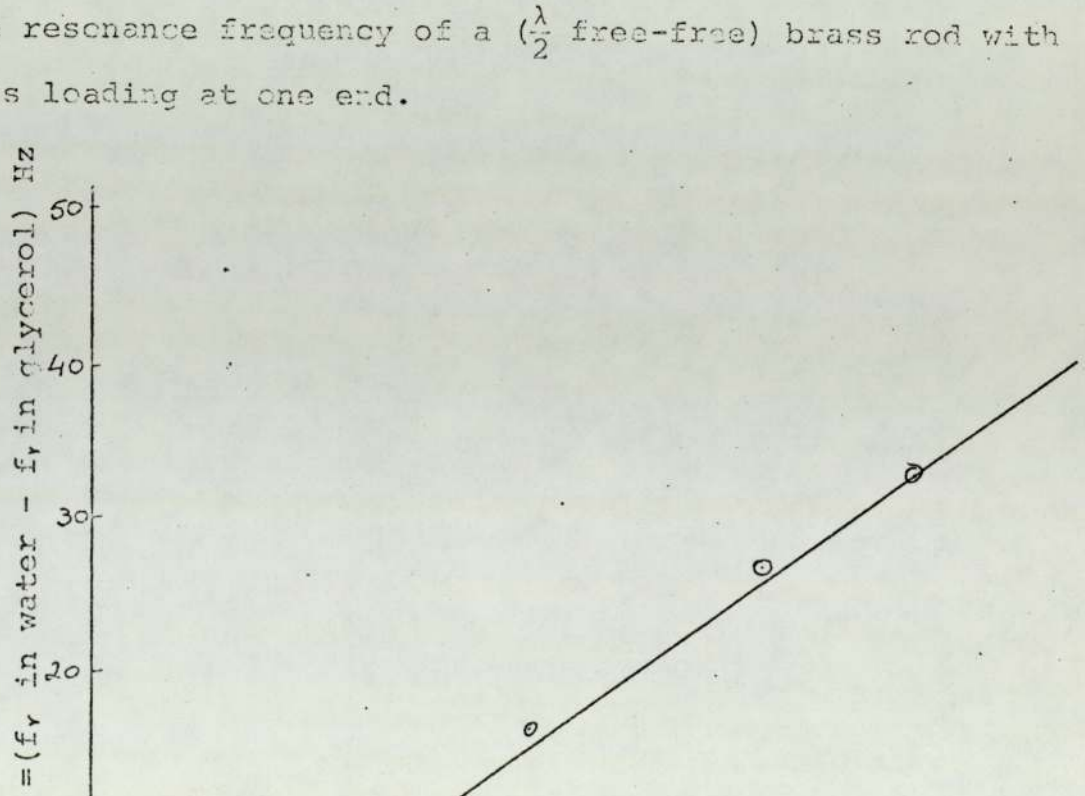

FIGURE 3.7.2 The change in the resonance frequency of the resonator with the diameter of the 'piston' sensor from water (ρ = 1.0 gms./c.c^3) to glycerol (ρ = 1.26 gms./c.c^3)

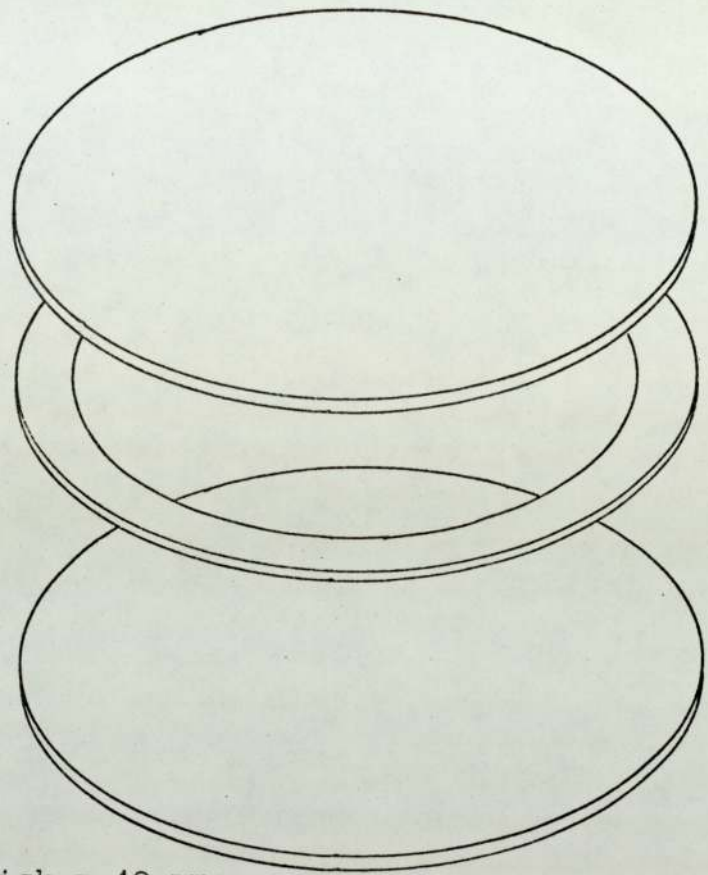

Radius of disk = 40 mms

Thickness of disks = 2 mms,

Outside radius of ring separator = 40 mms

Inside radius of ring separator = 35 mms

Thickness rádius of ring separator = 1.5 mm

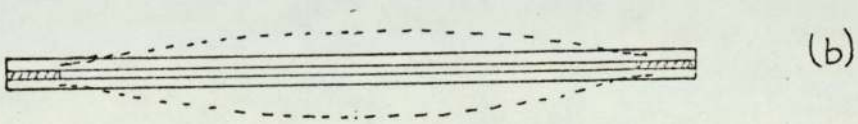

FIGURE 3.8.1.

The geometry of the 'oyster shell'.

(The two disks are brazed together at the periphery with the ring separator in between). This form of vibration will produce mainly acoustic radiation.

insensitive to density changes while retaining a high sensitivity to the fluidity of the surrounding medium. This property of the transducer is very useful for the measurement at hand, where an open loop electronic system is used so that retuning is not required as the density of the sludge pouring out of the bellmouth changes constantly.

By varying the radius of the disk or altering the resonance frequency of the transducer, it can be made to resonate in the very thick semi-liquids such as sludge.

Instead of a disk, a sphere for which the characteristics are given by Stokes law, clamped to the end of the line, undergoing translatory motion could be used as the sensor. A 50 mm diameter sphere was used and it was found that this type of transducer was fairly sensitive to consistency changes of sludge.

3.8 EXPERIMENTS WITH AN OYSTER SHELL

Although the design for the sludge consistency transducer had been completed and ready for on-line measurements at Mineworth, it was decided to investigate the effects of fluid loading on the so called oyster shell. Basically the oyster shell composes of two circular disks clamped together at the periphery with a small separation in between. An exploded view of the oyster shell is shown in Figure 3.8.1.(a). The fundamental mode of vibration is that of a clamped circular plate as shown in Figure 3.8.1.(b).

The shell is set into resonance by driving one disk at its centre as described before. When the driving signal frequency coincides with the resonant frequency of the disk, the second plate takes up energy via the clamped periphery, i.e. a node, and because of dynamic equilibrium its vibrations are in antiphase to that of the driven plate.

The fundamental resonant frequency of a clamped plate is given by:

$$f = 0.467c\left(\frac{h}{a^2}\right)$$

If the oyster shell, the internal radius, of the ring separator is taken as the radius of the clamped plate. Substituting the values for the thickness and radius, the theoretical resonant frequency of the shell is 3.8 KHz.

In practice the correct mode of vibration existed at 3.784 KHz with a good decrement. Since other spurious resonances were present this mode was verified with the microphone probe. With the shell surrounded by water contained in a bucket, it was found that the resonance frequency changed with the depth of shell. Figure 3.8.2. shows the variation in the resonance frequency with the depth of shell for two different heights of water in the bucket. This result can be explained by considering the flow field of liquid, shown in Figure 3.8.3, associated with the vibrations of the oyster shell. Since the two disks vibrate in antiphase and because of the absence of any nodal patterns on the surface of

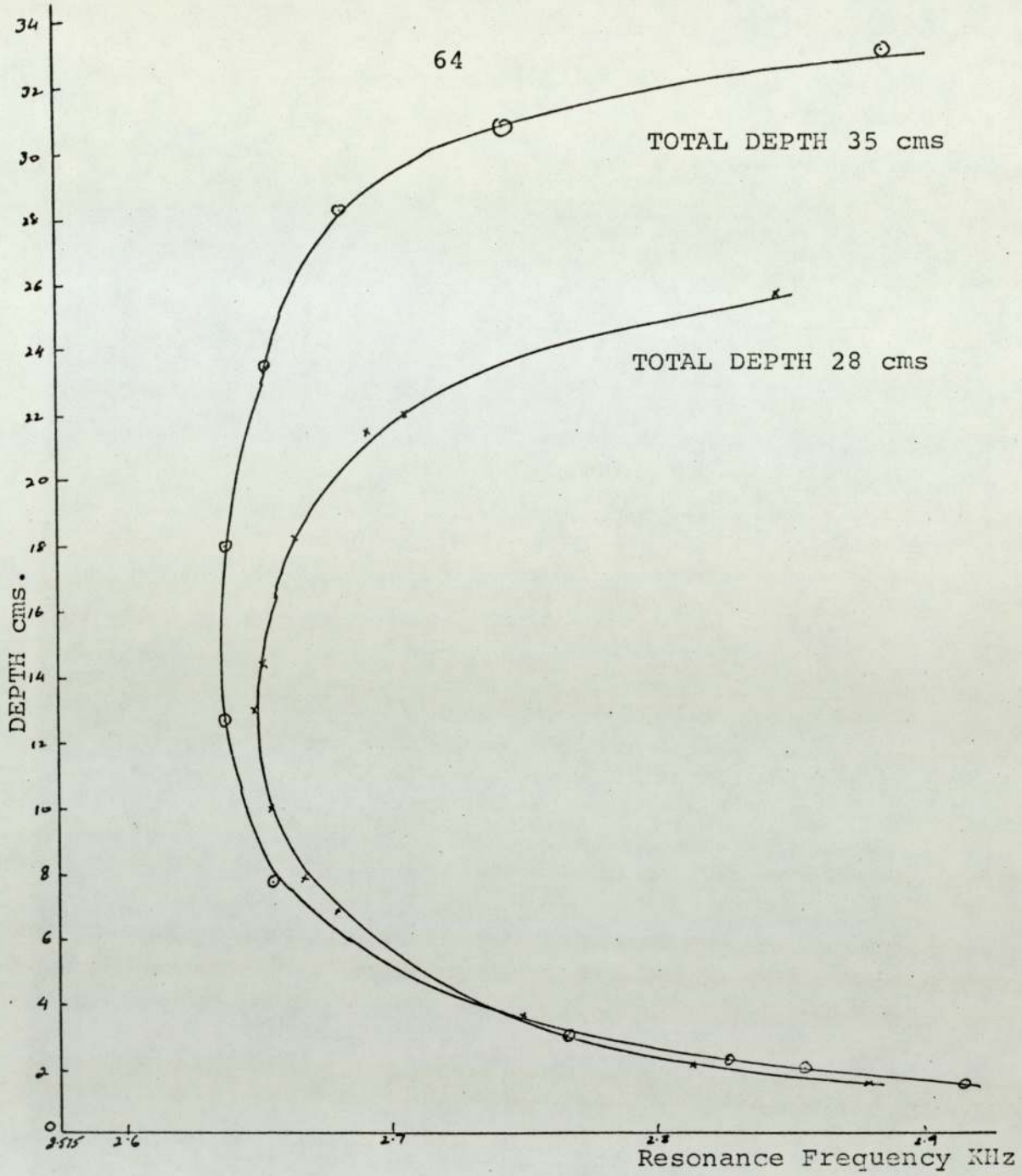

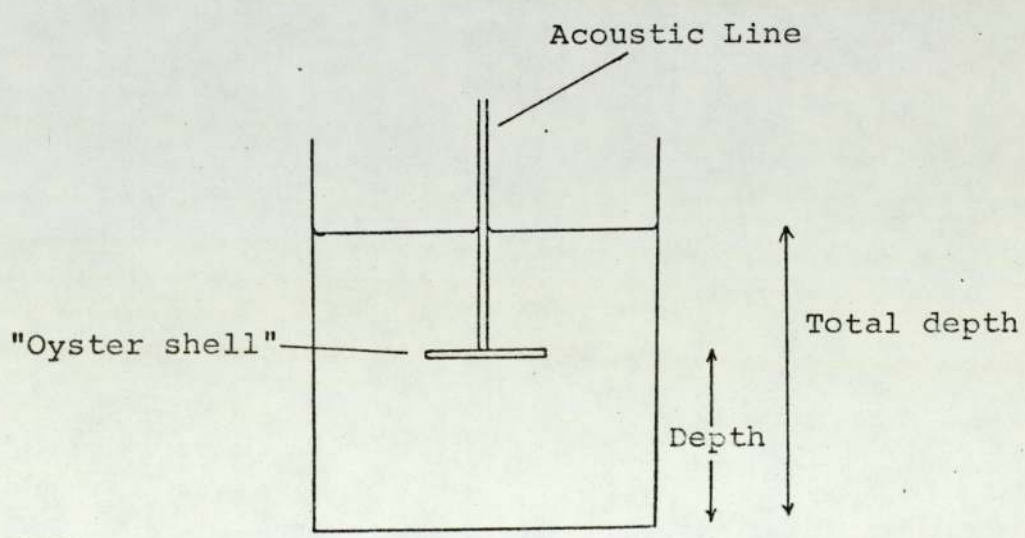

FIGURE 3.8.2.
The resonance frequency of oyster shell against depth.
The minimum occurs when shell is between the surface and bottom.

the disks, the energy field is not localised. The flow penetrates about 15cms into the water. From Figure 3.8.2. it is seen that true resonance frequency is 2.63 KHz, this being the frequency at which the oyster shell may be said to be surrounded by an infinite amount of water.

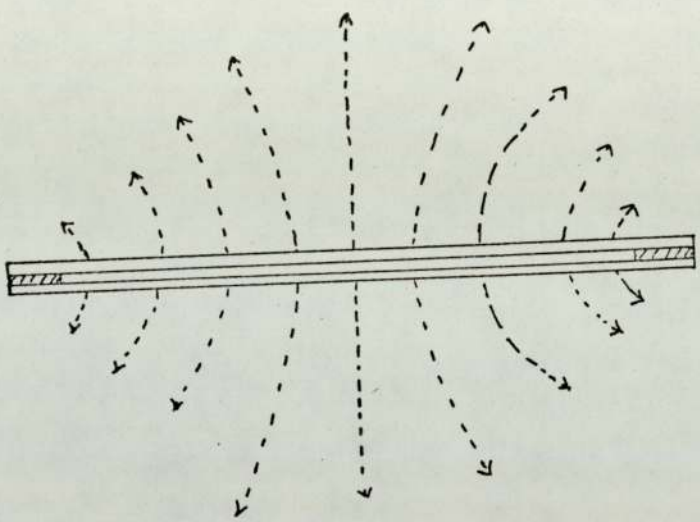

FIGURE 3.8.3.

The inertial loading on the shell decreases as it is moved towards the surface or to the bottom of the container. From the above results this transducer can not be used to measure density or other parameter of a liquid contained in a confined space. No further investigations were carried out. This type of transducer can be used as a sound radiator.

3.9. THE BUBBLE PROBLEM [27-30]

The settled primary sludge continuously decomposes

into liquid and gas as a result of chemical reactions. These gases are mainly methane and carbon dioxide. The rate of the chemical reaction is determined by the nature of the sludge and other chemical effluents that may be present. However, a continuous discharge of gas can be observed from the surface of the primary settling tanks and also in the bellmouth through which the settled sludge is discharged. Since the sludge is discharged at a high rate of flow past the consistency transducer it is envisaged that the bubble will only effect the readings momentarily. If the transducer readings are averaged over a small period of time than the instantaneous effects of bubbles so long as they are infrequent can be neglected. In other fields of consistency measurement such as the food or paper industry, the transducer may 'see' the bubbles for prolonged periods giving incorrect readings. Therefore, an investigation was undertaken to determine the effects of bubbles on fluid consistency transducers.

The presence of gas bubbles in water assumes great importance in the evaluation of the radiation of sound in underwater transducers. Exhaustive studies have been undertaken to investigate the scattering and attenuations of sound waves by the air bubbles. However, the present work has little to do with the sound radiation but nevertheless gas bubbles present within the energy field of the transducer will have similar effects.

The air bubbles in the water have a very large effect

on the attenuations of sound and on the elasticity of the water. Density of the water is little changed by the bubbles, but the compressibility of water changes drastically. This results in a change in the impedence presented to a submerged vibrating structure.

The measurements were made with the aid of the equipment shown schematically in Figure 3.9.1. The water container used was a transparent perspex aquarium of dimensions (30cms.×38cms.×60cms). The bubble rested against a very thin polythene diaphragm whose position could be adjusted. The size of the bubble could be varied by introducing more air into it with the help of a dropper of fine bore. The angle of contact between the bubble and the polythene was small this caused a spreading of the bubble to an oblate spheroidal shape. To prevent this spreading a spot of silicone grease was put on the diaphragm and the bubble clung to this area in an approximately spherical shape, although some distortion in the shape is inevitable because of the hydrostatic pressure. The size of the bubble was measured optically by the travelling microscope which traversed horizontally and vertically.

A detailed investigation of the effect of air bubbles on the resonance of the free edge disk was carried out. Figure 3.9.4. shows the changes in the resonance frequency of a disk caused by a bubble of mean diameter 7.4 mms, with its distance from the surface of the disk. This result verifies one of the important features of the

The equipment used to investigate the interaction of a bubbly liquid with the consistency sensor.

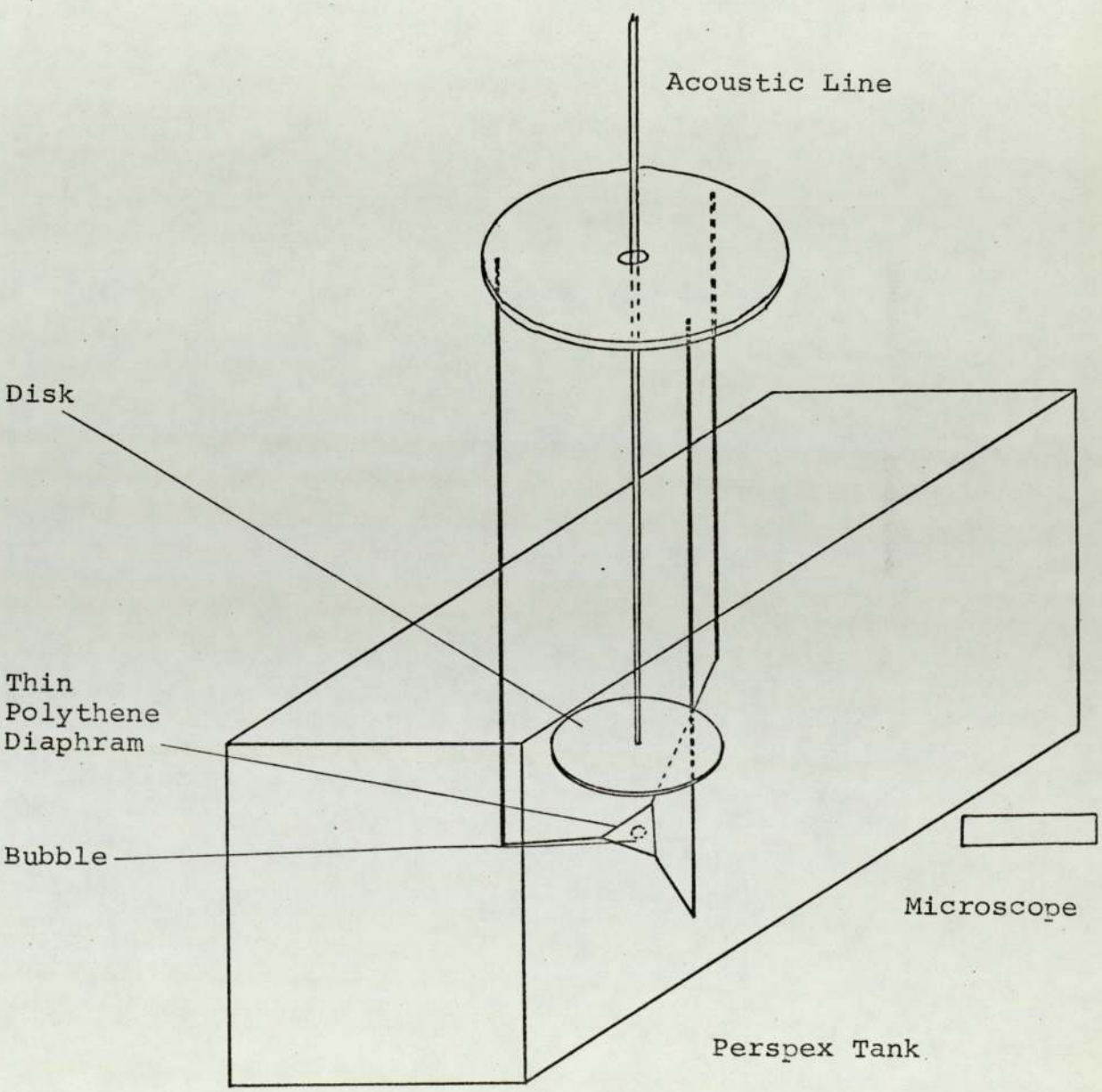

FIGURE 3.9.1.

sensor, that it will not be susceptible to bubbles beyond 3.5 mms since the energy field is very localised. This sensor will measure consistency of fluids in a confined space. Table 3.9.1. shows that variation of resonant frequency and the Q of the system, with bubble size. The separation between the diaphragm and the plate was approximately 0.5 cms.

Diameter of Bubble in mms	Resonance Frequecny in KHz	Q
1.15	3.534	108
0.145	3.498	Low Q
2.6	3.575	340
3.25	3.583	346
5.3	3.596	340

TABLE 3.9.1.

Figure 3.9.3. shows the dependence of the resonant frequency with the bubble diameter. This effect can be classified according to whether the radius of bubble is above or below a certain critical value. This being the size for which the bubble is set unto resonance.

The fundamental or pulsating resonant frequency of a bubble is defined as the frequency at which the stiffness of the gas in the bubble is tuned by the mass reactance

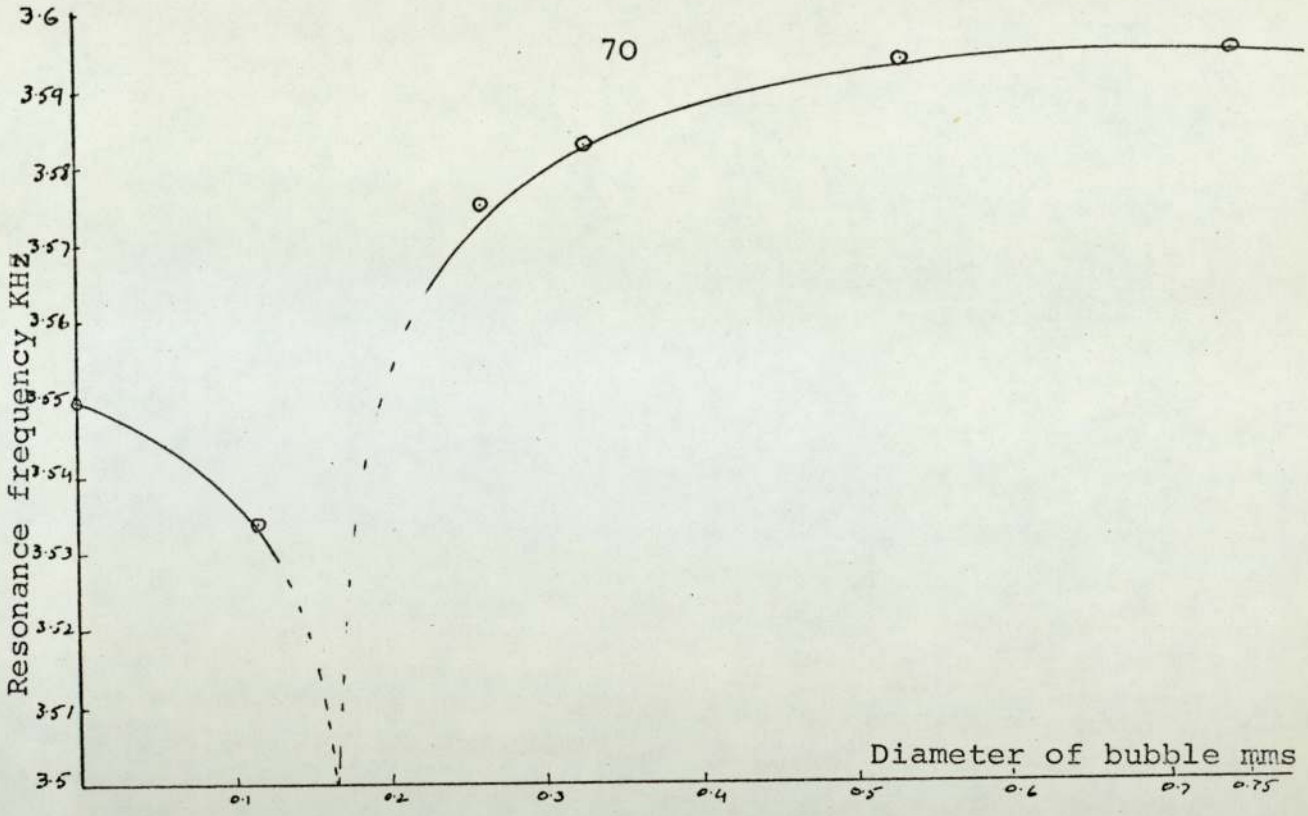

FIGURE 3.9.3.

The variation of a free edge disk resonant frequency with the bubble diameter. The bubble is held at a distance of 0.5 cm from the disk.

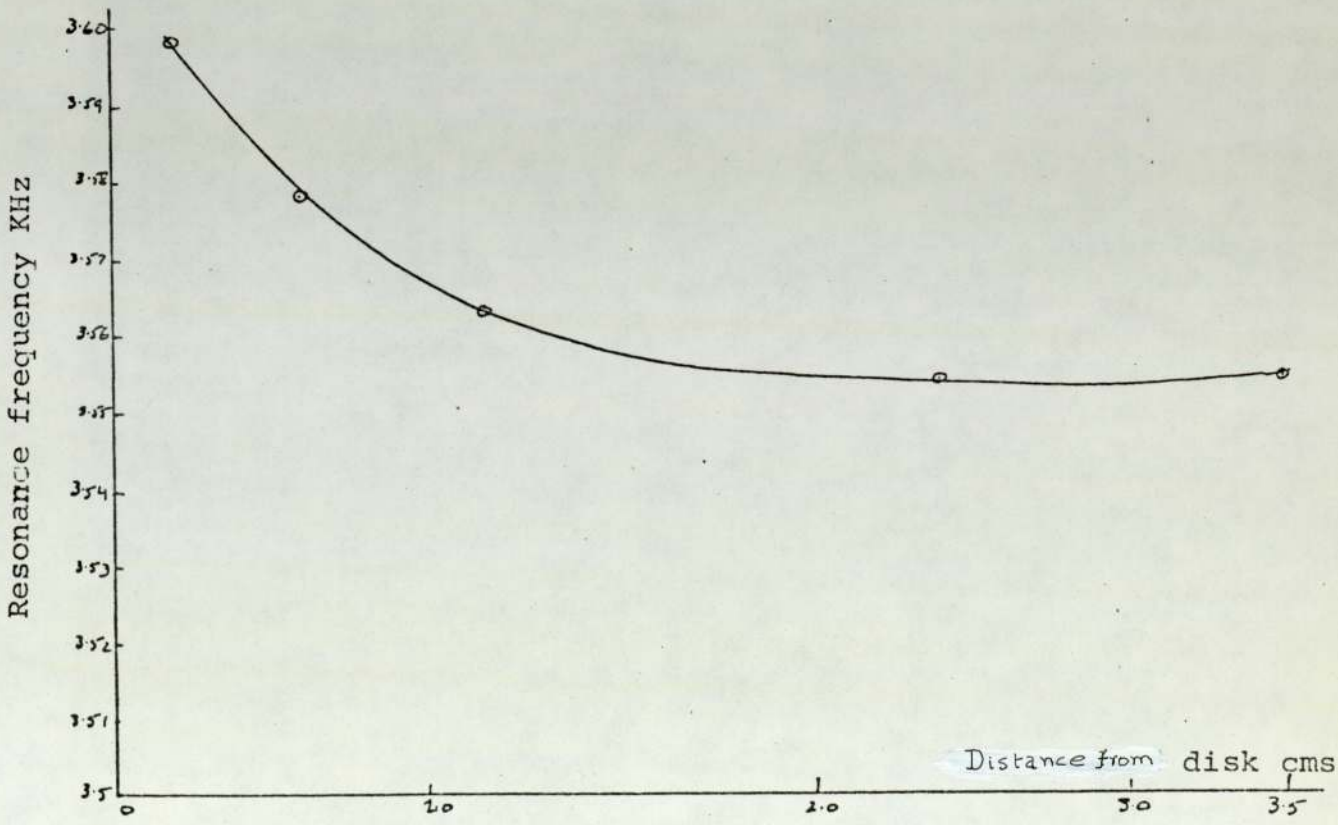

FIGURE 3.9.4.
The variation of resonance frequency with the distance of bubble from the free edge disk. (The bubble diameter=0.74 cms)

of the liquid around the bubble. This resonant frequency according to Minnaert[27] is given by:

$$f = \frac{(3\gamma P_o/\rho)^{\frac{1}{2}}}{2\pi R_o}$$

where P_o is the static pressure at which the bubble has the mean radius R_o, ρ is the density of the liquid and γ is the ratio of the specific heats (for air $\gamma = 1.4$). The above expression only holds for frequencies below 20 KHz. The resonant frequency for an air bubble near the surface can be obtained from

$$f = \frac{0.66}{2R_o}$$

Where f is in KHz and R_o is in centimetres. According to David and Thurston[28], bubbles which are excited below their resonant frequency oscillate in phase the incident field, the effective stiffness of the medium is reduced since the pressure variations act mostly on the bubble rather than the liquid. This results in the decrease of the resonance frequency of the coupled transducer-liquid system as shown in Figure 3.9.3. For resonant bubbles the 'Q' of the system decreases sharply. The resonance of the bubble is confirmed by observations through the microscope, at resonance the bubble wall becomes blurred. It is known that the resonant bubbles are much more effective scatterer and absorbers of sound than non-resonant bubbles. In the present case since the mass of the moving liquid associated with even a small resonant bubble, a considerable fraction of the field

energy can be stored in its vibrations. Most of this energy stored is absorbed by the following two processes: (a) heat conduction between gas and surrounding liquid (b) friction due to the viscosity of the surrounding liquid. These losses will be highest for resonant bubbles. From the results the experimental resonant bubble diameter is approximately 1.5 mm compared with the theoretical value of 1.8 mm.

For bubble sizes above resonance the bubble vibrations are out of phase with the incident field, effectively increasing the stiffness of the medium. This will cause the resonant frequency of the transducer to increase (see Figure 3.9.3.). For this state of affairs there is a small change in the 'Q' of the system. According to Mangulis there is no absorption of energy for non-resonant bubbles, only the velocity of sound in the medium will change.

The above results were confirmed for the oyster shell and the piston type sensor. Since the energy field in the liquid, due to the vibrations of these sensors is not localised, both sensors were susceptible to bubbles which were approximately 15 cm away.

It is clear from the above discussion that for consistency measurement with a vibrating transducer the presence of bubbles in the fluid is a source of error effecting both 'Q' factor and resonant frequency.

The sensors which produce very local energy fields are the most suitable and the free edge disk was therefore adopted for consistency measurements.

CHAPTER 4

VIBRATING BODY - FLUID INTERACTION

4.1. Introduction

When a resonator or a vibrating structure is immersed in a fluid there is a loading effect which changes the dynamics of the structure. In gasses the effect is only significant if the structure is very light or a thin layer of gas is involved such as the case of a condenser microphone.

In the case of real liquids there will always be an inertial loading but there may be an even stronger stiffness effect. Energy will be dissipated by the viscosity of the medium and by acoustic radiation. There are three classifications that may be given to the reaction forces on the resonator due to the liquid loading:

(a) The resonator stores additional kinetic energy in the liquid which has an inertial reaction on the resonator dynamics. This effectively is a net increase in the equivalent mass of the body and results in the lowering of its resonant frequency. In the simplest case of a Newtonian liquid which has viscosity only, the loading is inertia and dissipative. In real liquids a complex rheological model is necessary, the loading will vary with frequency and while there is always an energy loss there could be a stiffness term which exceeds the inertia loading

and results in a net increase in resonant frequency.

(b) The energy is radiated away from the resonator in the form of sound. Because of its great importance in the design of underwater sound generators it has been studied extensively in the literature. In general the radiation of sound decreases as the ratio of resonator size to acoustic wavelength in the fluid decreases.

(c) By virtue of the motion of the structure in the liquid, viscous drag forces are produced on the structure resulting in the dissipation of energy stored.

The magnitude of the three above mentioned effects are dependent on frequency of resonance, the mode of vibration, the geometry and mass of the resonator.

In the design of the consistency transducer the viscous dissipation effect (c) was maximised and the radiation effect (b) was minimised. In the step by step analysis given below the various effects are considered seperately as if the others were absent. Thus in analysing acoustic radiation the viscosity is neglected. The net performance is taken as the sum of the seperate effects. This simplifies the analysis of the fluid-loading of resonator considerably and it is easier to determine the condition under which the interaction effects reduce to those of the hydrodynamical nature, which forms the basis of consistency measurement. At a later stage the viscous damping will be discussed.

4.2. Brief Discussion of the Theory of Radiation

In the transducer radiation effects can cause errors due to standing waves in the fluid and to anomalies due to the presence of bubbles some distance from the transducer. Radiation also represents an unnecessary loss of energy from the transducer. The study was directed towards minimising acoustic radiation.

The sound radiation from simple vibrators have been analysed in the literature. Solutions have only been derived for a number of simple resonators such as spheres and ellipsoids and for square and circular membranes. To determine the acoustic radiation or fluid circulation due to vibrations, the viscosity is neglected. When it is required to determine the energy loss due to the fluid circulation it is assumed that the circulation is not affected by the viscosity. This will be valid for all but the very thickest of liquids.

In the literature the concept of the acoustic (or mechanical) impedence is used to describe the fluid-resonator interaction. The acoustic impedence (Z) is defined as the ratio of the total pressure at the surface of the resonator to the velocity of the resonator. The impedence will have a real (R) and imaginary(X) terms corresponding to the in phase and quadrature components of pressure and velocity. Therefore

$$Z = R + jX$$

With the parallel of the impedence of a transmitter in the theory of electromagnetic radiation, R represents the Ohmic part and X the reactive part of the impedence. The real component represents a pressure in phase with the velocity and is the energy radiated. The reactive term measures the amount of energy fluctuating between the resonator and the medium, it is non-dissipative. In general for a radiator the reactive term is always inductive (ie mass like) in nature whereas an antenna can be inductive or conductive depending on the length.

Figure 4.2.1. shows the acoustic impedence for various shapes of vibrators. The characteristics shown can be divided in two ranges, the high frequency and the low frequency limits. At short wavelengths, meaning $\frac{2\pi}{\lambda}a>2$, when the wavelength in the medium is smaller than the curvature of the radiating surface, then whatever the geometry of the resonator the acoustic impedence approximates to a plane acoustic wave which is purely resistive and equal ρC (characteristic impedence of medium). This range becomes important in the design of efficient sound generators.

In the low frequency limit, meaning $\frac{2\pi}{\lambda}a<1$, the radiation impedence tends to purely reactive and there is very little radiation of sound. Therefore low frequency resonators are of interest for consistency transducers because $\frac{2\pi a}{\lambda}$ falls with frequency.

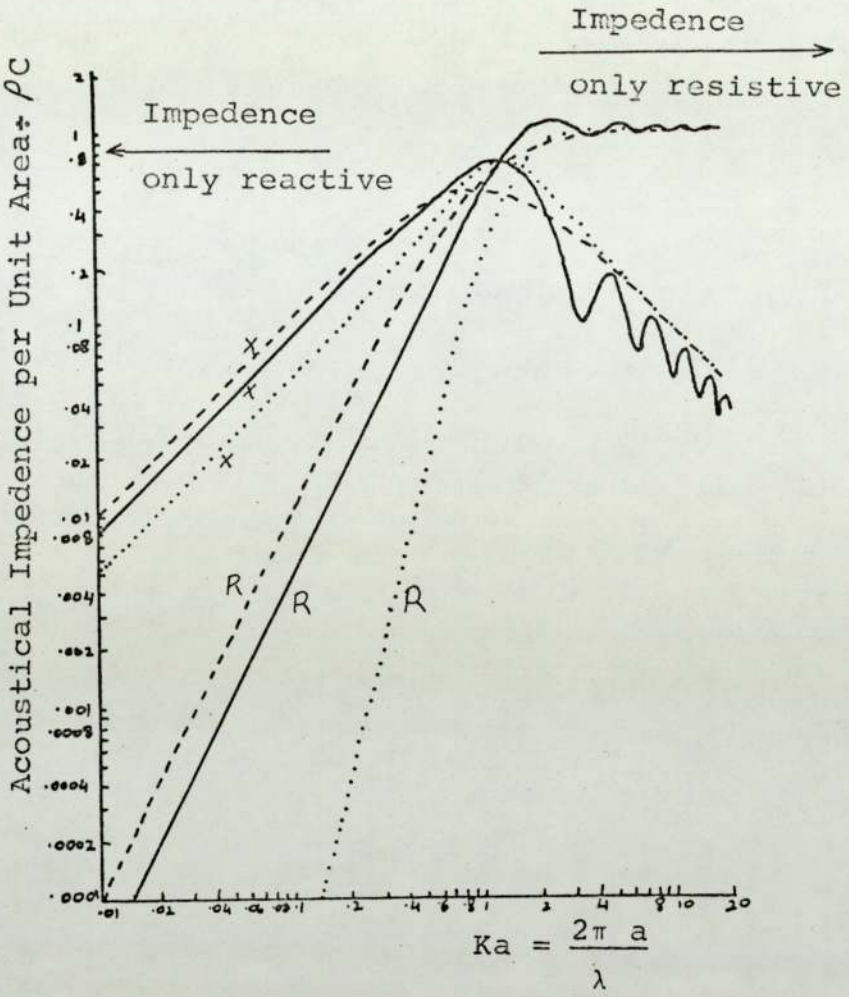

FIGURE 4.2.1.

The acoustical impedence (Z = R + jX) load per unit area divided by ρc as a function of Ka.

———— A vibrating piston of radius a set in an infinite ba ffle.

- - - - - - - - A pulsating sphere of radius a.

..... An oscillating sphere of radius a (See Section 5.1.0 Olson).

(Reproduced from Olson)[31]

4.3. Mass Loading of Sensors

As already stated the component of pressure which is in phase with the fluid velocity represents energy loss, the perpendicular component (reactive) represents energy stored. The kinetic energy of the medium contributes to this component and in most fluids it predominates. In thick liquids the stiffness effect can be the greater, as in the case of certain consistancies of sludge. This gives rise to the paradox that the resonator can have a higher frequency in sludge than in air. However, any stiffness loading of the sensors is neglected in the present analysis.

In the long wavelength limit the mass loading is computed from the hydrodynamic solution of the interaction problem which assumes that the liquid is incompressible and obeys the Laplace rather than the wave equation. This method is used particularly in the case of the free-edge disk.

4.3.1. Rigid Circular Disk

This case is taken first since it is reported most extensively in the literature. Data for a piston vibrating in free space was originally obtained by Wiener[33] who presented a numerical solution for the acoustical impedence. These theoretical results have been reproduced by Olson[31] where their use in the present development will subsequently be discussed. The resistive

and reactive acoustic impedence components of the load on one side of a piston vibrating in free space is shown in Figure 4.3.1.

The acoustic reactance load on one surface of the piston is given by

$$X_m = \text{Area of Piston.} \rho C.G. \qquad (4.3.1.)$$

The term G is a function of Ka, the value of which is obtained from Figure 4.3.1. The reactive curve can be approximated by a straight line such that

$$G = \frac{Ka}{1.9} \quad \text{for } Ka<2$$

Substituting this value of G in equation 4.3.1. and multiplying by 2 since the medium is present on both sides of the piston.

$$X_m = 2\pi a^2 \rho C \frac{Ka}{1.9} \qquad (4.3.2.)$$

The effective added mass due to the reaction of the medium on the vibrating plate is

$$M_m = 3.3 \rho a^3 \qquad (4.3.3.)$$

The next step in the discussion is to test equation (4.3.3.) experimentally. The system used to obtain experimental results is a longitudinally resonant brass rod, to one side of which is attached a disk of known radius and mass as shown in Figure 4.3.2.

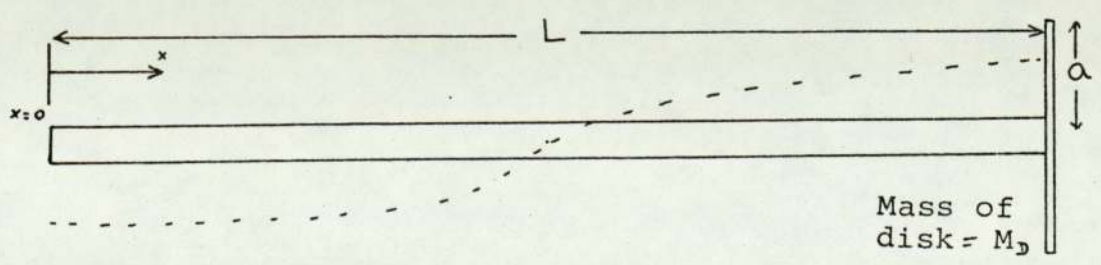

FIGURE 4.3.2.

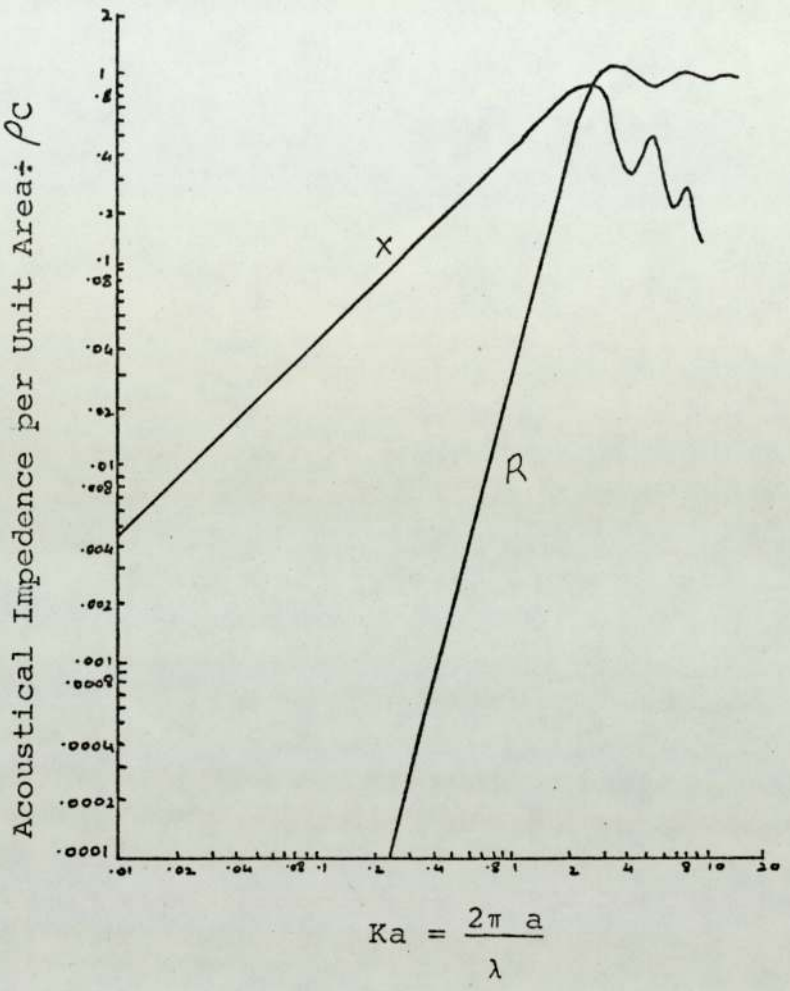

FIGURE 4.3.1.

The acoustical reactance, X and the acoustical resistance R load per unit area divided by ρC as a function of Ka for a vibrating piston of radius a in free space. By using low Ka values reactive loading is made predominant.

(Reproduced from Olson)[31]

[Frequency of vibration of piston ≒ 10 kHz. Typically a = 2 cms. therefore Ka ≒ .08.]

If the resonance frequency of the bar is much smaller than any resonance of the disk, then the system can be treated as free-free bar with a lumped mass M_D attached to its end. The wave equation for the bar is

$$\frac{\partial^2 \xi}{\partial t^2} = C_L^2 \quad \frac{\partial^2 \xi}{\partial x^2} \qquad (4.3.4.)$$

The solution of this equation is given by

$$\xi = \phi(t) \cdot \gamma(x) \qquad (4.3.5.)$$

Now $$\gamma = A \cos K_L x + B \sin K_L x$$

Where $K_L = \omega / C_L$

$$\frac{\partial \gamma}{\partial x} = -AK_L \sin K_L x + B K_L \cos K_L x \qquad (4.3.6.)$$

At the free end (x=0) for an antinode the strain $\frac{\partial \xi}{\partial x} = 0$. Substituting this boundary condition in equation (4.3.6.) implies that B = 0, therefore

$$\gamma = A \cos K_L x$$

Substituting this in equation (4.3.5.)

$$\xi = \phi(t) \; A \cos K_L x$$

$$\frac{\partial^2 \xi}{\partial t^2} = - \omega^2 \phi(t) \; A \cos K_L x$$

$$\frac{\partial \xi}{\partial x} = - \phi(t) \; A K_L \sin K_L x$$

At all points in the bar the stress forces must be balanced by the inertia forces. Therefore at the mass loaded end of the bar (at x = L)

$$EA \cdot \frac{\partial \xi}{\partial x} + M_D \frac{\partial^2 \xi}{\partial t^2} = 0 \qquad (4.3.7.)$$

Where E and A_o is Youngs Modulus and area of the bar respectively.

Substituting for $\frac{\partial \xi}{\partial x}$ and $\frac{\partial^2 \xi}{\partial t^2}$ from the above into equation (4.3.7.)

$$\frac{EA_o}{M_D} \not{p}(t) \not{A} K_L \text{Sin } K_L L + \omega^2 \not{p}(t) \not{A} \text{Cos } K_L L = 0 \quad \text{- - - -} \quad (4.3.8.)$$

Let $\sigma = \frac{M_D}{\rho_s A L}$ (where ρ_s = density of bar material) then equation (4.3.8.) can be shown to be

$$-\sigma K_L L = \text{Tan } K_L L \qquad (4.3.9.)$$

This is a transcedental equation the solution to which must be numerically computed. However, it is seen from equation (4.3.9.) that the resonant frequency of bar will be inversly proportional to the small mass attached to the end. This condition will only hold as long as σ is small (see Figure 4.3.2.) such that

$$\pi < K_L L > \frac{5\pi}{6}$$

for the fundamental mode. Under this condition

$$K_L L = \frac{\pi}{1+\sigma} \qquad (4.3.9'.)$$

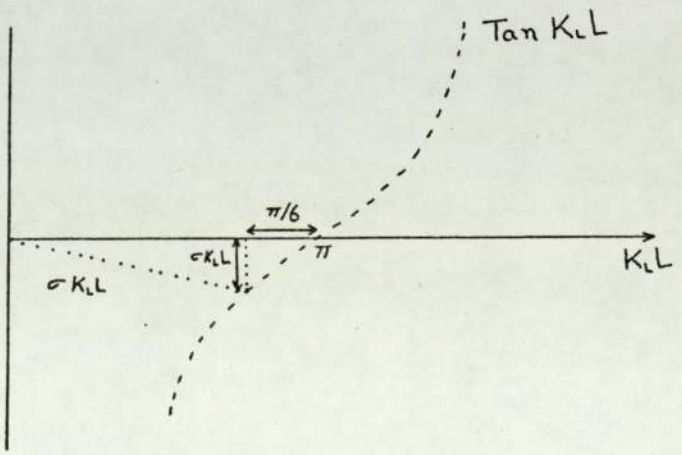

FIGURE 4.3.2.

Such a system has been investigated and the results obtained are shown in Table 3.7.1. Figure 3.7.1. shows the change in the resonance frequency with the mass attached to the end of the bar. This relationship is linear as predicted by equation (4.3.9′.). This graph shows that the decrease in the resonance frequency is 1 Hz per gram of mass attached to the end.

Figure 4.3.3. is a plot of the drop in resonance frequency Δf which occurs when the disk is immersed in water against a^3 where a is the radius of the disk attached to the end. The Δf is due to the extra mass of water M_m (equation (4.3.3.)) that is associated with the vibrations of the disk.

It has been demonstrated that the decrease in the resonance frequency of system studied is 1 Hz per gramme of mass attached to the end, therefore experimental M_m will be directly given by the gradient of curve in Figure 4.3.3. and is

$$M = 3.78\ a^3 \qquad \text{(since } \rho = 1 \text{ gm/cc for water)}$$

The experiment confirms that the added mass is proportional to the third power of the disk radius. The experiment constant is 15% greater than the theoretical value (3.3). The theory is based on a piston vibrating in an 'infinite baffle' driving into a semi-infinite medium. The experiment involves both faces of the disk and no baffle. There will therefore be an extra term arising from the circulation of the fluid from one side to the other. The experiment confirms the a^3 law, thus

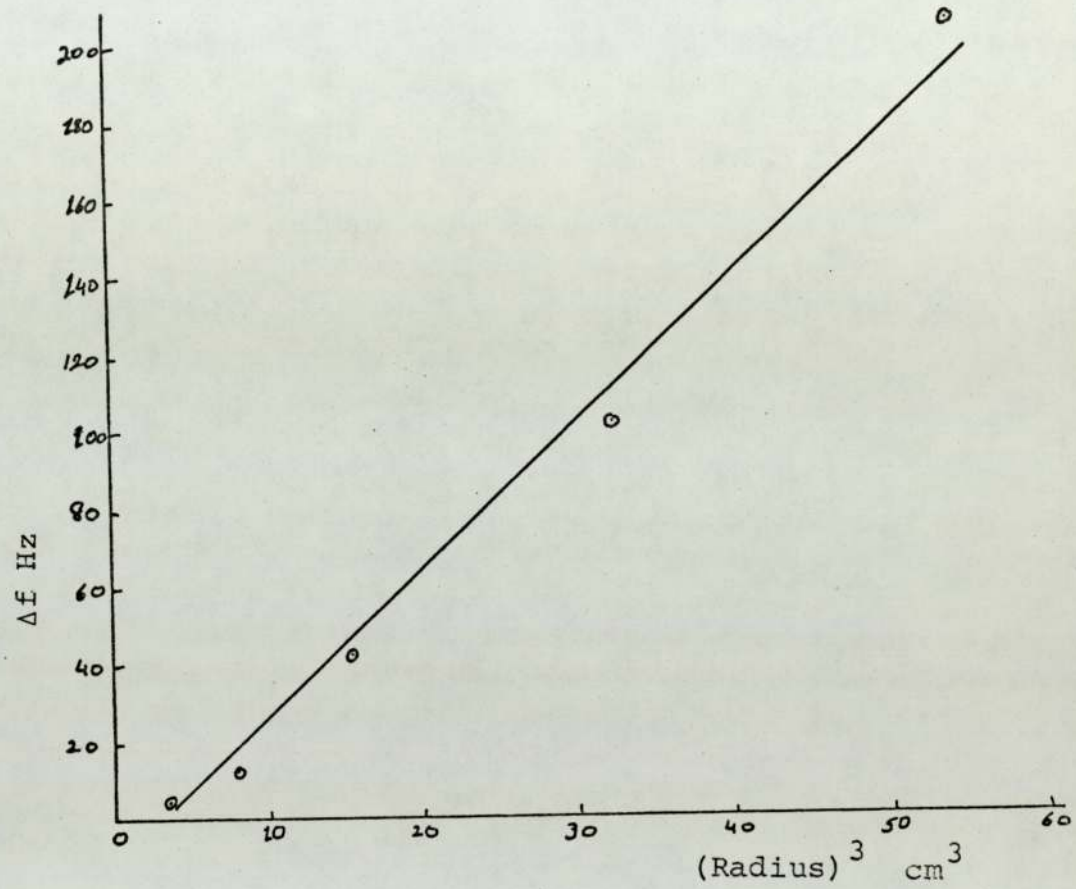

FIGURE 4.3.3

The drop in resonance frequency Δf which occurs when a disk of known radius a is immersed in water. This change in resonance frequency is due to the inertial loading by water.

[See Table 3.7.1. for data]

providing useful design information.

4.3.2. The "Oyster" Shell Configuration

This double disk shown in Figure 3.8.1. differs from the simple disk in that the two faces vibrate in phase ie. both move in and out together. There is therefore a minimum of fluid circulation. The clamping of the two disks round the circumference constitute dynamic clamping and allow the existing extensive analysis of the clamped plate to be used. This was originally studied by Lamb.[34] He considered an elastic circular plate, clamped at the circumference with water on one side, vibrating in its fundamental symmetrical mode. The dynamic deflection curve assumed for the plate was of the form

$$w(\gamma) = A' \left(1 - \frac{\gamma^2}{a^2}\right)^2$$

where w = normal diaphram

γ = distance from centre

a = radius

A' = function of time only [i.e. $\sin\omega t$]

The kinetic energy and potential energy, in vacuo, of the plate was calculated as suggested by Rayleigh.[35] Lamb then proceeded to work out the velocity potential Φ, at the surface of the disk from which he calculated the kinetic energy of the water by the use of the equation

$$T = \tfrac{1}{2} \rho \iint \Phi \frac{\partial \Phi}{\partial n} \, ds \qquad (4.3.10.)$$

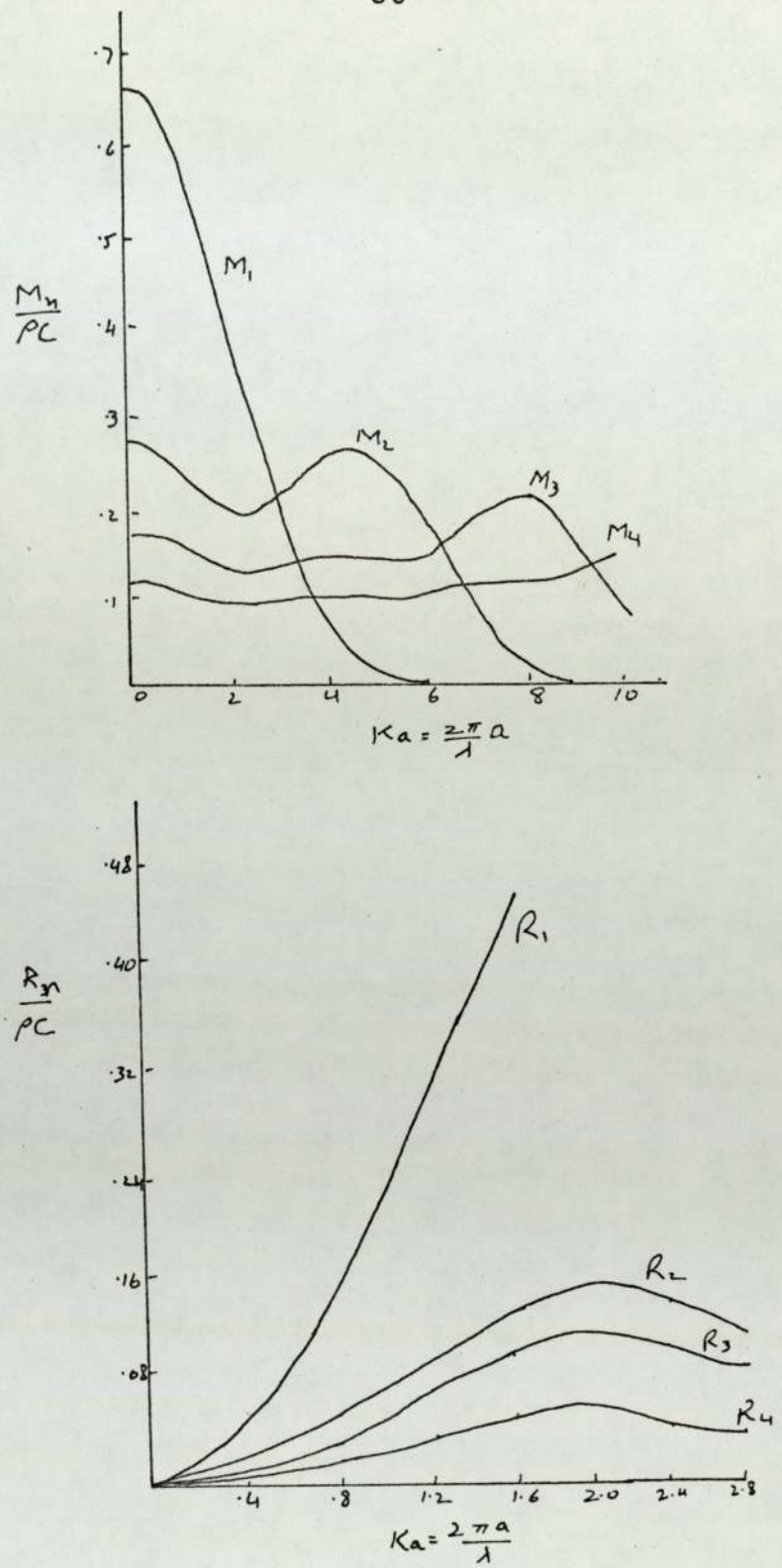

Figure 4.3.4.

The acoustic resistance R_n and mass M_n per unit area divided by ρC as a function of Ka for a clamped circular plate with the fluid loading on one side only. Data for the first four symmetrical flexural modes is given. The fundamental mode gives maxium resistance and reactance (at low frequency) loading.

(Reproduced from Lax[36])

$\frac{\partial \Phi}{\partial n}$ = normal velocity of surface.

ds = elemental area.

By equating the maximum kinetic to maximum strain energy the new resonance frequency of the plate was found. This method of analysis is used to calculate the inertia loading of a free-edge disk in Section 4.4.

A more rigorous analysis than Lamb for a circular clamped plate with fluid loading on one side has been carried out by Lax.[36] Important information about resonators that exhibit nodal line patterns is obtained from the paper by Lax. The acoustic impedence evaluated for various symmetrical modes of vibrations as a function of Ka is plotted in Figure 4.3.4. It is seen that the magnitude of the impedence decreases considerably for higher order modes compared to that for the fundamental. This is due to the regions of positive and negative amplitude partially compensating one another since some local pressure equalisation results between these regions.

Figure 4.3.5. shows the effect of the mass loading on the resonance frequency of the disk as a function of $\beta = \frac{\rho}{\rho_b} \frac{a}{h}$ where $\frac{\rho}{\rho_b}$ is the relative density of fluid to disk and $\frac{a}{h}$ is the ratio of radius to thickness of disk. One important assumption made by Lax is that of the disk being clamped in an infinite baffle. The vibrations of the two plates which constitute the oyster shell are such that each plate may be assumed to be in contact with liquid in infinite half space as shown in

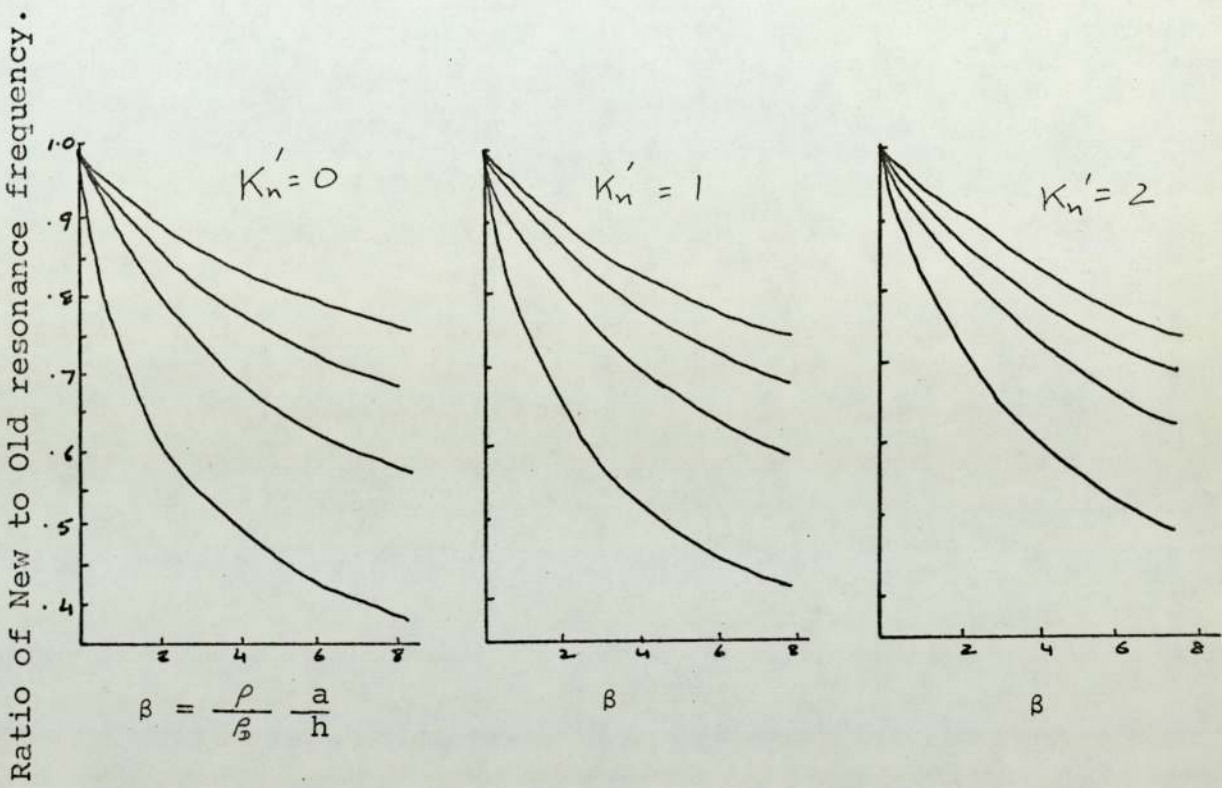

FIGURE 4.3.5.

Ratio of resonance frequency of liquid loaded and unloaded plate against $\beta = \frac{\rho}{\rho_s} \frac{a}{h}$

Figure 3.8.3., with an effective baffle in the plane of the shell. The air enclosed between the gap in the two disks had a neglegible effect on the vibrations of the oyster shell. The plates are made of steel with radius (a) and thickness (h) of 35 mms. and 2 mms. respectively. Therefore β as defined above has a value of 2.2. For low frequency as is the case here, the factor $K\acute{n} = \frac{2\pi a}{\lambda_a}$ where λ_a is the wavelength of sound in the water, may be assumed to be zero (although the value of $K\acute{n}$ obtained from experimental results is 0.3) From Figure 4.3.5. the ratio of frequency in air is 0.65 whereas from the experimental results this ratio is found to be 0.69. This small discrepancy can be firstly, due to the fact that $K\acute{n}$ is taken to be zero instead of 0.3 which will make the expected ratio higher than 0.65 and secondly, that there may be a small shift in the resonance frequency of the oyster shell due to the coupling between the transmission line and the shell (see page 36).

The good agreement between experiment and theory is considered to establish the assumption that the oyster shell resonator behaves as a double clamped plate.

4.3.3. The Inertia Loading of a Free Edge Disk

Various assumptions have to be made which will enable the determination of the resonant frequency of a liquid loaded free-edge circular disk. The procedure will

follow that outlined by Lamb[34] in his treatment of the loaded clamped edge disk. Basically this method involves the calculation of potential and kinetic energy of the disk unloaded, assuming that the dynamic deflection curve for the mode considered is known. The next step is to find the velocity potential, Φ, at the surface of the disk from which it is possible to determine the kinetic energy of the liquid by the use of the equation (4.3.10). This kinetic energy is added to the kinetic energy of the disk. The frequency can then be found by equating the new kinetic energy to the potential energy (strain energy) of the disk.

The assumptions made in this procedure are

(a) the liquid is incompressible i.e. there is no acoustic radiation, only under this condition it is possible to find the kinetic energy of liquid by using equation (4.3.10.). This means that there is no circulatory motion of the liquid particles in the flow field due to the resonator. For flow which is irrotational so that Φ is single valued, equation (4.3.10) is valid.

(b) The viscosity of the liquid does not affect the flow field.

(c) The plate vibrates in an infinite baffle.

The last assumption introduces a serious error in the calculation of the kinetic energy of liquid. It means that there is no flow of liquid around the periphery of the disk as shown in Figure 2.2.1. so that the fluid

particle velocity is normal to the surface of the plate at any instant. The shaded area in Figure 4.3.6. shows the assumed nature of the liquid pressure distribution over the surface of the disk.

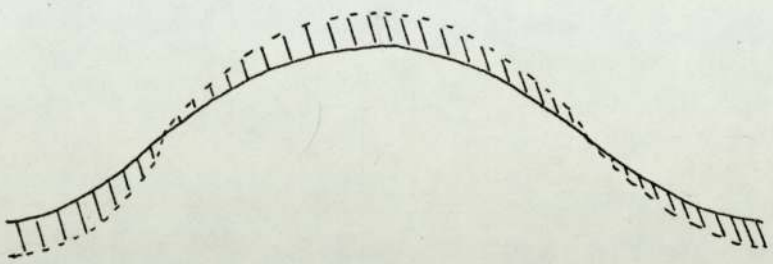

FIGURE 4.3.6.

The omission of any of the above assumptions will make the problem impossible to solve.

The dynamic deflection curve for a free edge disk is given by

$$w(\gamma) = I_o(\lambda_n \gamma) + A_1 J_o(\lambda_n \gamma) \qquad (4.3.11.)$$

where $A_1 = -\dfrac{I_1(\lambda_n a)}{J_1(\lambda_n a)}$

and λ_n is a constant which depends on the mode of vibration of disk, in the case of one nodal circle

$\lambda_n = \dfrac{3.01}{a}$ where a is the radius of the disk.

Equation (4.3.11.) can be written in the series form, writing $Z = \lambda_n \gamma$.

$$w(\gamma) = \left[1 + \tfrac{1}{4}(Z)^2 + \frac{(\frac{1}{2}Z)^4}{2^2} + \frac{(\frac{1}{2}Z)^6}{3}\right] + A_1\left[1 - \frac{Z^2}{2^2} + \frac{Z^4}{4.4^2} + \cdots\right]$$

Since for the fundamental mode $A_1 = -11.77$, the dynamic deflection for the plate can be written as

$$w(\gamma) = A'\left(1 + a_1\frac{\gamma^2}{a^2} + a_2\frac{\gamma^4}{a^4}\right) \qquad \text{Where } a_1 = -3, \tag{43.12}$$

$a_2 = 1.3$ and $A' = A_o \sin \omega t$

In symmetrical bending the potential energy of the disk is given by Timoshenko[37] to be

$$V_p = \pi D \int_0^a \left[\left(\frac{\partial^2 w}{\partial \gamma^2} + \frac{1}{\gamma}\frac{\partial w}{\partial \gamma}\right)^2 - 2(1-\mu)\frac{\partial^2 w}{\partial \gamma^2}\cdot\frac{1}{\gamma}\frac{\partial w}{\partial \gamma}\right] \gamma d\gamma \tag{4.3.13.}$$

where $D = \dfrac{Eh^3}{12(1-\mu^2)}$

μ = Poissons ratio

E = Youngs Modulus

h = Plate thickness

Substituting for $w(\gamma)$ from equation 4.3.12. into equation 4.3.13.

$$V_p = \frac{\pi D}{a^2}(A')^2 \times 11.0 \tag{4.3.14.}$$

The kinetic energy of the disk is

$$T_p = \pi \rho_p h \int_0^a \left(\frac{\partial w}{\partial t}\right)^2 \gamma d\gamma$$

$$= \pi \rho_p \frac{h}{2}(\dot{A}')^2 \rho_p a^2 \times 0.28 \tag{4.3.15.}$$

where ρ_p = density of disk material

The kinetic energy of a liquid in contact with surface vibrating with the shape given by equation (4.3.12.) has been calculated by Rayleigh[35] (Appendix A). Quoting directly the kinetic energy of the liquid on both sides of the plate is

$$Tw = \frac{8}{3}\rho(\dot{A}')^2 a^3 K \tag{4.3.16.}$$

where $K = \left[1 + \frac{14}{15}a_1 + \frac{5}{21}a_1^2 + \frac{314}{525}a_2 + \frac{214}{675}a_1 a_2 + \frac{89}{825}a_2^2\right]$

Equating the maximum kinetic to the maximum strain energy of the system frequency of the resonance is given by

$$f = \frac{1}{2\pi} C \frac{h}{a^2} \left[1.08\left(0.14 + \frac{8}{3\pi}\frac{\rho}{\rho_p}\frac{a}{h}K\right)\right]^{-\frac{1}{2}} \qquad (4.3.17)$$

where C = plate velocity of sound in material

$$= \left[\frac{E}{\rho_p(1-\mu^2)}\right]^{\frac{1}{2}}$$

Table 4.3.1. shows the results for various dimensions of the disk submerged in water. The theoretical resonant frequencies are obtained from equation(4.3.17). It is seen that on the average the expected resonant frequency is 16% lower than that obtained experimentally. The major part of this error is due to the calculation of the kinetic energy of water and in particular the determination of the velocity potential required to derive equation (4.3.16). The calculation does not consider the actual flow of liquid around the disk shown in Figure 2.2.1. but assumes a much simpler form of pressure presented to the disk (see figure 4.3.6.).

It has also been assumed that the dynamic deflection of the plate is unaltered by its immersion in a liquid. This is reasonable if the loaded Q is still high.

Disk Material	Radius in mms.	Thickness in mms.	Resonant frequency(air) kHz	f_r EXP. in water kHz.	f_r THEO. in water kHz.	$\frac{f_r \text{ EXP.} - f_r \text{ THEO.}}{f_r \text{ EXP.}} \times 100$
STEEL	40	3.0	4.1	3.25	2.8	14%
STEEL	35	1.0	2.16	1.29	0.900	14%
STEEL	30	1.0	2.39	1.66	1.36	18%
STEEL	38	3.2	4.8	3.78	3.19	15%
STEEL	35	1.5	3.03	1.93	1.53	22%
ALUMINIUM	38	3.2	4.76	3.05	2.4	21%

TABLE 4.3.1.

4.4. Oscillations of the Resonator in a Viscous Liquid[38-40]

So far in this chapter the effects of viscosity have been ignored in the discussion. The force recquired to accelerate a body through a fluid depends on the geometry of the body and the sorrounding boundaries, the nature of the motion and the physical properties of the fluid among which viscosity must be included. It has been pointed out that the presence of viscosity will make the mathemtics of the resonator-liquid system discussed above, unrealisable.

However, certain problems involving solid body oscillations and viscosity have been studied in the past. These include small oscillations performed by a plate in its own plane, spheres and cylinders undergoing torsional and translational oscillations. The viscous damping of rigid circular disk vibrating torsionally under the influence of elastic force or couple has also been analysed. Practical system of this kind are usefullin the measurement of viscosity of gases and liquids e.g. by the oscillating disk method (see Kestin and Pilarczyk[41]). The viscous damping of torsionally resonant rods is discussed in Chapter 7.

An exact analytical description of liquid resistance to the acceleration of a submerged solid is known for simple cases such as a sphere in rectilinear motion only. The viscous damping of flexurally resonant disk and the piston type motion of the disk is difficult to analyse. Therefore the damping of this type of sensor will be discussed only in conjunction with the experimental

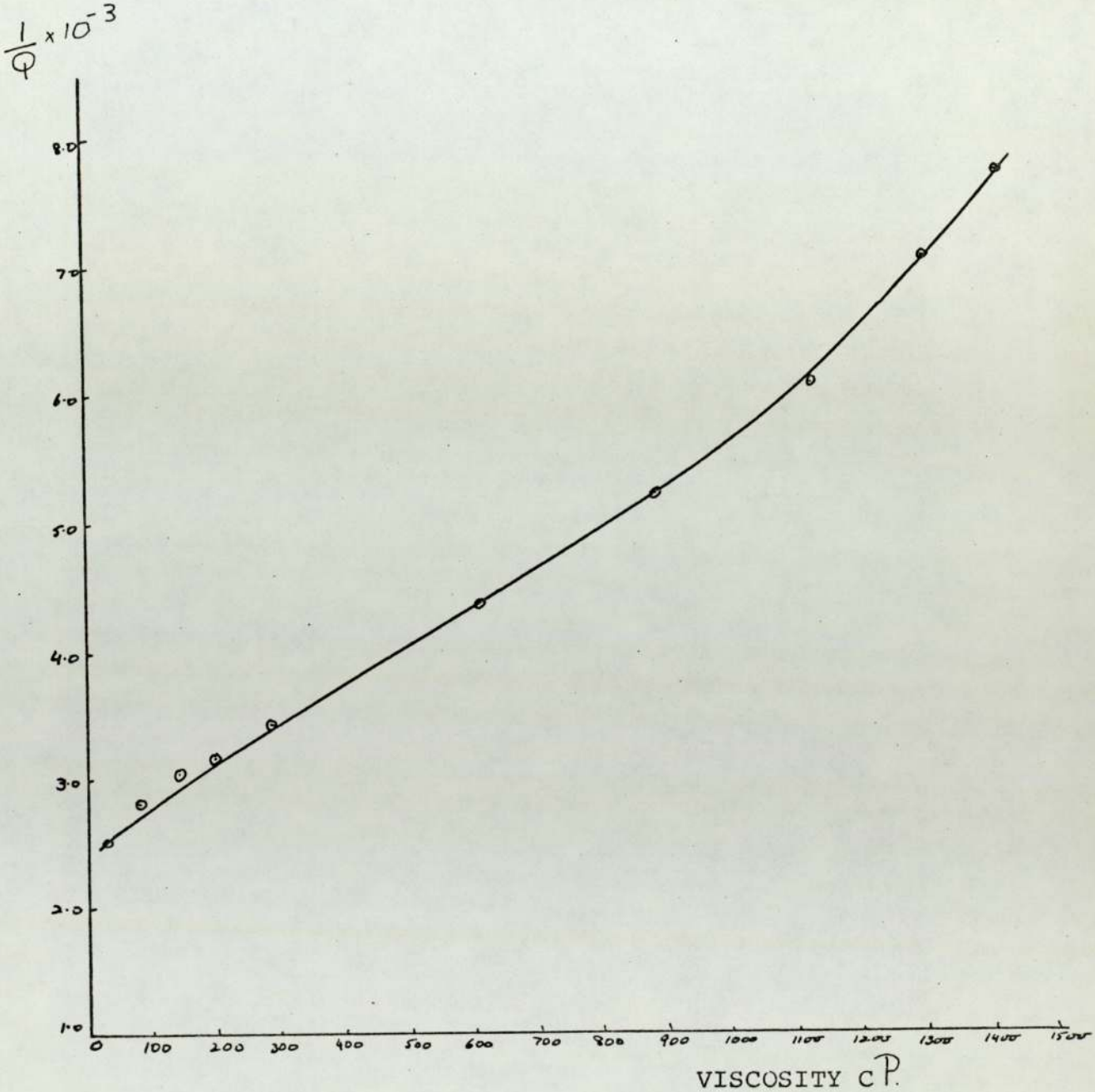

FIGURE 4.4.1.

The damping of the solid centre flexurally resonant disk as a function of the viscosity of the surrounding liquid. The disk geometry is shown on page 45. The resonant frequency in glycerol is 1.2 kHz.

results obtained. Basically, the damping of this type of resonator is due to the motion produced in the liquid, (the lines of flow are shown in Figure 2.2.1.).

It was decided to investigate the damping of the solid centre disk shown in Figure3.4.2.(page 45). The liquid chosen for the experiment was non-acquos glycerol since it is relatively easy to change its viscosity by altering the temperature. This method of changing the viscosity is desirable because once the experiment is set up external losses will be constant and the "Q" of the resonator will only change with the viscosity of glycerol.

Figure 4.4.1. shows the variation of losses with the viscosity of glycerol. It is that the losses are directly proportional to the viscosity. Throghout the experiment any changes in the density of glycerol with tempertaure were negligible, consequently the drive frequency of the transmitter was unaltered.

The damping of the flexurally resonant disk and the rigid disk motion showed similar results as above.

CHAPTER 5

ON-LINE PRIMARY SLUDGE CONSISTENCY MEASUREMENTS

5.1. Introduction

The transducer performance having been identified within fairly close limits, extended 'in situ' experiments were carried out to obtain user style results and to evaluate the effectiveness of the transducer. For on line measurements the industrial site chosen was the Minworth sewage works. In this chapter the experimental results obtained and various environmental difficulties encountered are discussed. Also, a concise description of the works at Minworth is given, with emphasis on the geometry of the primary settling tanks and the sludge withdrawl system, this being the main concern for the application of the transducer developed.

5.2. Treatment of Sewage

Figure 5.2.1. shows the sequence of treatment required in a sewage works. The first stage in the treatment is the removal of rags, grit and large solids. The large solids and rags are removed by passing the sewage through screens. The removal of such objects prevents any damage which may be caused to either pumps or pipeworks. The grit removal is included in most works to minimise damage

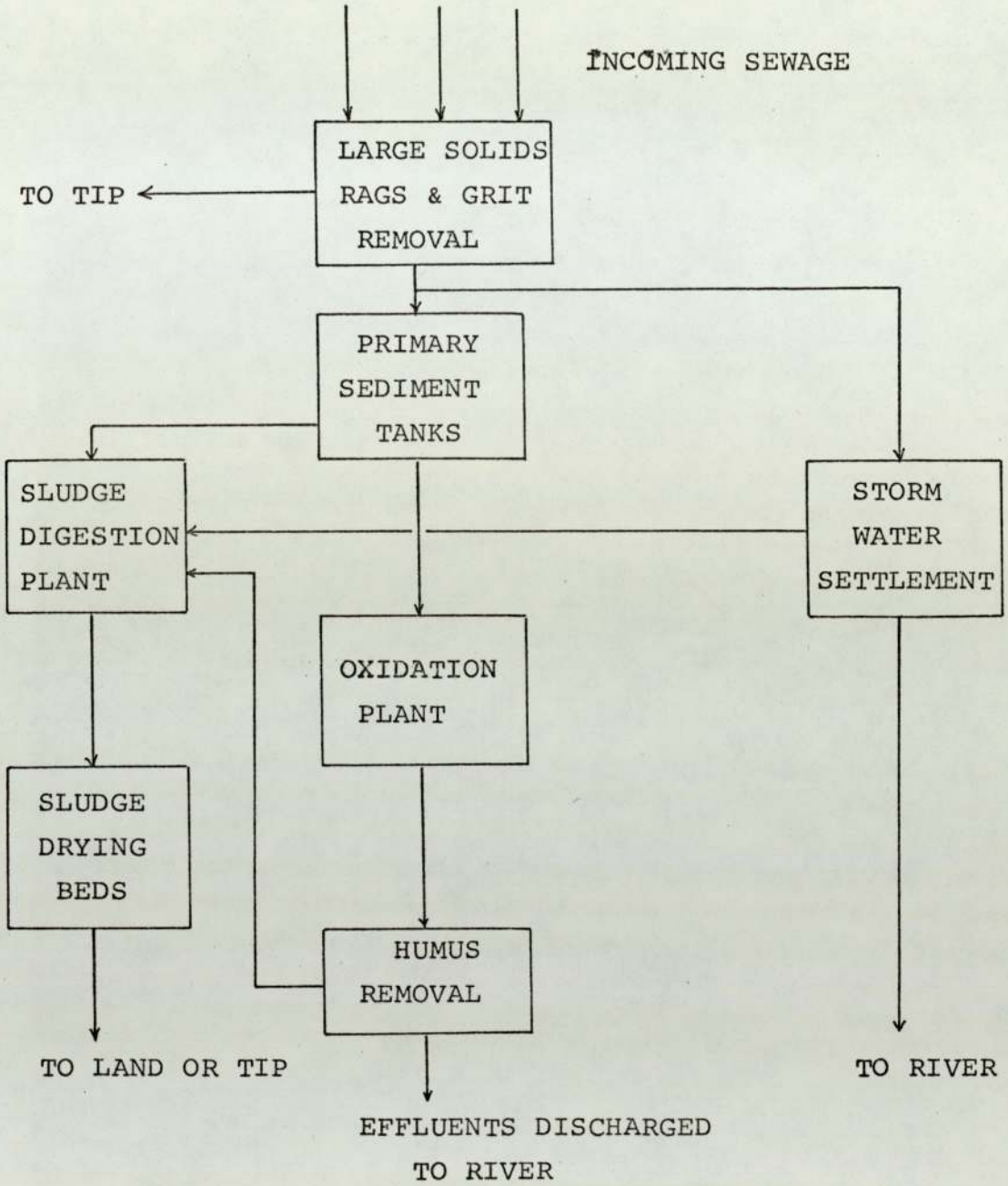

FIGURE 5.2.1.

Diagram showing sequence of treatment required in a Sewage Works.

to machinery as well as to prevent the accumulation of grit in the sedimentation tanks. Grit removal chambers are fairly shallow elongated channels designed to remove particles of S.G. 2.65 and size down to about 0.2 mm diameter. The deposition of grit is achieved by controlling the velocity of flow in the channel.

The sewage is then passed into the sedimentation tanks, the object of which is to maximise the removal of settleable solids known as sludge. The sewage from the grit removal channels is passed into large tanks, in which it is retained for periods of up to two days. In this time all the settleable solids collect at the bottom of the tank and are removed to the sludge digestion plant. The mechanics of sludge removal from the primary settling tanks will be described in detail in the following section, since this is the stage at which the consistency of the sludge withdrawn is monitored.

In the sludge digestion plant the sludge is retained for about a month at a temperature of about 20^{o}-30^{o}C. After digestion the sludge, which is now odourless, is pumped on to drying beds. The dried sludge which accounts for about 65% of the original solid, the rest being converted into gas and water, is removed mechanically and either used as soil conditioner in agriculture or taken to a tip. Alternatively, the digested sludge is dewatered mechanically and the dried sludge is burnt in a suitable incinerator, to reduce further the volume of the residue.

The unsettled impurities from the primary tanks are subjected to biological treatment. This process facilitates the removal of unsettleable solids and organic impurities. The oxygen from the air plays an important part at this stage of the treatment. The oxydation plants are of four different types:

(a) land treatment

(b) bacteria beds

(c) air blowing

(d) mechanical agitation.

Each of these four processes will produce solids which are removed in the humus tanks. The settled solids from the tanks are taken to the sludge digestion plant and the effluent produced at this stage is discharged into the river.

The storm water settling tanks are only used in wet weather when there is a greater amount of diluted sewage to be treated. The construction of these tanks is similar to the primary sedimentation tanks, but the sludge withdrawl from the storm tanks, is not remotely controlled.

5.3. The Primary Settling Tanks and the Sludge Withdrawl System

Sedimentation is one of the most important and widely used processes in the treatment of waste water. It reduces the amount of settleable solids suspended in the

sewage, which is achieved by retaining the waste water, for a period of time, in large settling tanks. The efficiency of the sedimentation tanks, depends on the settling characteristics of the suspended solids, on the geometry of the tank and the flow of effluents through the tanks. At Minworth rectangular tanks are used in which the flow is essentially rectlinear as shown in Figure 5.3.1. Sewage usually enters one end of the tank through a perforated baffle, travels the length of the tank and then exits at the opposite end through some type of effluent weir.

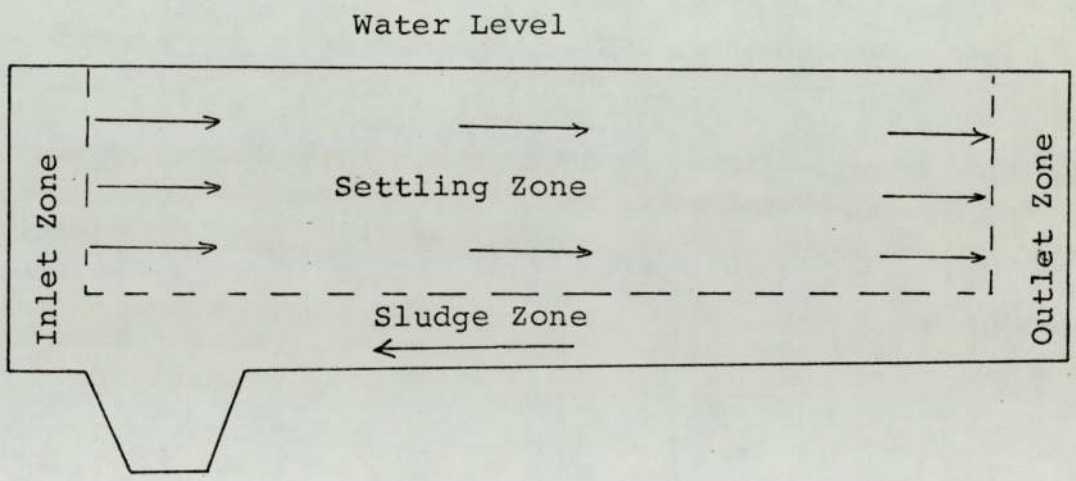

FIGURE 5.3.1.

The other more common tank geometry is circular in plan. Circular horizontal flow tank may be either centre feed with radial flow, peripheral feed with radial flow or peripheral feed with spiral flow. However, this type of tank is of no concern in the present investigation.

At Minworth eight rectangular tanks have been built

each 76.2 m. long, 48.4 m. wide, and 3 m. average depth, with the capacity per tank of 2.5 x 10^6 gallons. Each tank is further divided longitudinally by a ported wall. The bottom of the tank slopes at about 1 in 100 towards the inlet end where sludge hoppers are located. For each half of the rectangular tank at Minworth, three sludge hoppers are provided, each hopper being equipped with a separate draw off piping so that each can be desludged separately (see Figure 5.3.2.). Since the bottom of the tank is sloping towards the sludge hoppers, the sludge moves hydraulically into the hoppers. Sludge scraper mechanisms are used to prevent the sludge from sticking to the bottom and to help its flow. The speed of the sludge scraper mechanism is quite slow so as not to disrupt the settling process or to resuspend the settled solids. Scrapers with two booms per half tank with the traversing velocity maintained below 30 cms. per second are used to remove the sludge and the scum formed at the surface of the water. The total depth of the hopper is about 6 m.

The new sludge collected in the hoppers is removed under hydrostatic head to overflow telescopic valves (or adjustable bellmouth) located in a sludge inspection chamber. There is one inspection chamber per half tank so that three sludge hoppers can be desludged and monitored at one bellmouth. The quality of the sludge withdrawn is visually inspected via closed circuit television installed in the inspection chamber. The end point of

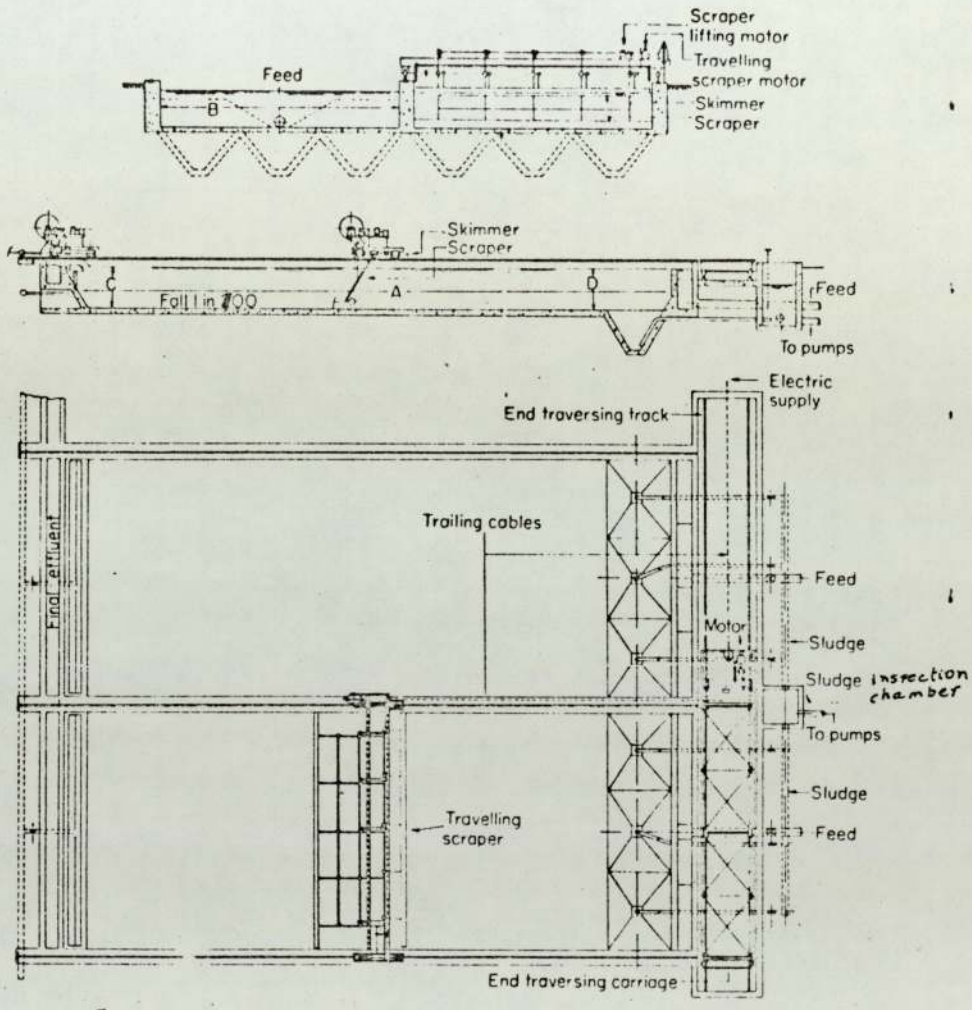

Fig. 53.2.—Rectangular sedimentation tanks with travelling scraper and transporter carriage

By courtesy of Hartleys (Stoke-on-Trent), Ltd.

the desludging process is recognised when water breakthrough occurs. At this instant the appearance of the emerging liquid changes from matt to highly reflecting surface and the appropriate outlet valve of hopper is closed by remote control. Each hopper is desludged separately.

The new sludge collected in the inspection chamber is continuously gravitated to primary sludge digestion plant pumphouse for further treatment as described earlier.

The transducer developed is designed to measure the consistency of the sludge withdrawn through the bellmouth, in an effort to replace the closed crcuit television system and to automate the desludging process.

Plate 5.3.1.(a) and (b)show the settling tanks and the inspection chamber with a transducer, respectively.

5.4 Preparation for Minworth

A number of disks with resonant frequency ranging from 1KHz to 4KHz in the flexural mode having one nodal circle were selected. After laboratory tests on a range of calibrating liquids, primary sludge was used with the most promising disks. Typically a 'Q' factor of about 300 in water was reduced to 90 in stationary sludge. Stirring and mixing the sludge had little effect on the 'Q' indicating that a macromeasurement on the body of the fluid was being made. From the laboratory experiments with sludge it was concluded that while the changes in

(a) The primary sedimentation tank.

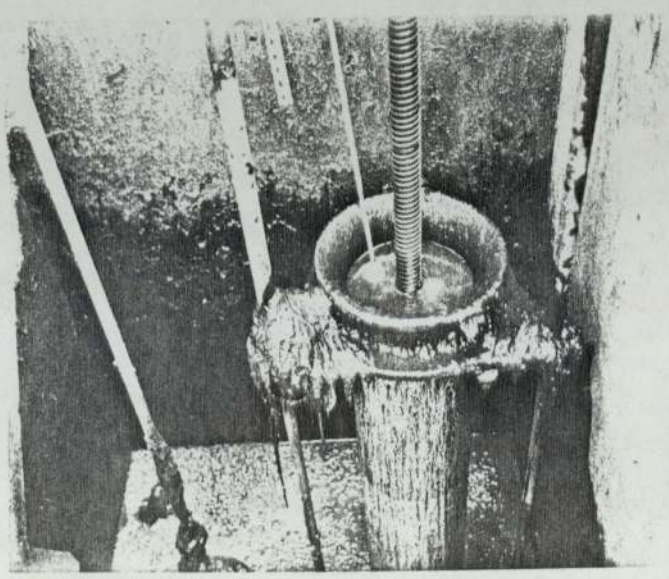

(b) The inspection chamber with a transducer located in the bellmouth

PLATE 5.3.1.

resonant frequency were quite measureable, it was at once apparent that the 'Q' factor is the most significant parameter to measure. It was decided that for each measuring cycle of two seconds duration the natural i.e. decrement period and the 'Q' of the transducer were to be measured digitally and recorded on a dual pen recorder using D to A converters.

The electronic system used for on-line measurements is schematically shown in Figure 5.4.1. For these experiments an open loop system was used in which a long burst of oscillations from the transmitter drives the line. At the end of the burst the energy stored decays in the characteristic exponential law at the natural period of the transducer (Figure 2.4.4.(a)). The period is readily measured by timing ten oscillations of the decrement using a one MHz clock as described on page 145. If the energy used to drive the line is held constant by keeping the burst length, repitition rate and the transmitted voltage fixed then a simple measure of the change in the 'Q' of the system is obtained by measuring the amplitude of oscillations at a fixed point in the decrement. The electronic circuitry required to measure this amplitude digitally is explained on page 148.

An experiment was performed to calibrate the 'Q' of a system with the amplitude of oscillation of the decrement for a disk with the solid centre driven by a robust line (Page 56). The sensor was submerged in the glycerol so that the 'Q' of the transducer could

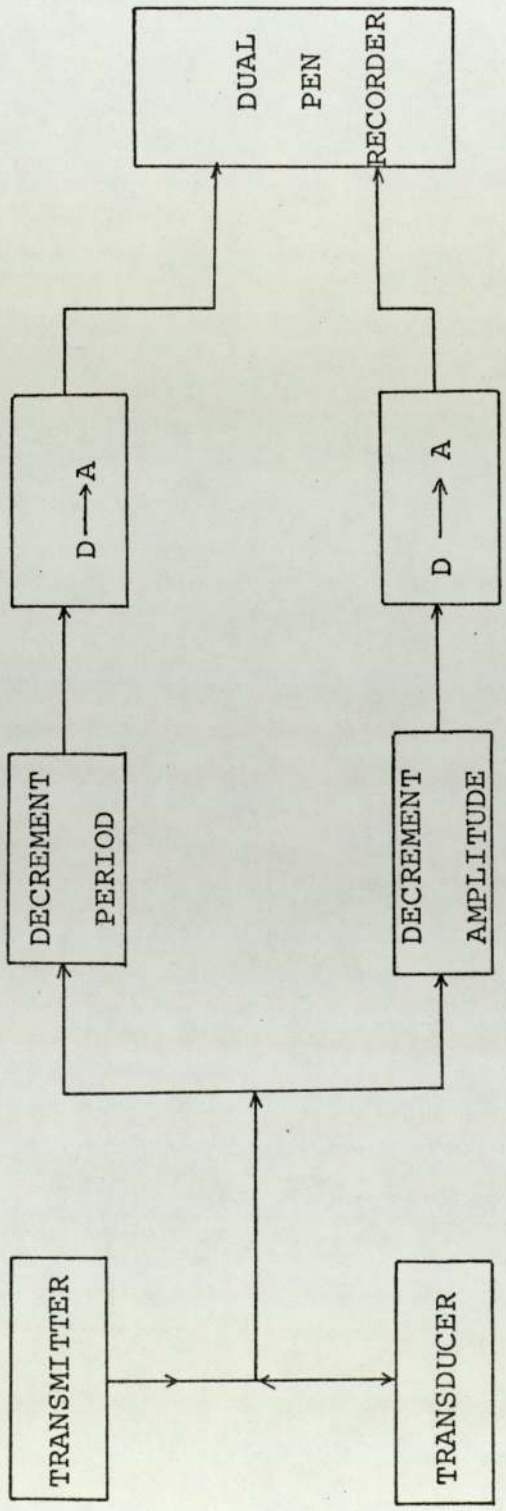

FIGURE 5.4.1.

Block diagram of the system used for on-line sludge consistency measurement at Minworth.

(The decrement amplitude is stored digitally).

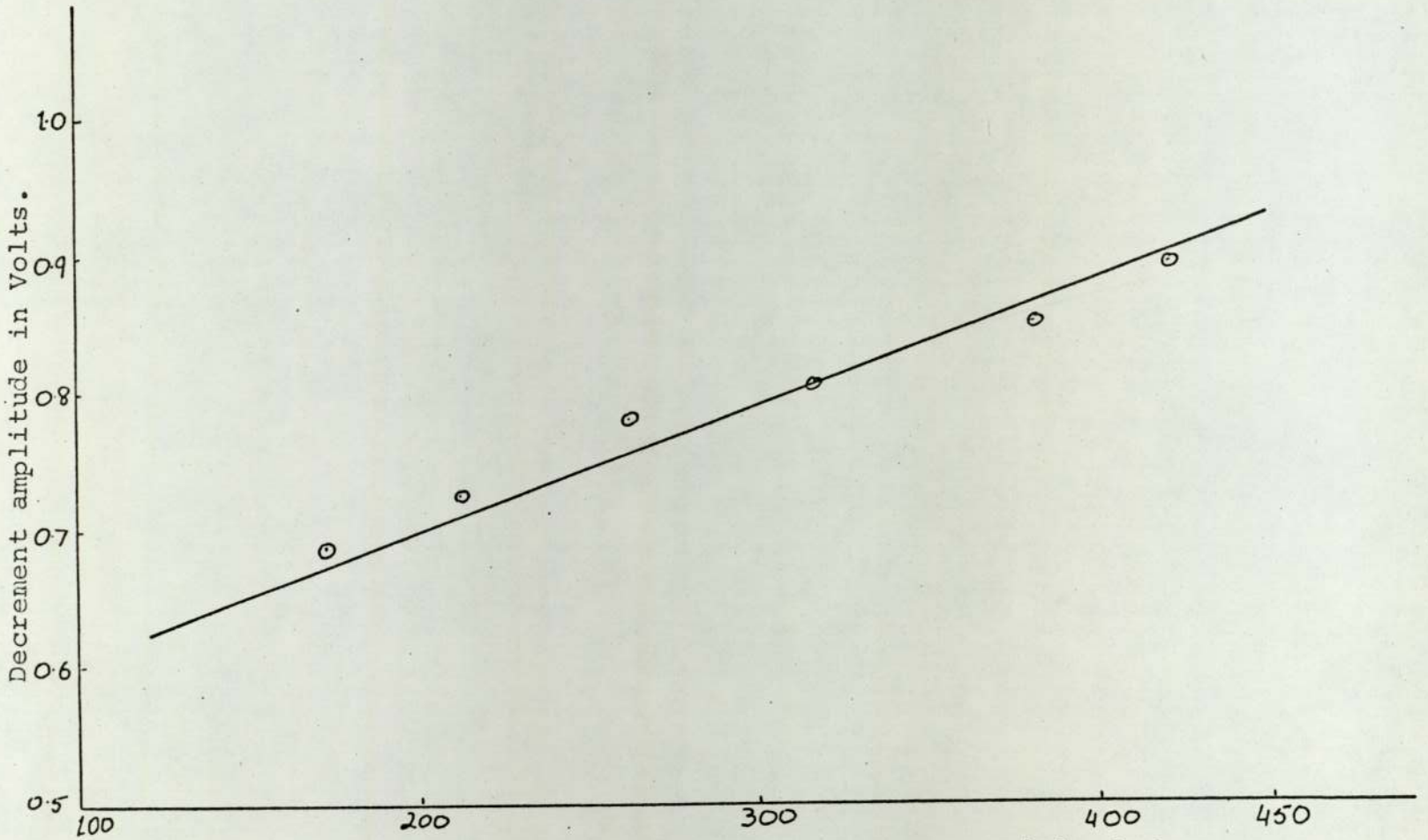

FIGURE 5.4.2.

The decrement amplitude as a function of the 'Q' of the transducer.
This callibration curve is for the solid centre disk with the robust line (page 56).

be changed by varying the temperature of the glycerol. A burst length of 40 pulses, 60 volts peak to peak and a repitition rate of 3 Hz was used to set the transducer into resonance. The 'Q' at resonance was calculated from the envelope of the decrement displayed on the oscilloscope, and it is plotted in Figure 5.4.2., against the positive peak amplitude of the 6th pulse of the decrement. It is seen that the relationship between 'Q' and decrement amplitude is linear. Although the pulse amplitude only changes from 0.9 V to 0.6 V for a corresponding change in 'Q' of 400 to 120, however this resolution would be sufficient to differentiate between water and sludge. In the fully designed system, the 'Q' would be computed from the ratio of two peak amplitudes with the use of equation 2.3.1.

A range of probes were prepared for trials at Minworth. Among these were the probes with uniform thickness disk and solid centre disk, vibrating in the flapping mode, as shown on pages 37 and 45 respectively. Also a probe was prepared in which the sensing end could be fitted with a range of small (non resonant) disks, so that the probe resonates with the disk undergoing a piston type motion. Alternatively the probe may be fitted with a sphere undergoing translational motion as the consistency sensing element. The supports for the line resonator and the mounting for the magnet used to bias the magnetostrictive launcher is shown in Figure 5.4.3. The line is supported through rubber bungs located at two nodal points for a full wavelength resonator. The

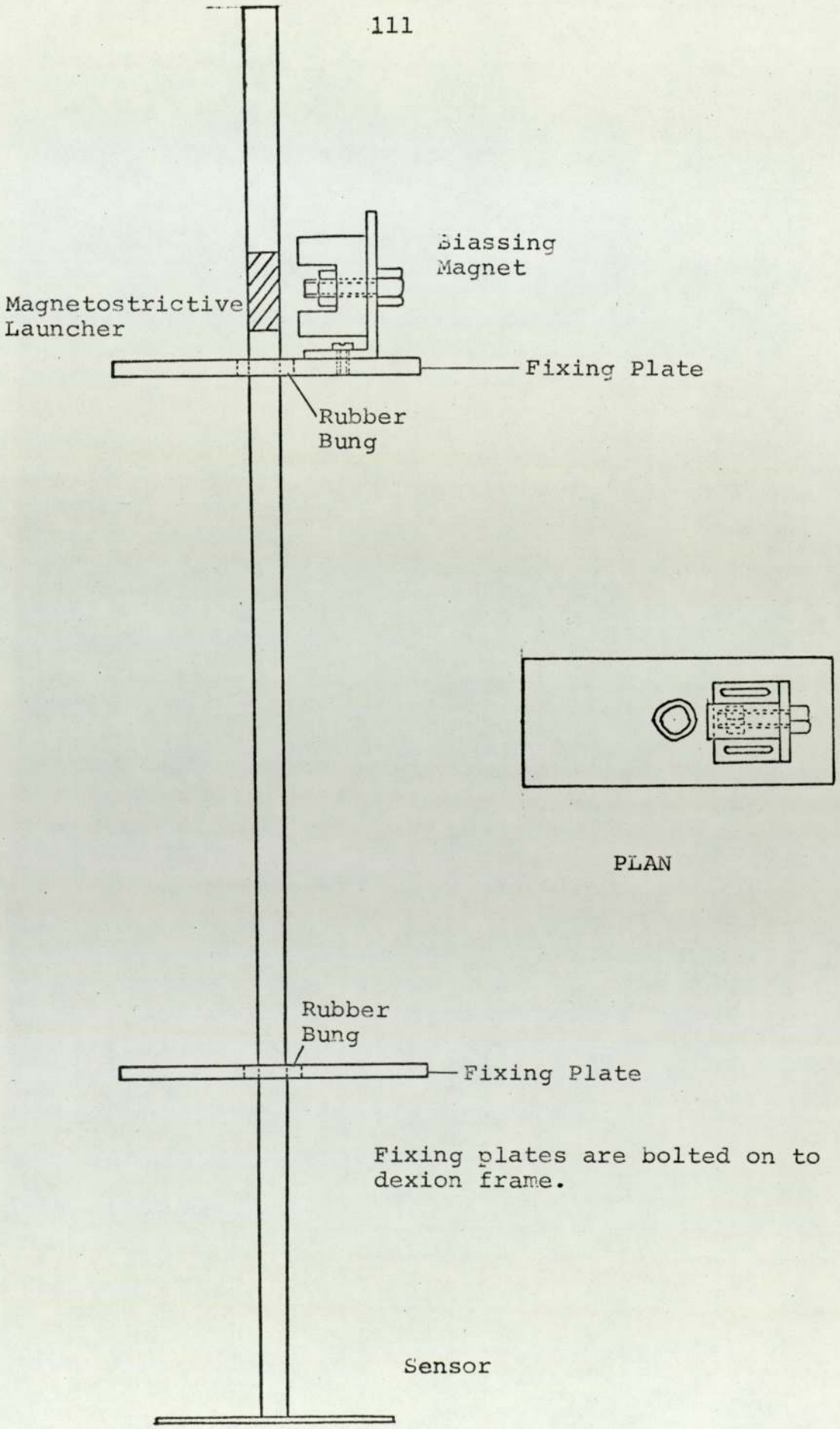

FIGURE 5.4.3.

The transducer and mounting used for on-line measurements.

supports have to be tight enough to withstand the upward thrust produced by the high speed of sludge against the sensor. The support losses can be reduced virtually to zero by locating the rubber bungs at the two nodes. This arrangement was found to be adequate for the Minworth trials.

The mounting for the magnet is such that its position can be altered for the correct biasing of the launcher. The steel fixing plates are attached to a dexion frame so that the transducer can be held by hand with the sensor submerged in the bellmouth.

5.5. Measurements at Minworth

The primary settling tank chosen to carry out the measurements was tank no. 4. This was the nearest tank to the sludge pump house in which the electronic equipment is arranged as shown in plate 5.5.1. for protection against the weather. The signal to and from the transducer is taken by a lead long enough to reach the inspection chamber in which the transducer is held in position by hand. The valves and penstocks required for desludging this tank were all switched to local control so that any one of the three hoppers could be desludged at will and also the speed of sludge in the telescopic valve could be controlled conveniently.

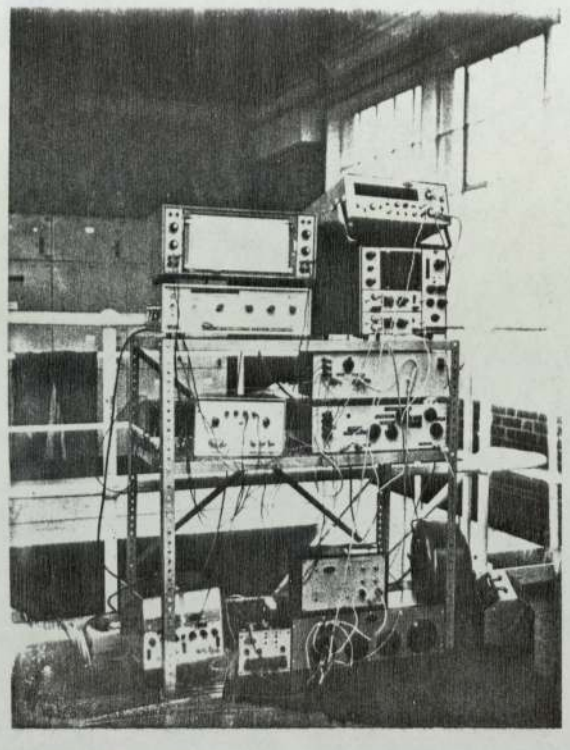

PLATE 5.5.1.

The electronic equipment used stored in the primary sludge pumphouse.

5.5.1. The Flexurally Vibrating Disk

The first type of transducer used for the measurement was the type with the flexurally resonant disk used as the sensor. The two forms of sensing disks are shown in pages 57 and 56 which will be called disk 1 and 2 respectively. One of the hoppers was desludged so that it contained a very low concentration of solid matter and one other hopper contained thick new sludge with heavy solid concentration.

Both types of transducers were found to be very sensitive to the presence of sludge. The 'Q' of the transducers 1 and 2 changed from 200 to 20 and 350 to 30 respectively as the liquid changed from water to sludge. The frequency of resonance in sludge for both transducers varied over the range indicated in Table 5.5.1. Since an open loop transmitter was used it was necessary to constantly retune the drive frequency to resonance.

	Frequency in water	'Q' in water	Frequency in sludge KHz	'Q' in sludge
Disk 1	1.130 KHz	200	1.120 - 1.145	20
Disk 2	1.460 KHz	350	1.430 - 1.470	30

TABLE 5.5.1.

This will not be necessary when feedback frequency control

is used. This result exemplifies the complex rheological nature of sludge. It can present stiffness or mass loading to the sensor resulting in either increase or decrease of the resonance frequency from that in water. The transducer clearly detected the breakthrough of water after the desludging of the second hopper was complete. This was confirmed by visual inspection. At this point a good steady decrement of high'Q' was obtained.

The above experiment was repeated on different days and on the whole, the results obtained were consistent.

A problem encountered from time to time arises from long glutenous fibres and sludge saturated rags which are always present. These wrap themselves round the sensor and give a low 'Q' reading. The transducer 1 was the more prone to rag accumulation than transducer 2. This is to be expected in view of the method used to terminate the line to the disk. The blocking of the sensor was more severe in the early stages of desludging a hopper in which the sludge had been standing for sometime if it had been raining the previous day, since a storm increases the rag contents of sewage. The solution to this problem may be to provide a local screen for the transducer.

Although the breakthrough of water was easily detected, the flexurally resonant disk was found to be over sensitive to sludge. Since a constant retuning of the drive frequency was required to maintain resonance,

these two transducers were not suitable for obtaining a continuous readout of decrement frequency and amplitude.

5.5.2. Rigid Disk used as Sensor

In this transducer the circular disk undergoes piston type motion. This type of sensor has advantages because the sensitivity of the transducer can easily be altered by changing the diameter of the plate. One end of the robust line was tapped so that disks of various diameters could be screwed to the line. In these experiments the only setting up required is to tune the drive frequency to the decrement by placing the sensor in a bucket of water and tuning for maximum decrement amplitude. A difference between drive frequency and resonator frequency will not effect the measured period but if excessive could reduce the amplitude of the decrement and hence give a low reading for 'Q'. This limit was not reached in these experiments.

In the most comprehensive experiments three hoppers could be drained at one bellmouth. In addition the transducer could be removed and dipped into a barrel containing stationary water. Hopper one, which had already been desludged, contained very low density sludge, hopper two contained thick new sludge with heavy solid concentration and hopper three contained a sensibly uniform sludge. The head of liquid at the bellmouth was set to a level which ensured a normal

fast sludge rate which showed the characteristic 'gushing' movement past the sensor. The control valves enabled the switching from hopper to hopper to be carried out without interruption thus giving a continuous transducer reading.

Figure 5.5.1. shows the period and decrement amplitude over a thirty minute experiment. Having been set for water the drive frequency was not changed throughout the run. A few minutes in air were followed by a few minutes in still water. The sensor was put in the bellmouth and held in position by hand. Hopper one sludge (mainly water) showed small fluctuations in period and amplitude, the amplitude being significantly lower than for water. The insensitivity of readings to fluid velocity was very evident and highly satisfactory. The emptying was switched to hopper two, the very thick sludge. Wide amplitude fluctuatuions were observed, at times the amplitude being almost zero and associated changes in period of about 1%. The fluctuations were caused by genuine variations in consistency which was very evident by direct observations. Switching to hopper three giving a uniform intermediate sludge seven minutes of quite steady readings were obtained. Removing the probe and placing it in the water barrel returned the readings to their original values, establishing the stability of the measuring system.

The results given are for a steel plate of 5 cms. diameter used as the sensor. The problem of the rag accumulation was again encountered particularly during

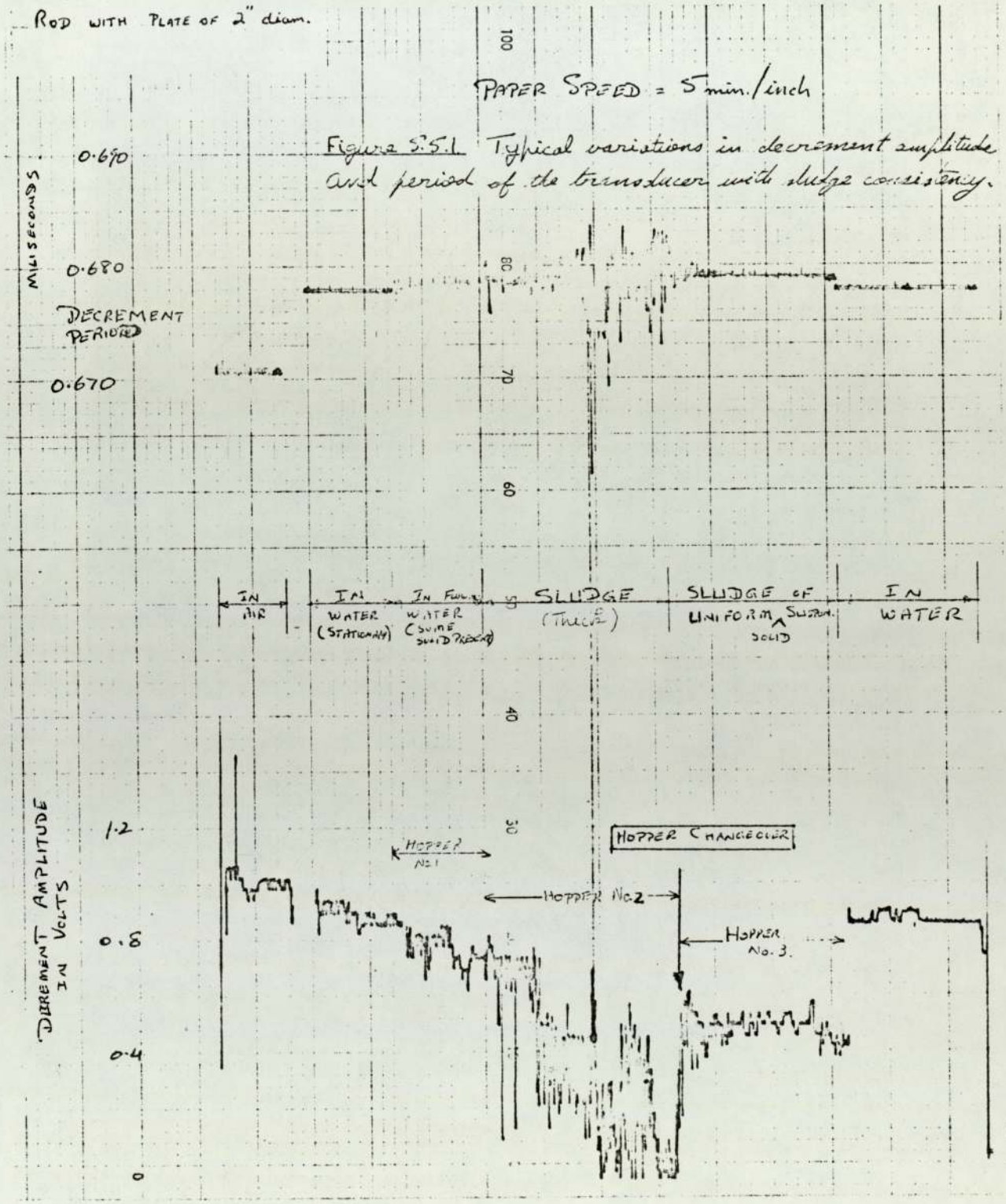

Figure 5.5.1 Typical variations in decrement amplitude and period of the transducer with sludge consistency.

the emptying of the very thick sludge in hopper two. Separate tests with small spheres used as sensing elements were preformed. The readings obtained were typical of those obtained for disks, furthermore it was found that this probe was less susceptible to the attachment of rags.

5.6 Conclusion

The experiments have established two of the requirements of the transducer as a measuring system:

(a) A meaningful readout parameter of the fluid was obtained over a full desludging cycle and this is as significant a measure of sludge consistency as that obtained by direct observations.

(b) The high velocity flow of fluid round the sensing end of the transducer, effects due to the momentum of the fluid and the impact of suspended matter does not influence the readings.

A formal technological solution for the sludge transducer has been reached. The problem of the attachment of filament/rags needs further investigations. Protection of the transducer is unsatisfactory as this could isolate it from the flow of sludge.

An alternative form of the transducer which employs the fluid damping of torsionally resonant rod was subsequently developed and is described in Chapter 7. This transducer can be located at the bottom of the

hopper instead of the bellmouth. It is envisaged that in its nature this arrangement will not be vulnerable to rag accumulation and has a self clearing action (Figure 5.5.2.).

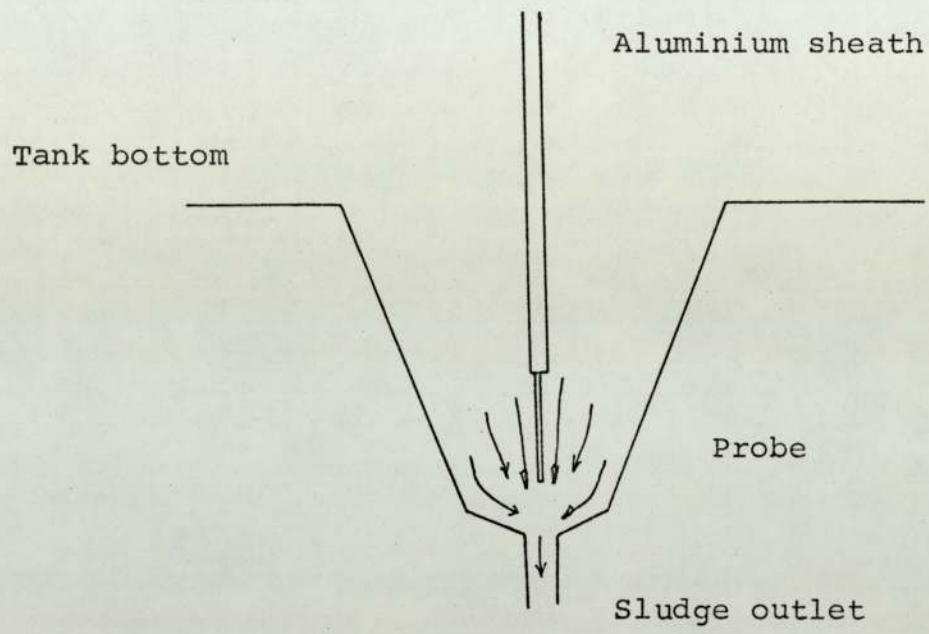

FIGURE 5.5.2.

Only a small development effort is required to close the frequency loop and maintain the drive oscillator at the transducer frequency. This needs to be done particularly in the case of flexurally resonant disk sensor. The decrement amplitude was measured by using a peak detector and stored in an A to D converter. This was found to be satisfactory for the low frequency of the transducer. But a better readout stability may be achieved by using the ratio of two oscillations, say 10 periods apart than relying of a single amplitude reading.

In the present form the line is one wavelength long, having modes at ¼ the length from each end. The

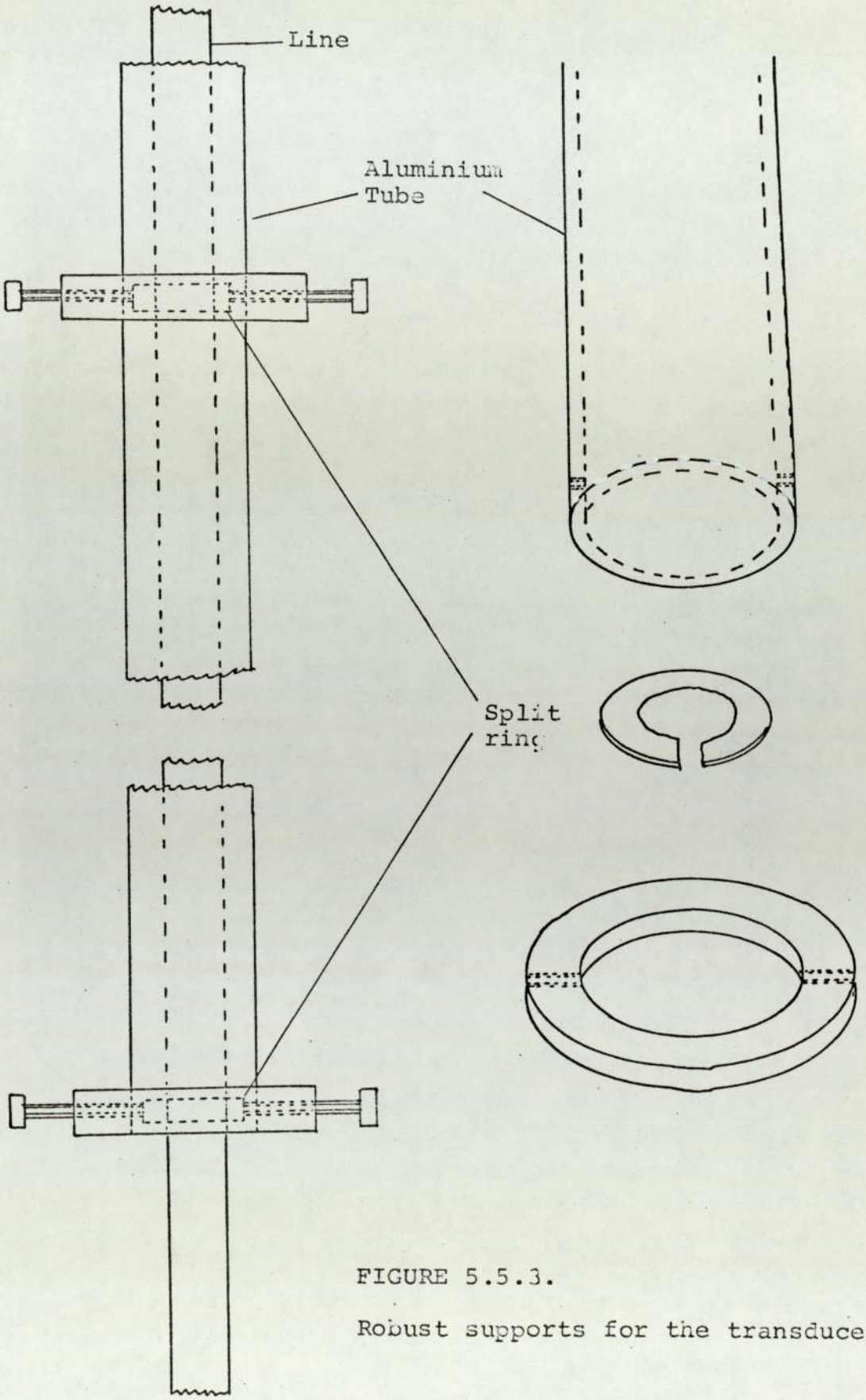

FIGURE 5.5.3.

Robust supports for the transducer

line is supported at the node using rubber bungs. Improvement in the transducer supports is achieved by solidly attaching disks to the line at the nodes. It was found that this arrangement did not affect the transducer performance and constituted an extremely robust and practical support. The details of the supports and protective sheath for the line are shown in Figure 5.5.3. The biassing magnet for the magnetostrictive launcher can be replaced by two small bar magnets which form integral parts of the line as shown in Figure 5.5.4.

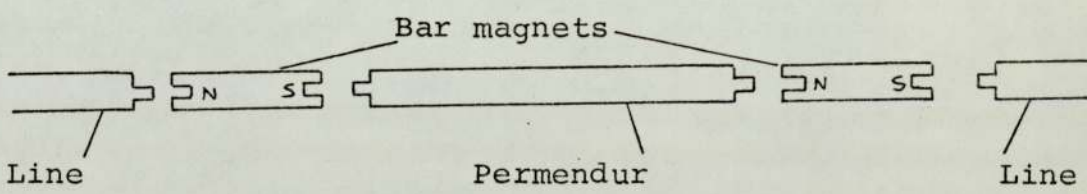

FIGURE 5.5.4.

With this system there is a very efficient magnetic coupling to the permendur.

The magnets were made of Feroba which is an extremely hard material to machine. The machining was carried out on the unmagnetised form of the bar magnets using a diamond grinding wheel after which the magnetisation was done on a (Newport Instruments) electomagnet.

Typically a decrement amplitude of 7.5.V was obtained with this biassing system compared to 11.0 V when the bias is augmented by an external magnet.

CHAPTER 6

THE ELECTRONIC SYSTEM

6.1. INTRODUCTION

The electronic system is an essential part of the on-line consistency transducer. Its function as described in Chapter 5, is to set the transducer into resonance, measure the decrement period and the decrement amplitude. The transmitter generates a burst of electrical pulses which are converted into acoustic pulses at the magnetostrictive launcher. The transducer decrement, which appears at the resonance, is converted back to electrical oscillations at the launcher. It is known that energy stored in the transducer decays exponentially at the natural frequency of the resonator independent of the transmitted frequency. The decrement period and therefore the resonance frequency of the transducer, is determined by timing ten oscillations of the decrement using a 1 MHz clock. It has been shown experimentally that the 'Q' of a resonator can be calibrated against the decrement amplitude and that this relationship is linear (see Figure 5.2). Therefore a circuit is designed to measure the positive peak amplitude of a decrement oscillation.

Thus the electronic system required to perform these three functions can be divided into the following separate systems:

(a) Transmitter,

(b) Decrement Period Measurement,

(c) Decrement Amplitude Measurement.

An extensive use of T.T.L. digital integrated circuits have been made in the construction of the electronic systems. The above systems are independent of each other and will be described separately.

6.2 TRANSMITTER

The function of the transmitter is to generate a burst of pulses of

(a) Variable frequency from a voltage controlled oscillator,

(b) Variable burst length and repitition rate.

These variables should be independent of each other. The burst length may be varied from 1 to 999 and the maximum repitition rate is 50 per second and can be reduced to one every three seconds by dividing the 50 Hz through a chain of divide by 2 flip-flops.

A schematic block diagram of the transmitter is shown in Figure 6.2.1. It basically consists of a voltage controlled oscillator, a repitition rate oscillator a counter to control the burst length, gating circuits and a transistor push-pull amplifier to drive the magnetostrictive launcher.

6.2.1. VOLTAGE CONTROL OSCILLATOR

The circuit diagram of the V.C.O. is shown in Figure 6.2.2. The oscillator is made by cross-coupling two monostables M_1 and M_2. The frequency is varied by

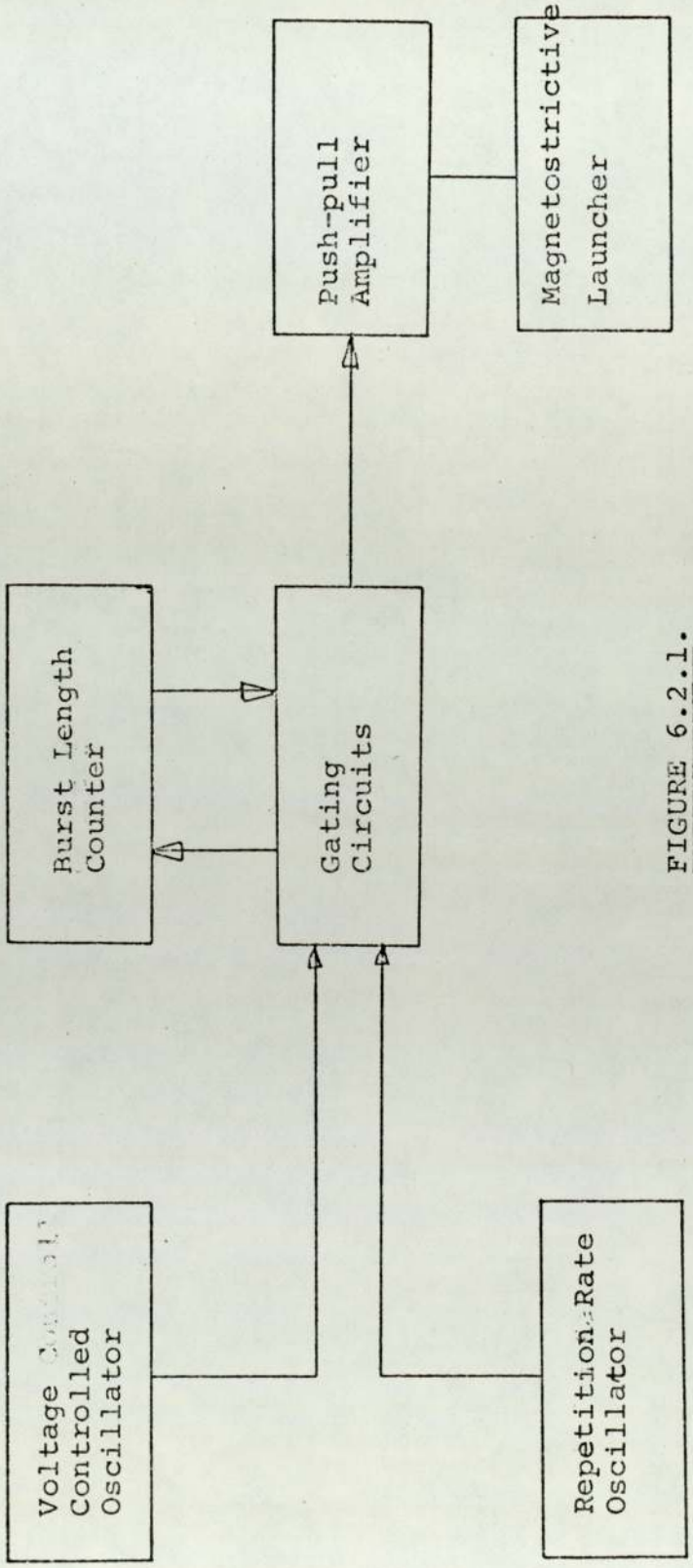

FIGURE 6.2.1.

A Block Diagram of the Transmitter

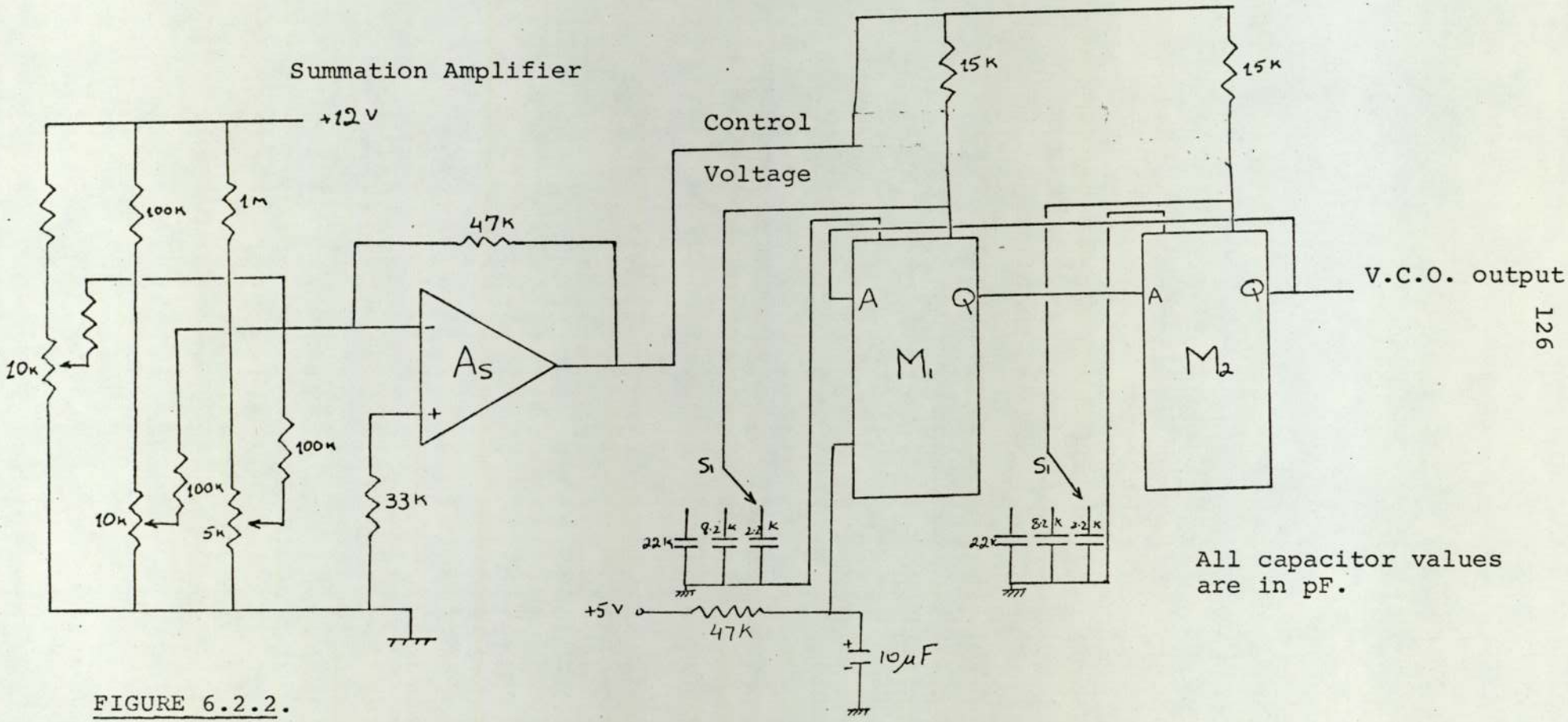

FIGURE 6.2.2.

Voltage Controlled Oscillator

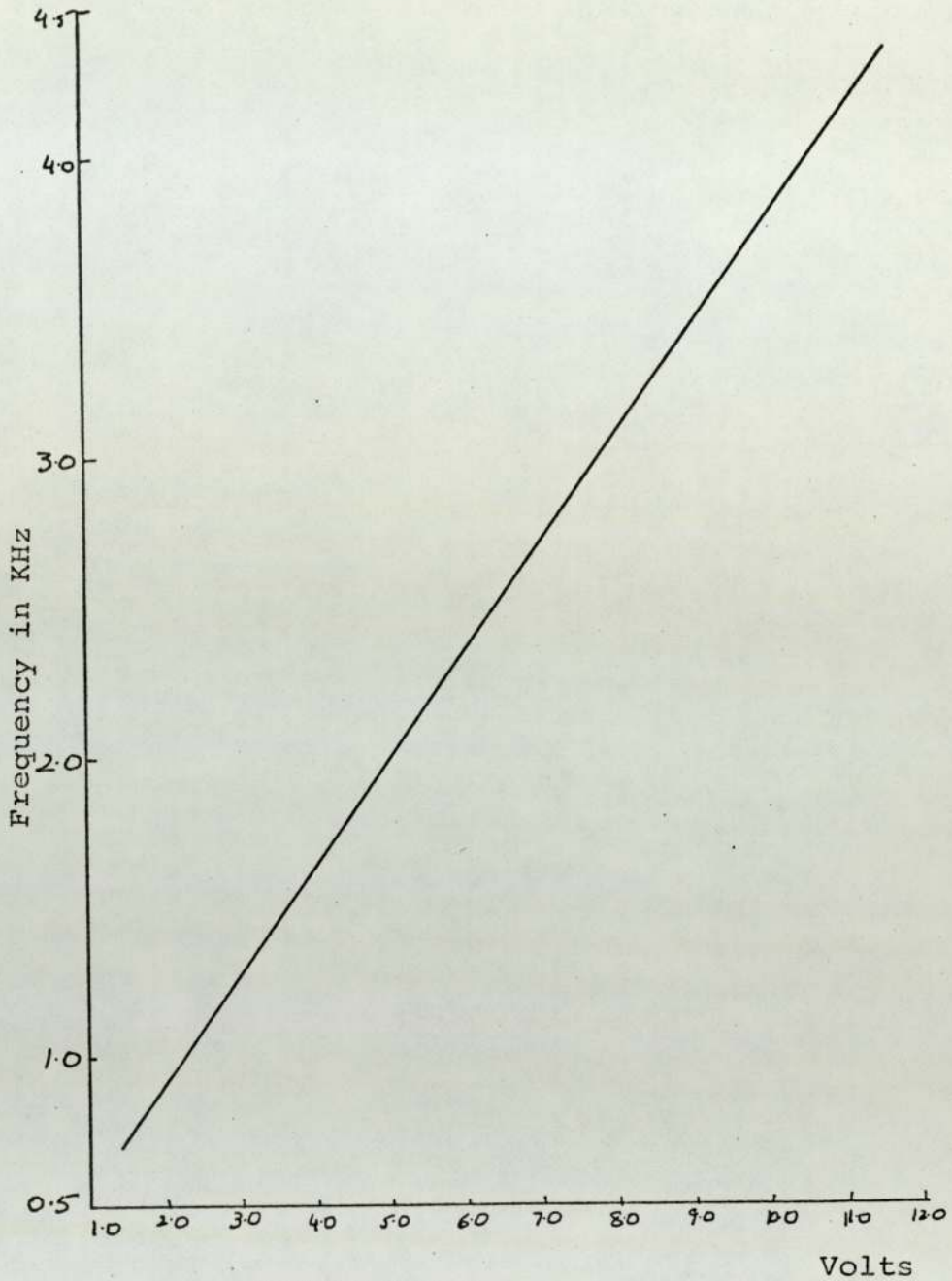

FIGURE 6.2.3.

Voltage controlled oscillator characteristics.

V.C.O. sensitivity = $\frac{2.5}{7}$

= 0.33 KHz/Volt

(The control voltage is measured at the output of the summation amplifier Fig.6.2.2.)

varying the base voltage on the transistors T_1 and T_2. The control voltage for both coarse and fine frequency control is obtained from potential divider chains through a summation amplifier A_s . The frequency is varied over three ranges by the timing capacitors on the monostables. The calibration of V.C.O. relating voltage to frequency is shown in Figure 6.2.3.

The RC network at M_4 ensures that the oscillator starts relibly with the supply. Once switched on the oscillator runs continuously.

6.2.2 PULSE REPETITION FREQUENCY GENERATOR

This oscillator is locked to the mains frequency. The 50 Hz 1 volt peak to peak signal is obtained from an oscilloscope and it must be amplified to be compatible with T.T.L.

The circuit diagram is shown in Figure 6.2.4. The amplified signal is passed through a chain of flip-flops acting as divide by 2 elements. The repetition rate is selected by switch S_2. The 330Ω resisters on this switch ensures that the unused points are pulled down to the low level state of T.T.L.

The monostable M_3 gives a short pulse when the output of the Nand gate N_1 changes from high to low level.

6.2.3. BURST LENGTH COUNTER AND GATING CIRCUITS

The circuit diagram is shown in Figure 6.2.5. and

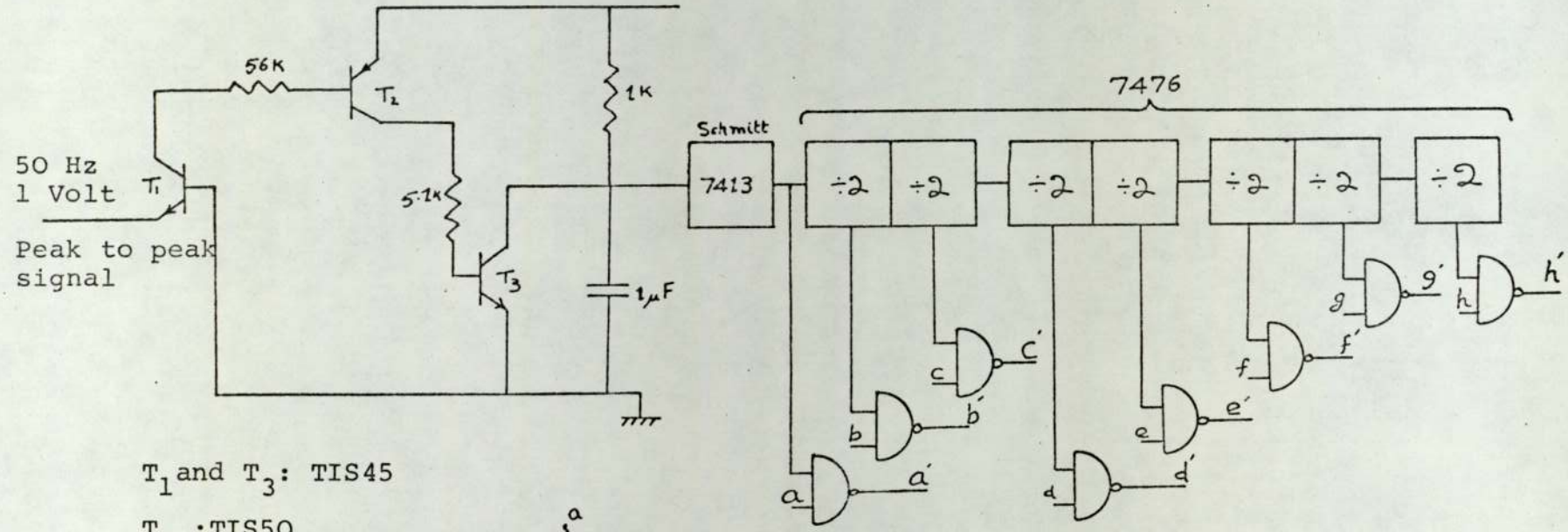

T_1 and T_3: TIS45

T_2 :TIS50

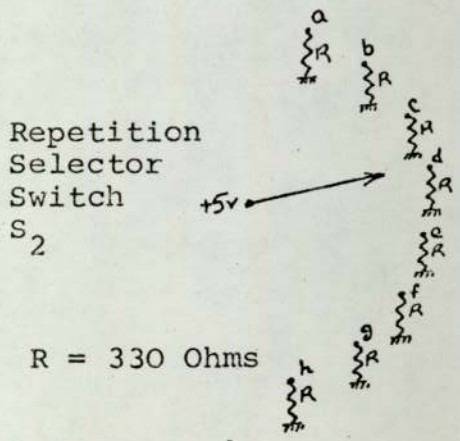

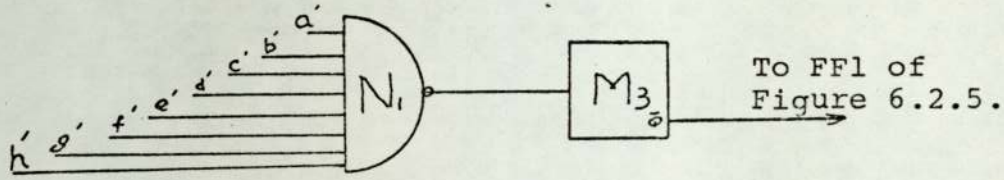

FIGURE 6.2.4.

Burst Repetition Frequency System

the associated waveforms at various points is given in Figure 6.2.6.

The sequence of events is started by the transition of high to low level of the output of N_1 which generates a pulse of short duration at the output of M_3. The $\overline{Q}$ of M_3 is used to preset F.F.1. When over the 'count enable' for the b.c.d. counters is high, the counter is inhibited and all the outputs are reset to zero. Therefore the input count pulses will only be counted when the 'count enable' is low. The input count pulses are derived from the Q of F.F.2, which are generated by the combination of gates I_1 and N_2.

The b.c.d. count is continuously converted to decimal system by the b.c.d. to decimal decoders, the outputs of which are connected to the thumb-wheel switches TW_1, TW_2, and TW_3. The burst length is controlled by setting these switched to any number from 0 to 999. When the set numbers of pulses have been counted, the N_3 generates a short pulse which is used to close the loop by clearing F.F.1.

The combination of gates N_4, N_5, N_6, and I_1 with F.F.3 which is a D-type flip-flop generates a complimentary set of pulses. The Q's of F.F.2 and F.F.3 are used to drive the push-pull amplifier.

6.2.4 PUSH-PULL AMPLIFIER

The circuit diagram is shown in Figure 6.2.7. The transistors T_1 and T_2 are used to drive the push-pull

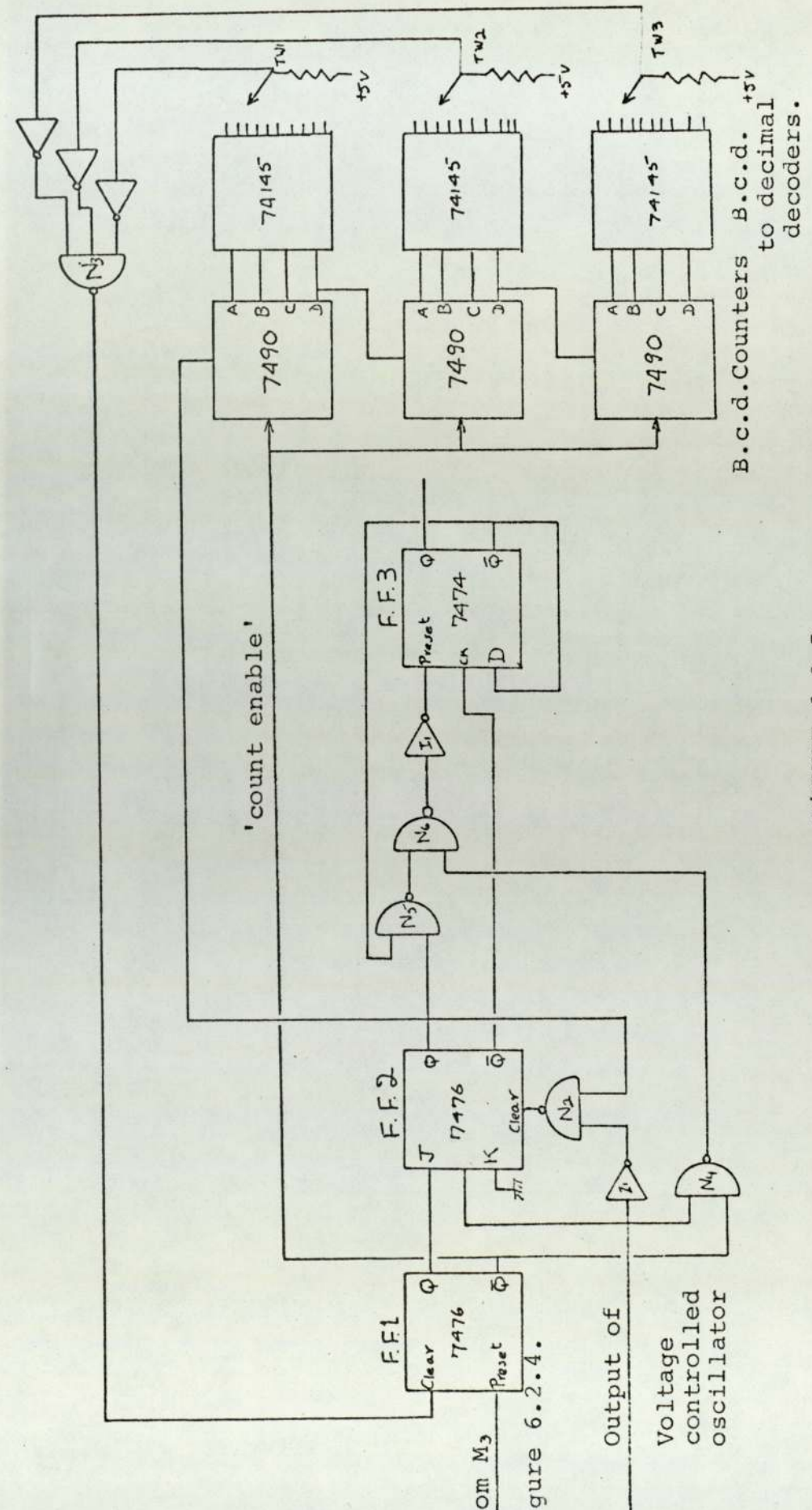

FIGURE 6.2.5.

Burst Length Counter and Gating Circuits

Figure 6.2.4.

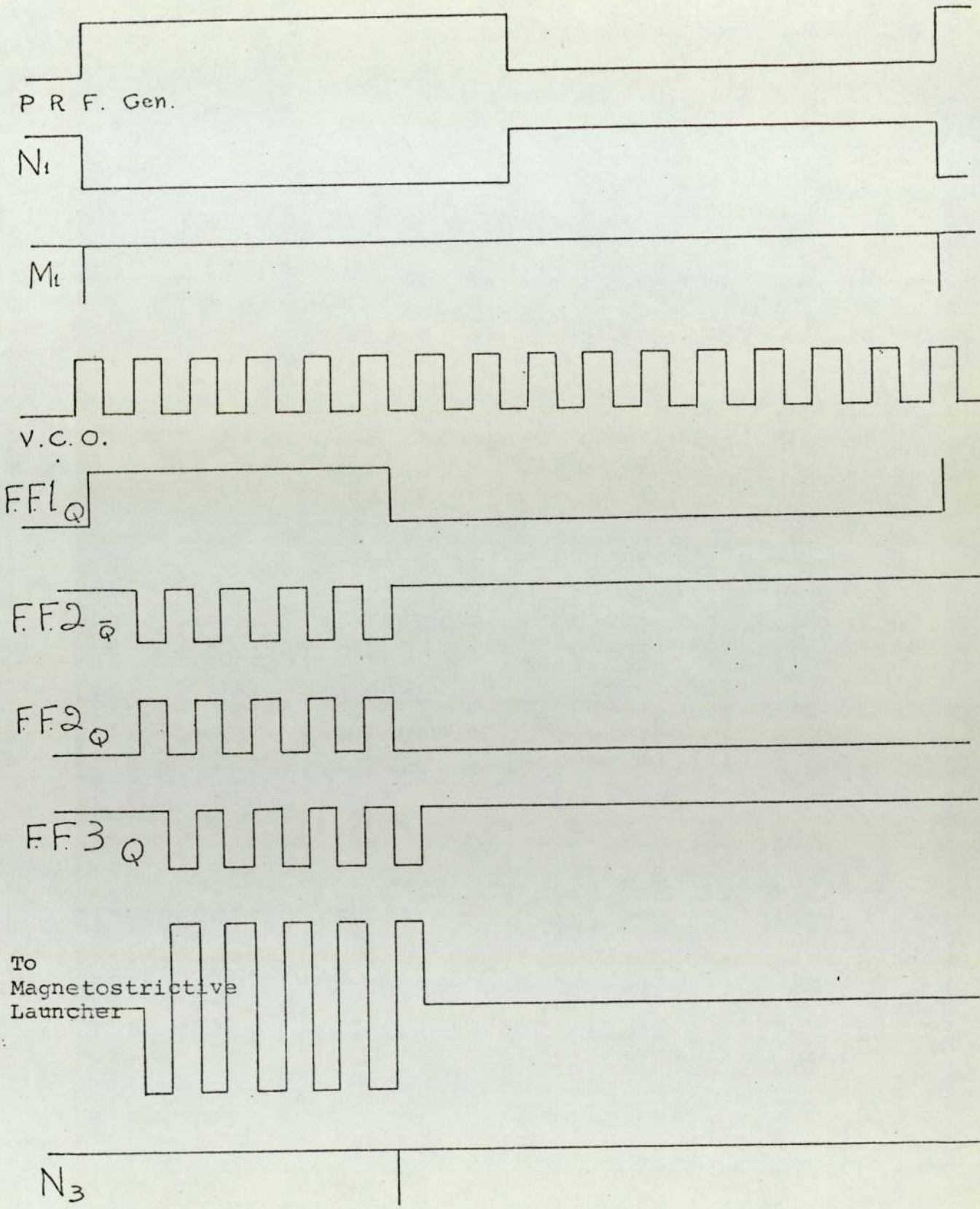

FIGURE 6.2.6.

Waveforms at various points on the Transmitter

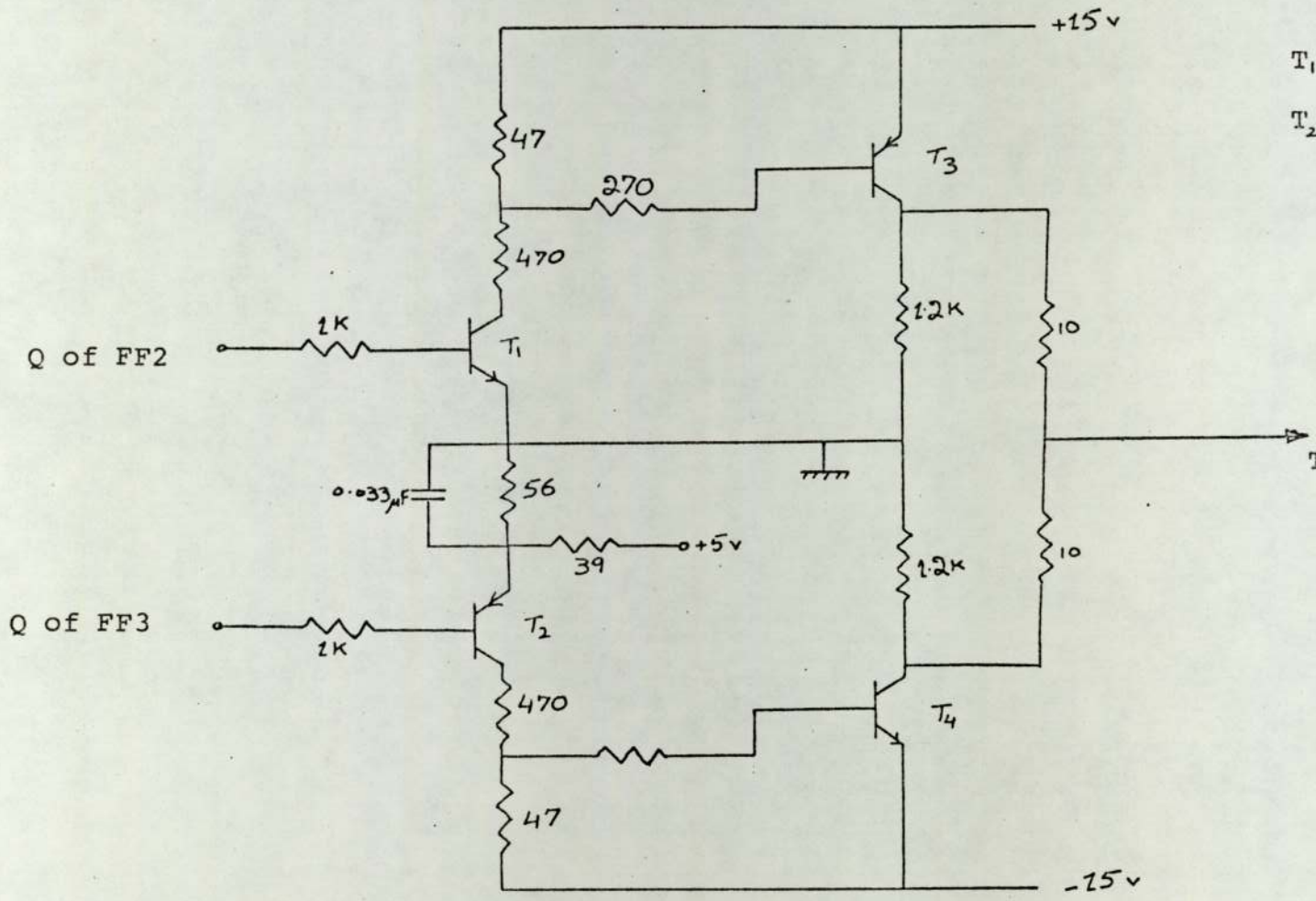

T_1 and T_4: 2N2218

T_2 and T_3: 2N2904

FIGURE 6.2.7.

The Push-Pull Amplifier

amplifier which is a complimentary pair of transistors T_3 and T_4. These produce a burst of transmitter pulses of +15V to -15V amplitude to drive the magnetostrictive transducer as shown in Figure 6.2.6. and Figure 6.2.7.

The frequency response of the transmitter is only limited by the switching characteristics of the transistors in the push-pull amplifier. The circuit described will function reliably for frequency up to 100 KHz. Beyond this range the storage time of the transistors is too high and the output of the amplifier is distorted.

For the low frequency (<5 KHz) fluid consistency transducer the amplifier frequency response is not important but the power handling capacity of the amplifier described is limited. An increase in the drive to the coil is needed for the permendur magnetostrictive launcher in the robust brass line. Therefore a similar amplifier is constructed with power transistors so that burst transmitter pulses of +30V to -30V amplitude are generated.

6.3. DECREMENT PERIOD MEASUREMENT

The function of this circuit is to amplify and process the decrement period measurement. Processing of the decrement involves generation of square pulses for T.T.L. circuit operation and sampling of the decrement to provide pulses to enable period measurement by timing a 1 MHz clock. Diagrams of the analogue and T.T.L. circuits required are given in Figure 6.3.1. and Figure 6.3.2.

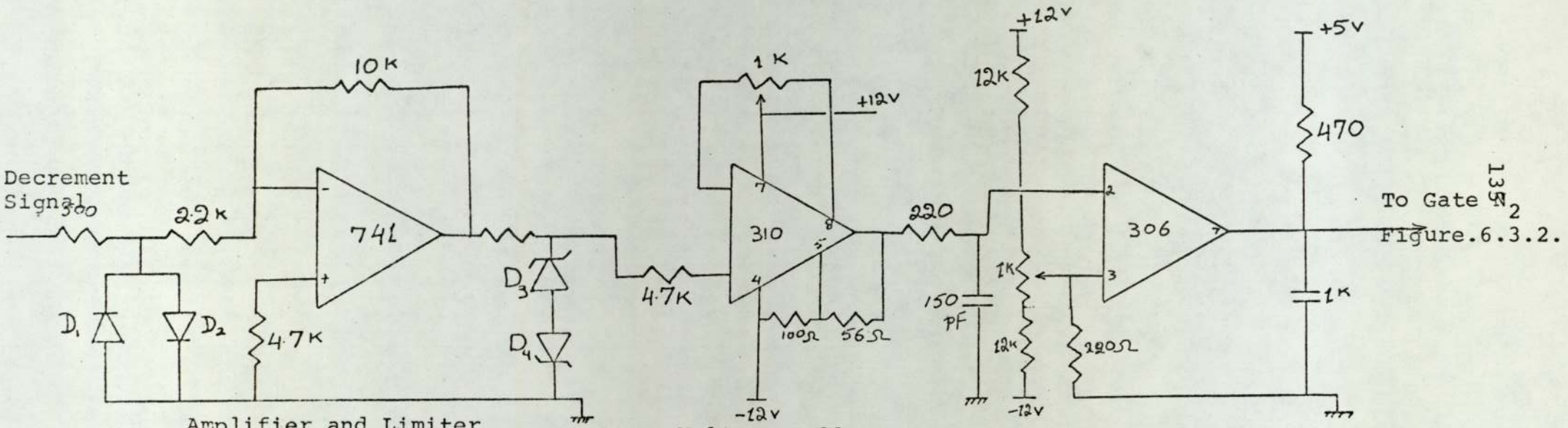

FIGURE 6.3.1.

The processing of the decrement signal for period measurement

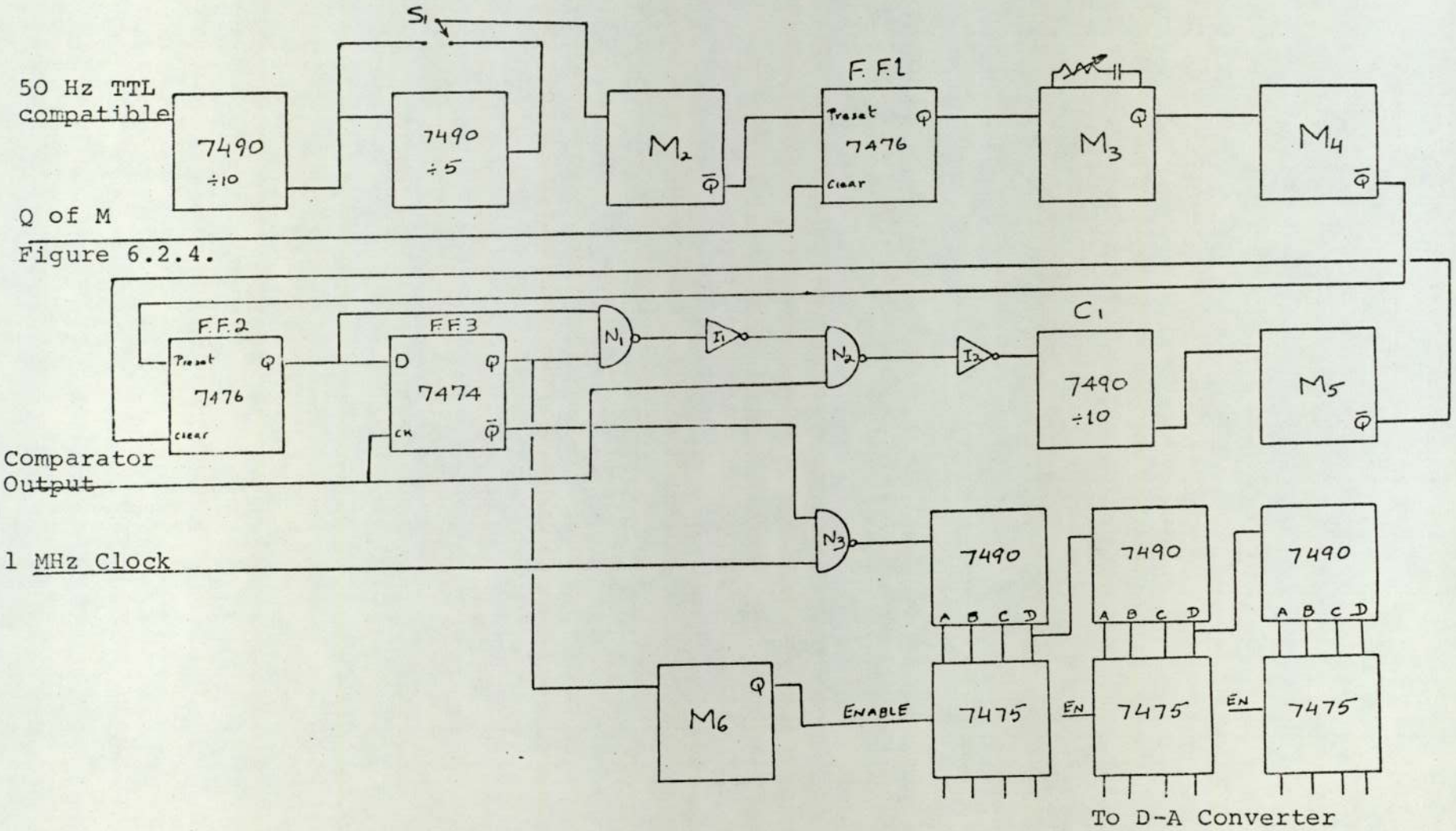

FIGURE 6.3.2.
Decrement Period Measurement

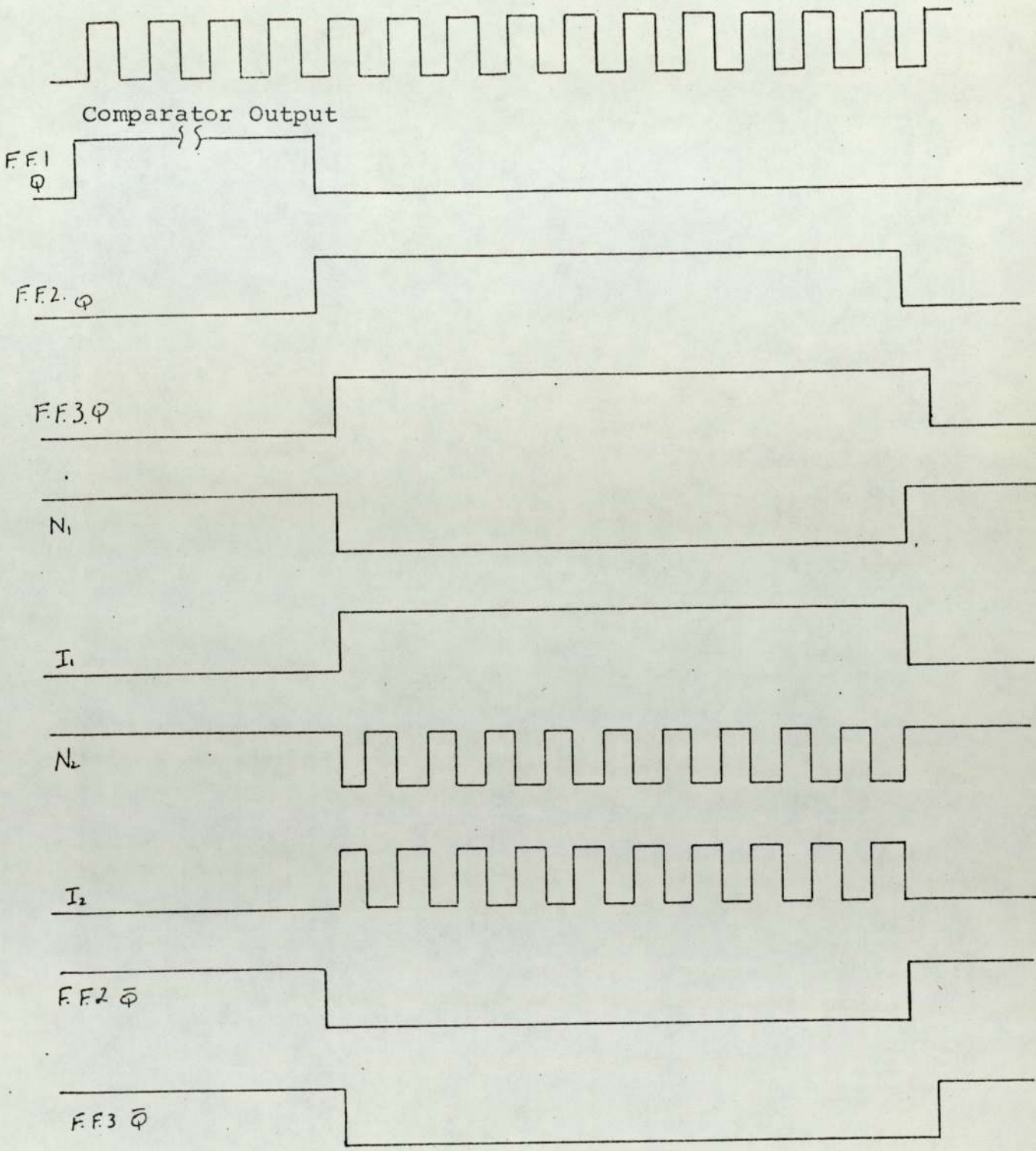

FIGURE 6.3.3.

Waveforms for various points for the decrement period measurement.

respectively. The waveforms at various points in the circuitry are shown in Figure 6.3.3.

6.3.1. INPUT AMPLIFIER

The transducer signal comprises of the high voltage transmitted burst and the relatively low voltage of the decrement. To limit the saturation of the amplifier and the comparator the input is clamped to ±0.6 V by clamping diodes D_1 and D_2. The gain of the amplifier can be adjusted by the feedback resistor to provide sufficient decrement amplitude for the comparator. The zener diodes D_3 and D_4 are used as an extra precaution to ensure that the output of the amplifier never exceeds ±5 V as this is the allowed voltage swing at the input of the comparator. The amplifier is the standard integrated circuit type SN72741.

6.3.2. VOLTAGE FOLLOWER AND THE ZERO-CROSSING COMPARATOR

The voltage follower acts as a buffer for the comparator. The voltage follower and the comparator is the integrated type LM310 and LM306 respectively. The comparator has a strobe facility enabling it to operate only for the required period.

The amplified transducer signal is applied at the input and the strobe, generated by F.F.4., is arranged to give comparator output for the decrement. During the rest of the period the comparator is off as shown in Figure 6.3.3. The comparator output is compatible with T.T.L. circuits.

6.3.4. GATING CIRCUIT FOR THE PERIOD MEASUREMENT

The gating circuit is shown in Figure 6.3.2. The sampling rate is determined by switch S_1, this rate can either be 5 or 1 per second. The sequence of events is started by a short pulse from monostable M_2 which sets the Q output of the flip-flop F.F.1. high. At the end of the next transmit burst, the output of the F.F.1. is set to low level by a short pulse from gate N_3 Figure 6.2.5. At this point in time the monostable M_3 is triggered. The duration of output pulse M_3 can be altered by varying its timing resistor. This enables the sampling position in the decrement to be changed. The negative going edge of the Q of M_3 generates a pulse at M_4 which sets the Q of F.F.2. high.

Combination of gates N_1, I_1, N_2 and I_2 together with the counter C_1 (b.c.d. counter SN7490) produces a pulse at the output of F.F.3., a D-type flip-flop; of duration equivalent to the period of ten oscillations of the decrement signal.

The $\bar{Q}$ of F.F.3. and a stable 1 MHz clock are gated through gate N_3 the output pulses of which are counted by the three b.c.d. counters shown. These counters will only measure the three least significant figures of the decrement period. This is suffiecient to determine the total change in the resonant frequency of the transducer with the properties of the surrounding liquid.

At the end of the count period a pulse is generated by the monostable M_6 which enables the data present

at the input of the latches (SN7475) to be transferred to the output. The data at the output of the latches is displayed on chart recorder via a D-A converter. The maximum error in the period measurement is ±0.1μS, which is inherent in the digital system. The other form of error which remains constant and is neligible, is due to the delay time in the various T.T.L. gates.

6.3.5. EXPERIMENTAL RESULTS

The results obtained for the decrement period measurement are shown in Figure 6.3.4.

(a) Trace 1 which shows the general behaviour of the electronic circuitry, clearly indicating the ±0.1μ inherent error of the system.

(b) Trace 2 shows the changes in the decrement signal period with the transmitted signal period. It is seen that the decrement changes by $\frac{1}{15}$th of the transmitted change. This change is basically due to the variation in the decrement amplitude with the transmitter frequency Since the comparator (Figure 6.3.1.) triggers at a finite voltage level (other than zero) as shown in Figure 6.3.5. then for a decrement signal of same frequency but different amplitudes (i.e. exponential decay of stored energy) then an error in the period measurement of $(\Delta T_2 - \Delta T_1)$ will be introduced for each oscillation. This error cummulates for the ten oscillation in the decrement.

This error is evidenced in Trace 3.

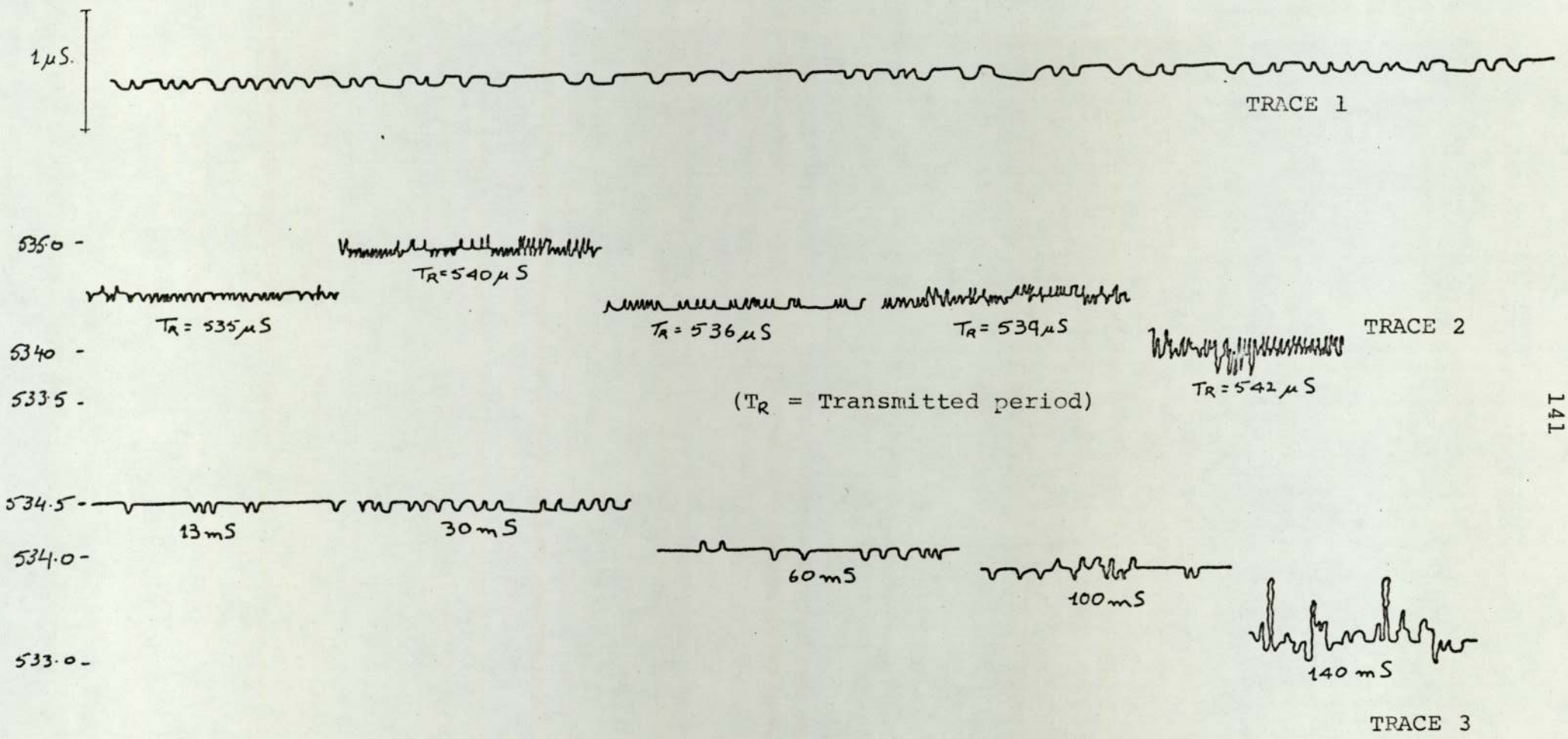

FIGURE 6.3.4.

The variation of the decrement period with (a) Transmitted Period (Trace 2),
(b) Various positions in the decrement (all times are measured from the end of transmitted burst) (TRACE 3).

(c) Trace 3 shows the variation of the decrement period with the sampling position in the decrement for a constant transmitter frequency. All times are measured after the end of the transmitted burst.

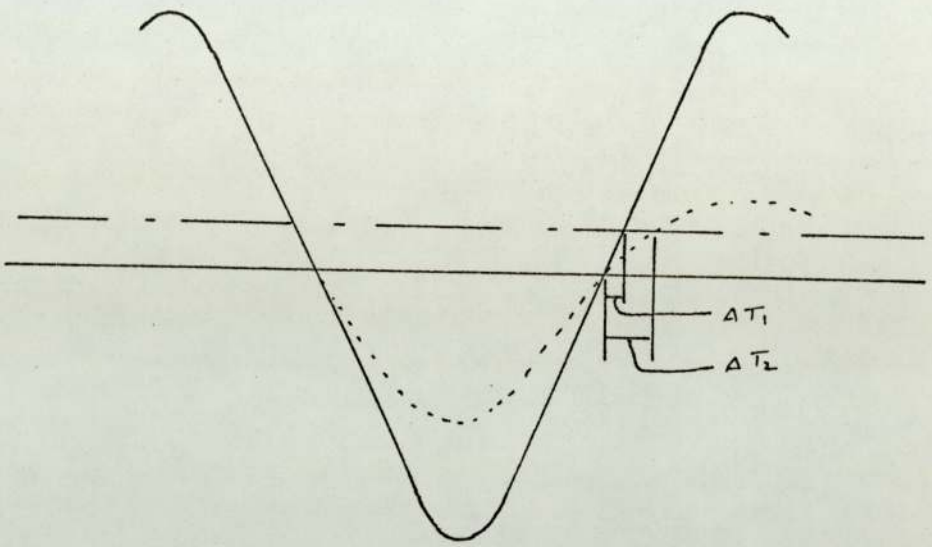

Figure 6.3.5.

6.4. DECREMENT AMPLITUDE MEASUREMENT

The function of this circuit is to measure the amplitude of one selected oscillation of the decrement and hold the signal for display until the next cycle of measurement. This is, in effect, a sample and hold circuit. The decision to hold the infomation digitally was made because of the relatively long hold time. An analogue hold system would be susceptible to drift errors and component deterioration with time.

The block diagram of the system is shown in Figure 6.4.1. The circuitry is shown in Figure 6.4.2. and the corresponding waveforms at the various points in the circuit are shown in Figure 6.4.3. The transducer signal is applied to an attenuator which is used to ensure that the decrement signal will not exceed +1V. This limitation is imposed by the D

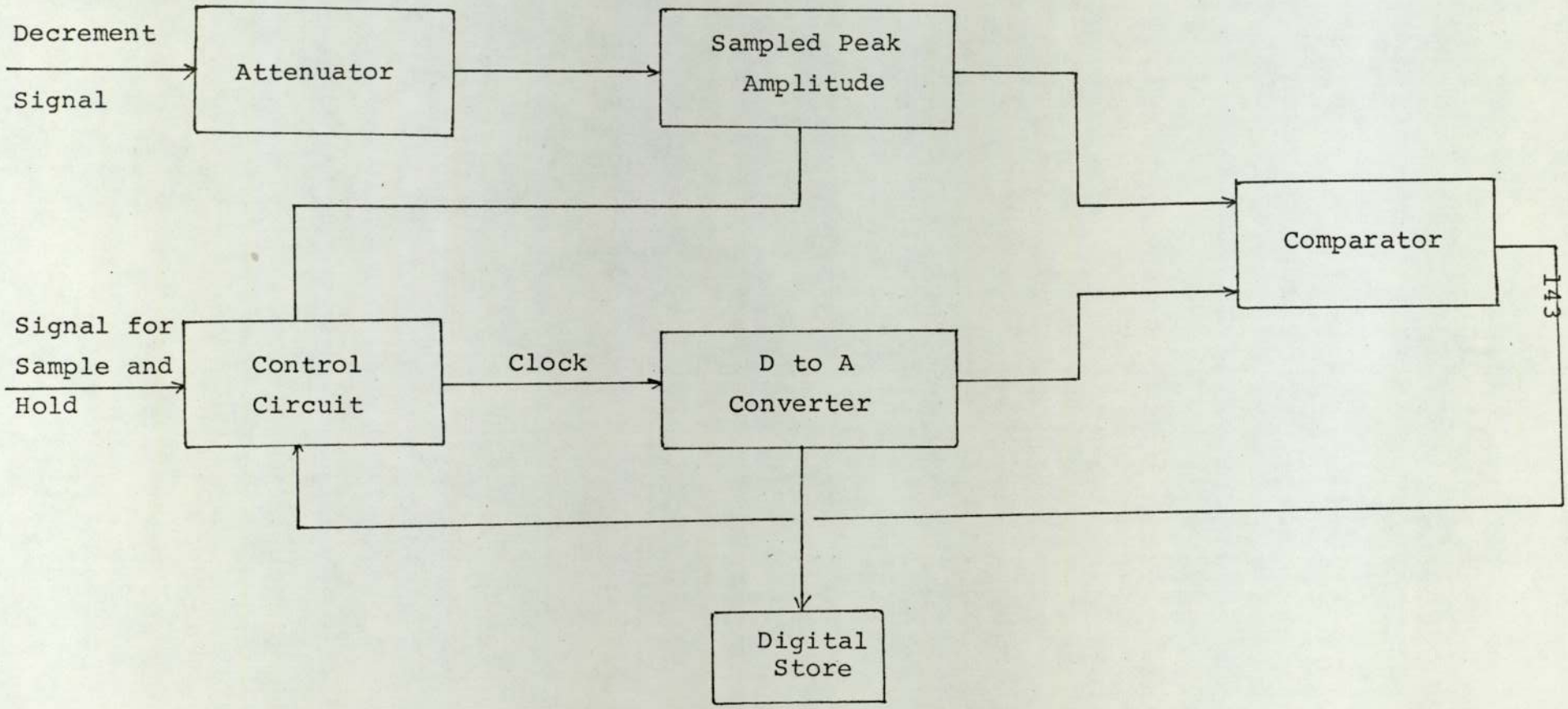

Figure 6.4.1. The block diagram for the decrement amplitude measurement.

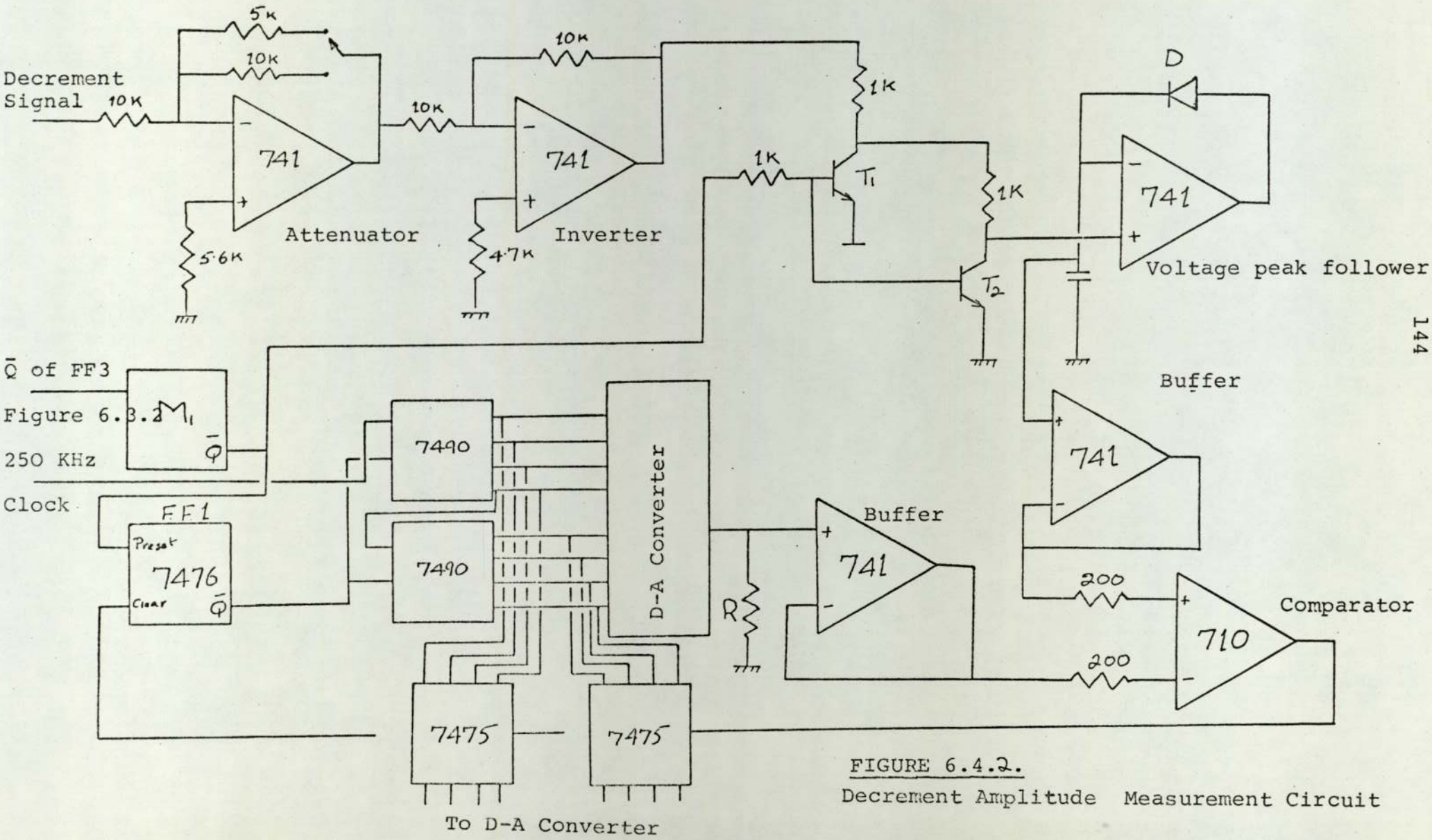

FIGURE 6.4.2.

Decrement Amplitude Measurement Circuit

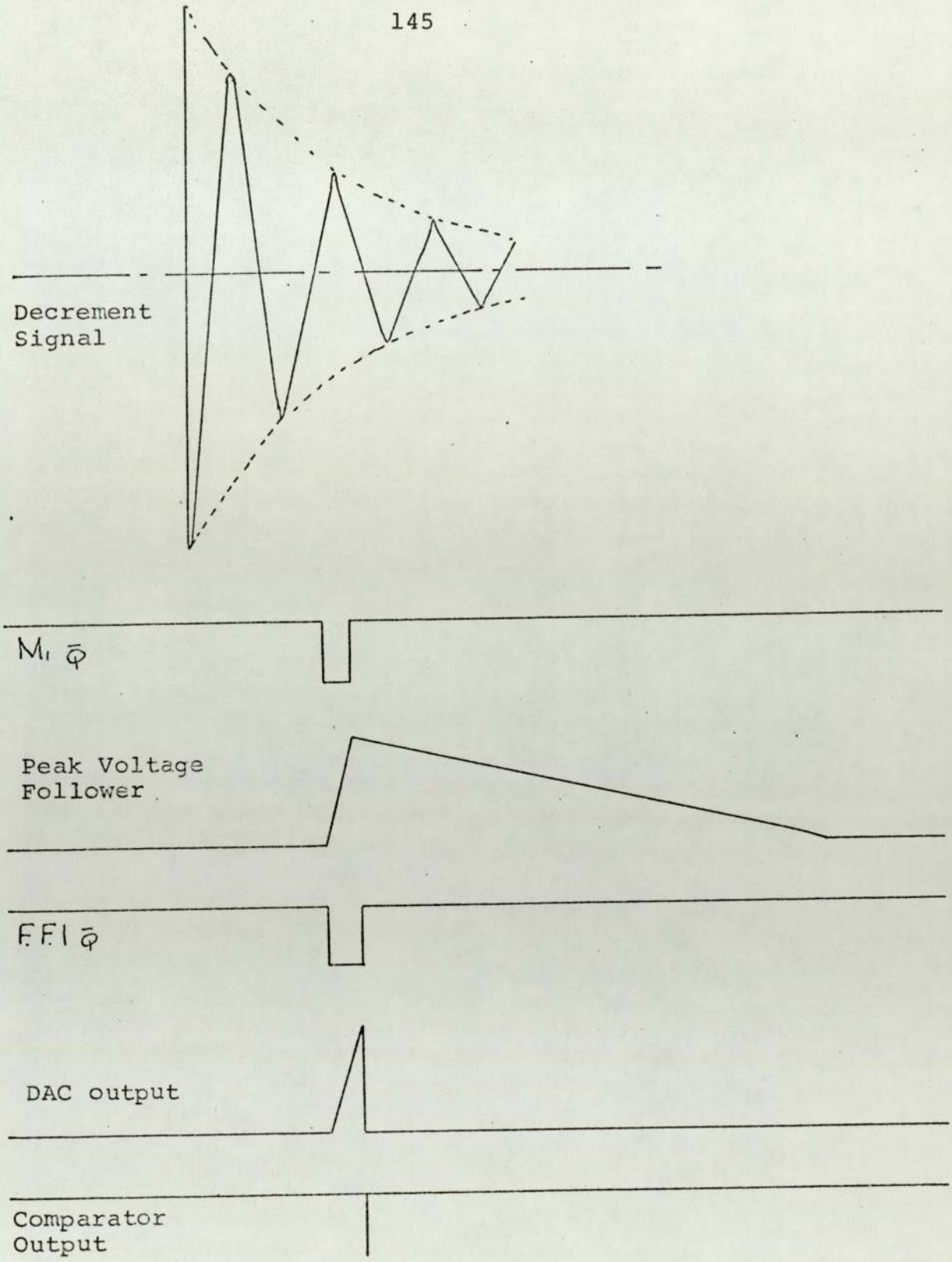

FIGURE 6.4.3.

Waveforms at various points for decrement amplitude measurement.

to A convertor used. The DAC used is a Datel DAC 9 current output model which is converted to give a full scale output of 0.99 V by the resistor R of 704 ohms. The digital input for the DAC is obtained from the two b.c.d. counters.

It was decided to measure the peak amplitude of the first oscillation used to measure the decrement period. The Q of the D-type flip-flop in Figure 6.3.2. is used to generate a pulse at the monostable M_1, the duration of which just exceeds 0.25 T, where T is the decrement period. This pulse is used to switch on transistors T_1 and T_2. The capacitor C is charged to the peak amplitude of the oscillator through a diode D in the feedback of a voltage follower. This charge is applied to the input of a voltage comparator through a buffer. The second input to the comparator is obtained via another voltage follower (used as a buffer) from the DAC. When the two amplitudes are equal the comparator generates a pulse which is used to transfer the data to the output of the latches (SN7475). The comparator output also resets the flip-flop.

This data is held at the latches until it is updating at the next cycle of the measurement. The charge on the capacitor C discharges through the amplifier (input bias current) and the diode (reverse leakage current).

A clock of 250 KHz for the b.c.d. counters was sufficient to ensure that the DAC output followed the charge on the capacitor C adequately. At the end of the meauring cycle the counters are reset to zero by the Q of the flip-flop F.F.1.

CHAPTER 7

DAMPING OF A TORSIONALLY VIBRATING ROD BY THE SURROUNDING MEDIUM

7.1 INTRODUCTION

This is an alternative approach to that described previously for measuring consistency. The basic principle of this method is to measure the damping of torsionally resonant robust rod due to the surrounding fluid. Torsional oscillations in the rod will be very susceptible to viscous damping since most of the vibrational energy is confined to the surface of the rod. A unit used to drive and detect the torsional oscillations is similar in principle to the moving coil galvanometer, a detailed drawing being shown in Figure 7.1.1. The flat coil is wound in a rectangular former which is solidly inset into the end of the rod. The coil is placed between the poles of a "C-core" electromagnet which provides a magnetic field parallel to the plane of the coil, so that the application of an alternating signal to the coil produces an alternating signal; and by the reciprocity of this electrodynamic principle the motion of the coil in the field will generate an electrical signal in the coil. Therefore the basis of driving and detection of resonance is that a short burst of a.c. pulses are applied to the coil and the driving frequency is adjusted until a decrement, indicating the resonance of the rod, is obtained at the end of the burst. The drive frequency is equal to the rod frequency when

the decrement, which is always at the rod frequency, is a maximum.

In driving the rod the torque on the coil is proportional to BANi where B is the flux density, AN is area-turns product and i is the current. For the detection of resonance the emf induced in the coil is proportional to BAN $\dot{\theta}$ where $\dot{\theta}$ is the rotational rate. This drive is very efficient and large amplitudes can readily be obtained even when the rod is heavily damped.

An important feature of this driving system is its wide band performance, which gives excellent results for frequencies up to 10 KHz. Within this range the efficiency of the system was found to be independent of frequency. Another advantage of this method of excitation is that 'drive' and 'detection' takes place in the same part of the rod and it also eliminates undesired types of vibrations, such as longitudinal, since energy only in the form of torsional waves is generated. Rods or tubes of any material can be utilised.

The energy losses at the supports are minimised by locating them at the nodes. To obtain a robust structure the full wavelength resonance was used, having two nodes located at $\frac{\lambda}{4}$ from each end. An excellent robust structure was obtained by supporting the rod at these points with rubber bungs or grommets, giving a very rigid support combined with a low loss.

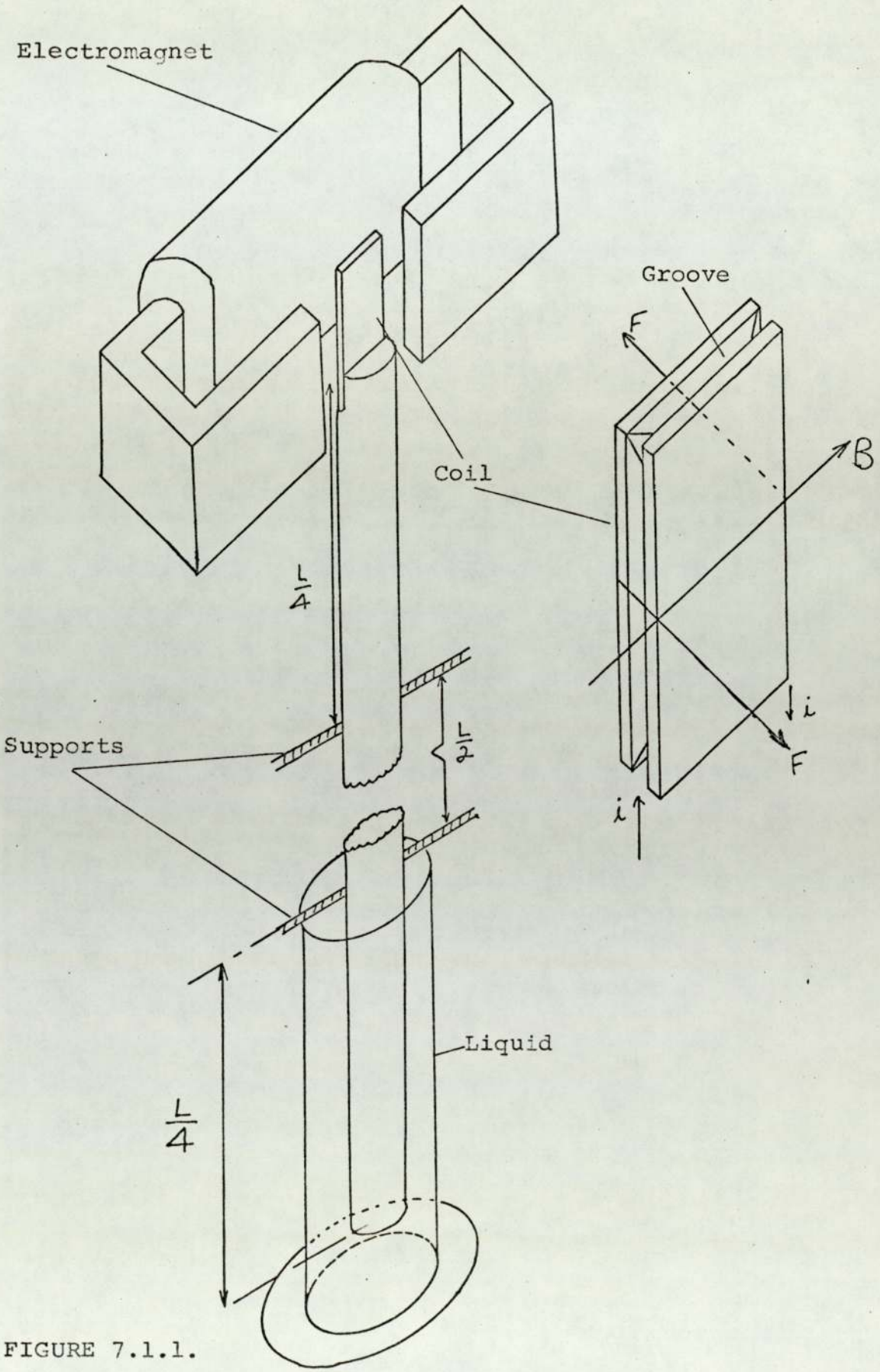

FIGURE 7.1.1.

Illustrates the 'drive' and 'detect' system for the torsionally resonant damped rod.

7.2. THEORETICAL ANALYSIS

When a plate vibrating parallel to its plane is immersed in a fluid, there is an impedence loading of the plate. The loading due to a simple Newtonian liquid has been derived by Lamb[49]. His theory is the basis of numerous viscometers. Of these the Ultra-Viscoson, an instrument devised by Roth and Rich[20], is the most versatile. They have analysed the impedence loading of a thin strip vibrating in a visco-elastic medium. This analysis is equally relevant to the fluid-loading of a rod carrying torsional waves, a system investigated in this work. Therefore the theory pertaining to the Ultra-Viscoson will be discussed at length.

The Ultra-Viscoson consists of a thin metal strip excited magnetostrictively in its fundamental longitudinal frequency. The vibrations of this strip are then calibrated with fluids of known properties. In the general case the loading of the surface of the strip can be expressed by the use of the concept of driving point impedence, defined as

$$z_o = R_o + j\, x_o = \frac{Y_x}{\partial \xi / \partial t} \qquad 7.2.1.$$

where Y_x is the shear stress produced in the visco-elastic medium by a transverse or a shear wave of frequency ω travelling in the y direction, and $\partial \xi / \partial t$ is the particle velocity in the medium at the surface of the strip in the x direction (see Figure 7.2.1.).

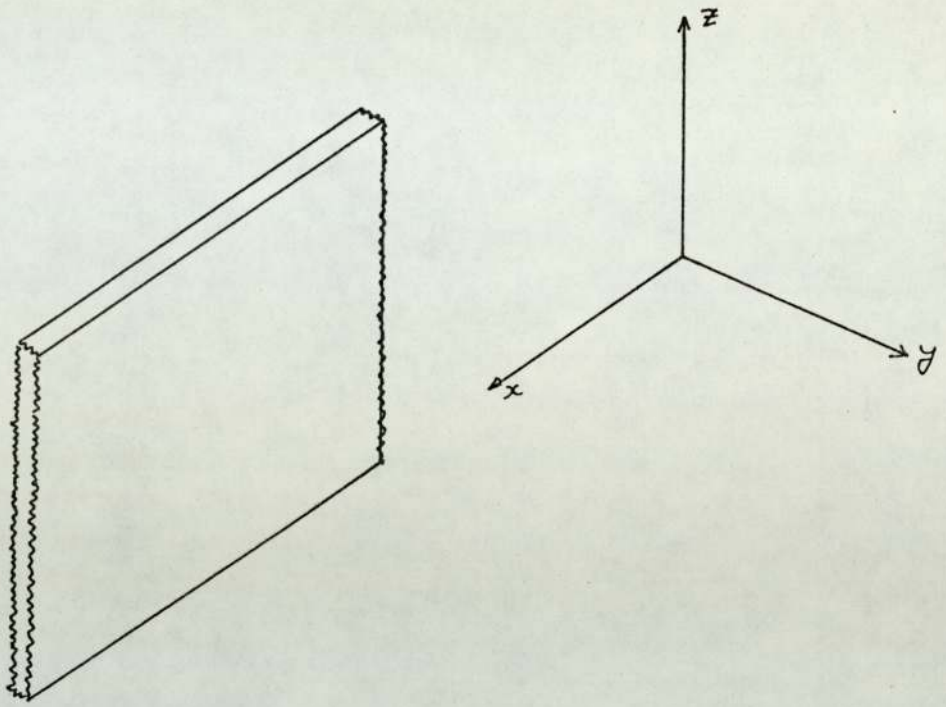

FIGURE 7.2.1.

In equation (7.2.1.), R_o represents the losses due to the medium and the imaginary term X_o mass or stiffness term. If this term is positive, it increases the effective mass of the system resulting in the lowering of the resonance frequency and if it is negative then it increases the effective stiffness of the system thereby increasing the resonance frequency.

For a non-Newtonian fluid (suspensions, slurries, polymers etc.) which is defined as one for which rate of shear is not directly proportional to shear stress, as the magnitude and the frequency of shear stress is varied, the impedence z_o will be magnitude and frequency sensitive giving rise to a complex fluid model.

It is seen from equation (7.2.1.) $\left[\gamma_x = \frac{\partial \varepsilon}{\partial t}(R_o + jX_o)\right]$

that there is a phase difference between the strain produced and the applied stress. The strain can be resolved, in terms of fluid properties, in to two time phase components, firstly the strain in phase with the applied stress, dependent on the rigidity coefficient function g, and secondly the strain in quadrature with the applied stress dependent on the viscosity coefficient function η. Since for real fluids both these coefficients are functions of frequency, all vibrating probe viscometers measure the dynamic viscosity coefficient at known rates of stress.

The shear stress Yx is related to the shear strain by

$$Y_x = g\frac{\partial \xi}{\partial y} + \eta\frac{\partial^2 \xi}{\partial t \partial y} \qquad (7.2.2.)$$

The shear wave propogation equation in the visco-elastic medium of density ρ_o is given by

$$\rho_o \frac{\partial^2 \xi}{\partial t^2} = \frac{\partial Y_x}{\partial y}$$

and substituting for Y_x from equation (7.2.2.)

$$\rho_o \frac{\partial^2 \xi}{\partial t^2} = g\frac{\partial^2 \xi}{\partial y^2} + \eta\frac{\partial^3 \xi}{\partial t \partial y^2} \qquad (7.2.3.)$$

Assuming the particle displacement to be given by the relationship $\xi(y,t) = e^{\Gamma y} e^{j\omega t}$, where Γ is the propogation constant, and substituting in equation (7.2.3.) it is

found that

$$\Gamma \doteq \pm \left[\frac{j\omega \rho_o}{\eta + g/j\omega} \right]^{\frac{1}{2}}$$

Therefore the solution for particle displacement is

$$\xi = \left[A\, e^{-\Gamma y} + B e^{\Gamma y} \right] e^{j\omega t} \qquad (7.2.4.)$$

This equation represents two waves travelling in opposite directions with amplitude coefficients of A and B. For the present purpose, where shear wave propogates less than a mm. or so due to the high attenuation of shear wave in liquids, it can be assumed that the medium is infinite and that waves propogate outward only. The distance, d, over which the amplitude of shear wave in a viscous medium decreases by a factor e, is called the skin depth and is given by

$$d = \left[\frac{2\eta}{\rho\omega} \right]^{\frac{1}{2}}$$

For example, for a fairly thick liquid of η = 500 CP ρ_o = 1 gm/c.c. and frequency of 1.0 KHz, the skin depth is 0.035 cms., for water this figure is further reduced by a factor of 20. Therefore with the absence of reflected waves the coefficient B is zero and equation (7.2.4.) can be written as

$$\xi = \xi_o e^{-\Gamma y}\, e^{j\omega t} \qquad (7.2.5.)$$

where ξ_o is the displacement amplitude at y = o. By

substituting into equation (7.2.2.).

$$Yx = (g + j\omega\eta)\Gamma \qquad (7.2.6.)$$

Substituting equations (7.2.5.) and (7.2.6.) into (7.2.1.) the driving point impedence for an infinite medium is

$$Z_o = \frac{Yx}{\partial\xi/\partial t} = \pm\left[j\omega\rho_o\left(\eta + \frac{g}{j\omega}\right)\right]^{\frac{1}{2}} \qquad (7.2.7.)$$

In the authors case only viscous medium was experimentally investigated, then taking g = O, equation (7.2.7) reduces to

$$Z_o = \left[\frac{\omega\rho_o\eta}{2}\right]^{\frac{1}{2}}(1 + j) = R_o + jx_o \qquad (7.2.8.)$$

The damping arises from the real part of equation (7.2.8.) and for very thick liquids encountered in this work, it could be very large. This damping can be reduced by using low frequency resonators.

For the thick liquids the thin strip would be critically damped (therefore no decrement signal). A rod, however, having a large mass to area ratio would still have an effective resonance in very thick liquids. The low frequency resonators in conjunction with other design parameters enabled good decrement to be achieved.

The imaginary term of the driving point impedence lowers the resonant frequency of the rod. In actual practice this increase in the vibrating mass is negligibly small and the change in the resonant frequency of the resonator from air to a heavy medium could not be detected.

7.2.2. DAMPING OF TORSIONALLY VIBRATING ROD

In the authors case a torsionally resonant rod, as shown in Figure 7.2.2., is used. A torsionally vibrating rod has features which could be an advantage as a consistency transducer:-

(a) There is no acoustic radiation since there is no component of vibration perpendicular to the surface as in a longitudinally vibrating rod which has a radial component due to Poissons ratio coupling.

(b) There is a design capability of adjusting the fluid loaded 'Q' factor by using a tube. Thus a thin walled aluminium tube would have high sensitivity and a solid steel rod a low sensitivity.

(c) The use of a rod or tube without the associated vibrating plate would avoid accumulation of fibrous solids by allowing an uninterrupted flow of fluid.

Let the tangential velocity of an element of area dS be $\dot{\xi}_o$ Sin ωt. The viscous loss due to this element in time dt is (by analogy with the electrical case, $i^2 R$).

$$R_o \dot{\xi}_o^2 \text{ Sin}^2 \omega t \text{ ds dt} \qquad (7.2.9.)$$

Where R_o is the real part of the impedence given by equation (7.2.8.).

Since the tangential velocity varies along the length of rod, minimum at the node and maximum at the

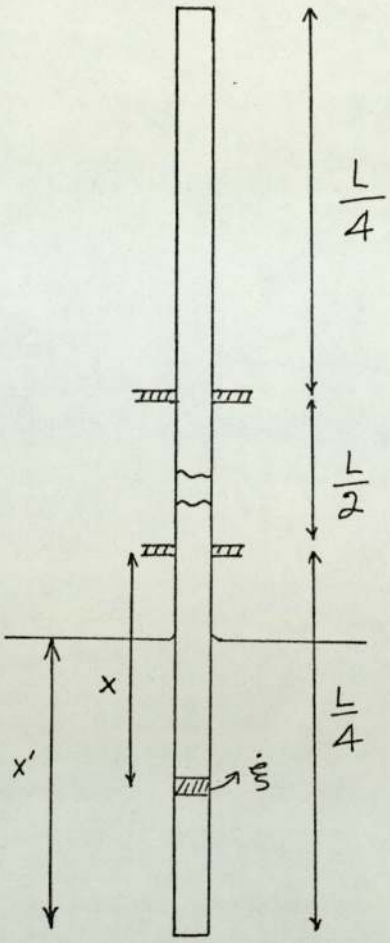

FIGURE 7.2.2.

antinode, $\dot{\xi}_o$ is taken as

$$\dot{\xi}_o = \hat{\dot{\xi}}_o \text{Sin} \frac{2\pi}{L} x$$

where $\hat{\dot{\xi}}_o$ is the maximum velocity at the antinode. Substituting for $\dot{\xi}_o$ in equation (7.2.9.) and integrating over one period of oscillation, the energy lost due to viscous damping is

$$\Delta E_L = R_o \hat{\dot{\xi}}_o^2 \frac{\pi}{2\omega} \text{Sin}^2 \frac{2\pi}{L} x \, ds$$

Taking ds as $2\pi r \delta x$ where r is the radius of the rod, the viscous loss for the immersed length of rod is

$$E_L = R_o(\dot{\hat{\xi}})^2 \frac{\pi^2}{\omega} \gamma \int_{\frac{L}{4}-x'}^{\frac{L}{2}} \sin^2 \frac{2\pi}{L} \; x \; dx$$

$$= R_o \; (\dot{\hat{\xi}}_o)^2 \frac{\pi^2}{\omega} \gamma \left[x' + \frac{L}{4\pi} \sin \frac{4\pi}{L} \; x' \right]$$

(7.2.10.)

Therefore the Q of the system is related to the depth of immersion by

$$\frac{1}{Q} \propto \left[x' + \frac{L}{4\pi} \sin \frac{4\pi}{L} \; x' \right] \qquad (7.2.11.)$$

7.3. EXPERIMENTAL RESULTS

The experimental system is shown in Figure 7.1.1. The wide band electromechanical drive unit has already been described. The frequency of a burst of A.C. current in the coil is adjusted to the second harmonic resonance in the rod, making the two support points nodes. As in the other transducers the decrement at the end of the drive period was observed. The supports were carefully positioned at the nodes to minimise the support loss.

The coil is wound on a rectangular shaped metal piece of dimensions (3.7 cm x 1.0 cm x 0.5 cm). A groove of depth 3.5 mms and width of 3.5 mm wide is cut into the edges of the metal piece as shown. A coil of 200 turns of s.w.g. is wound into the groove. The

fixing of the coil to the line is important and a good integral joint was obtained by recessing it to a depth of about 1.3 cm in the rod. Very good electromechanical coupling was achieved by this method and typically, with a burst length of 150 pulses, 30 volts and repetition rate of 3 Hz resulted in the initial decrement signal amplitude of about one volt with a very high Q. A brass rod of diameter 0.86 cm and length of 1.22 m was found to resonate at a frequency of 1.569 KHz with a Q of approximately 8000 in air. This is near the theoretical value for the metal.

Table 7.3.1. shows the variation of Q with the depth of immersion in one of the silicone calibrating fluid of ρ_o = 1 gm/c.c. and η = 200 C.P. These results are shown graphically in Figure 7.3.2. It is seen from this graph that it is not necessary to measure the level of the liquid accurately if the level is close to the nodal position.

It is evident from equation (7.2.11.) that the reciprocal of 'Q' is directly proportional to

$$(x' + \frac{L\pi}{4} \text{ Sin } \frac{4\pi}{L} x');$$

this indeed is the case as seen from Figure 7.3.3. A corroborating test of the foregoing theory was performed using silicone fluids of constant density (ρ_o=1.0 gm/c.c.) and various viscosities. Table 7.3.2. shows the variation of Q with the viscosity of the liquids. The reciprocal of Q is plotted against η in Figure 7.3.4; the relationship is found to be linear as predicted

$(\frac{\lambda}{4} = \frac{L}{4} = 30.5$ cms.)

Depth x' in cms	$x' + \frac{L}{4\pi} \text{Sin} \frac{4\pi}{L} x'$	Q	$\frac{1}{Q} \times 10^{-3}$
1.5	2.99	1160	0.99
3.6	7.12	930	1.08
6.5	12.45	610	1.64
12.1	21.33	370	2.7
16.2	25.85	270	3.7
21.1	29.1	250	4.0
24.6	29.9	250	4.0

TABLE 7.3.1.

from equation (7.2.10.).

The resonant frequency of the rod did not change by a measureable amount when it was immersed in the liquids, showing that the reative part of equation (7.2.8.) is negligible for this design.

7.4. CONCLUSION

The design parameters have been verified by the experiments. This method of measuring visco-elastic properties of fluids can be optimised to give excellent results for a variety of fluid consistencies.

FIGURE 7.3.2.

Shows the dependence of Q with the depth of immersion.

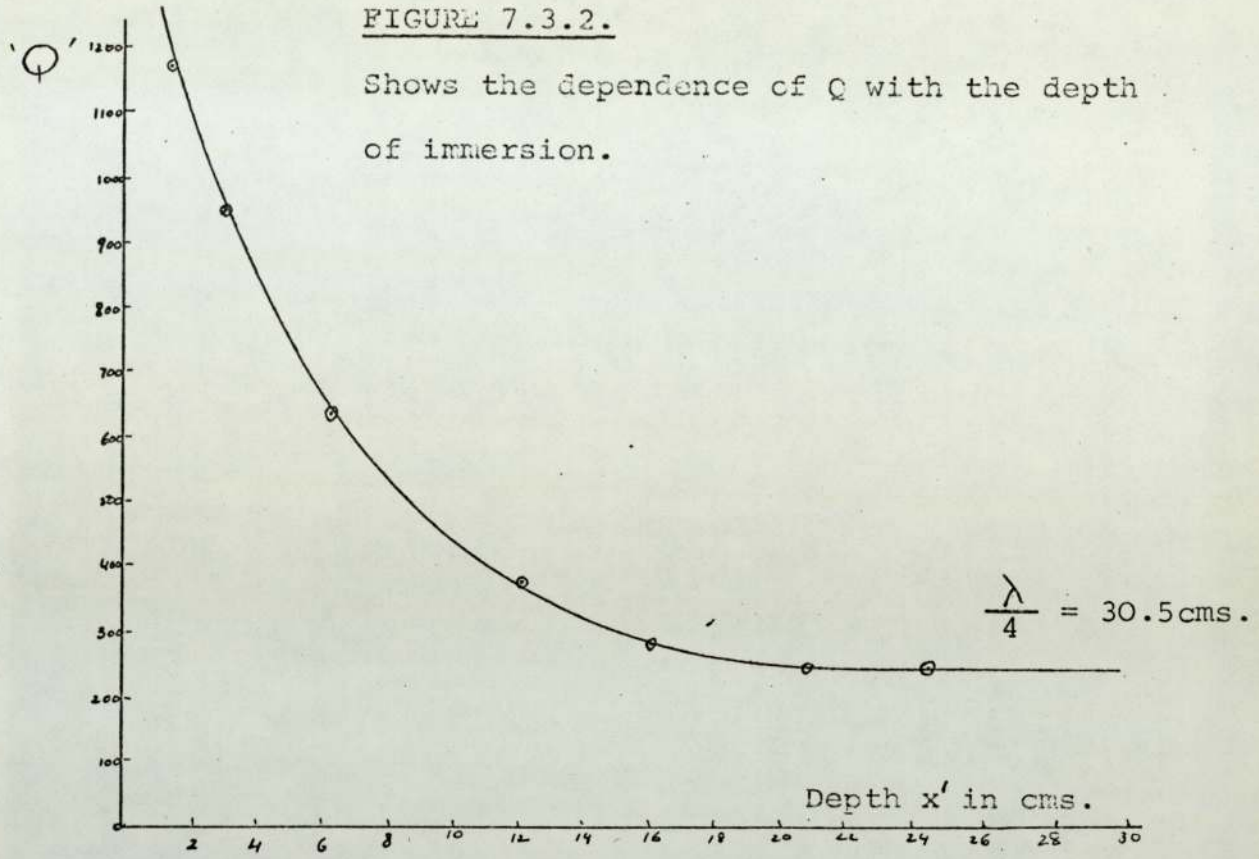

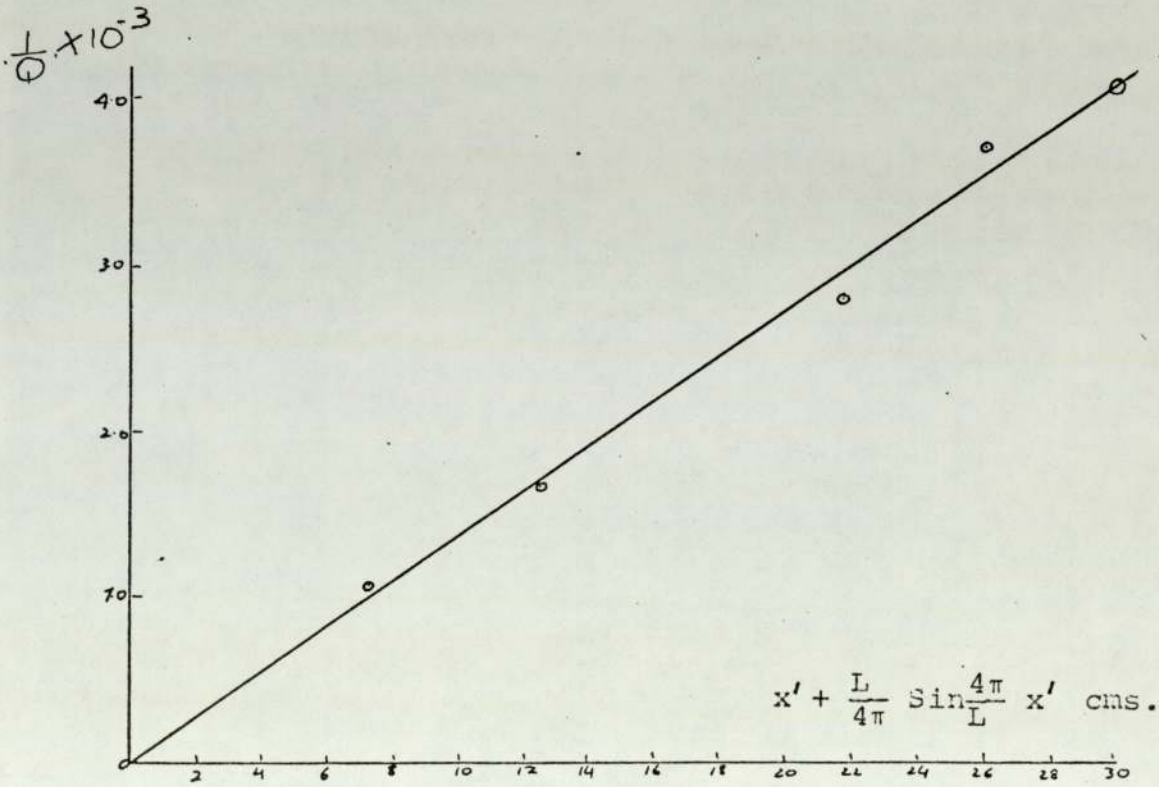

FIGURE 7.3.3.

The variation of the loss $(\frac{1}{Q})$ against $x' + \frac{L}{4\pi} \sin \frac{4\pi}{L} x'$ where x' is the depth of immersion..

η in C.P.	$\sqrt{\eta}$	$\dot{Q}$	$\frac{1}{\dot{Q}} \times 10^{-3}$
50	7.07	560	1.78
100	10	400	2.5
200	14.4	280	3.5
500	22.4	180	5.56

TABLE 7.3.2.

The high loss liquids of this work require rather massive rods while very low loss liquids would require a design incorporating a narrow walled tube of low density material.

The torsionally resonant rods have various advantages over the longitudinally vibrating probe devised by Roth and Rich. Firstly no acoustic waves are generated into the fluid, resulting in the absence of radiation damping, secondly the uncertain damping due to the edges of the strip is absent.

Although an exact expression for the Q of the system can be found, taking into account the losses due to the end of the rod, an absoulte is not recquired for the present application, since only a rough indication of the sludge 'fluidity' is needed. However, it has been demonstrated by the experiments and theory that a

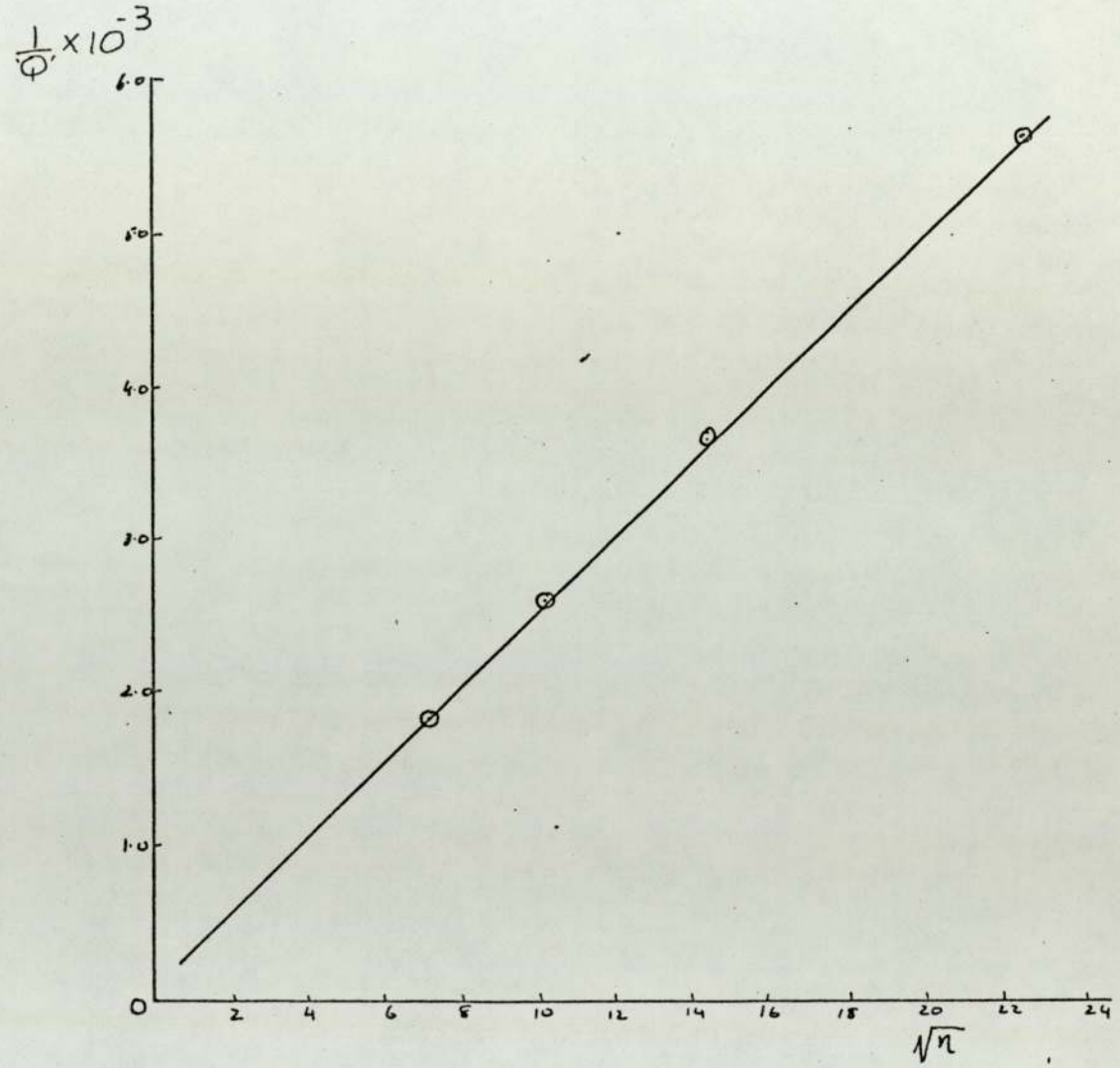

FIGURE 7.3.4.

Shows the loss $(\frac{1}{Q})$ against $\sqrt{n}$

wide range of fluids can be measured by changing the parameter of the rod.

7.5. APPLICATION TO PRIMARY SLUDGE MEASUREMENT

The problem encountered with the probe placed in the bellmouth was that the long glutenous fibres and sludge saturated rags, which are always present, wrap themselves round the sensor and give a low 'Q' reading. The sensor had to be cleaned from time to time. It is envisaged that if the rod is placed in the mouth of the outlet of the hopper, this clogging will not occur since the flow of sludge in this case is parallel to the rod and the chance of rags being retained is minimised.

Part of the rod and the exciting system can be enclosed in a water tight enclosures, so that only a $\lambda/4$ length is protruding and exposed to sludge. The whole probe arrangement can be held in position, in the outlet of the hopper, by an appropriate mechanical arrangement attached to the sides of the primary settling tank.

APPENDIX 1

The Impedence of a Flexurally Resonant Free Edge Disk

The impedence of any mechanical system is defined as the ratio of the driving force F to the velocity $\dot{w}$ in the direction of the force at its point of application thus

$$z = \frac{F}{\dot{w}}$$

This impedence has a real and imaginary part corresponding to the equivalent mass and stiffness respectively, at the point under consideration. At the resonance of the vibrating system the impedence can be written as

$$z = j\omega Meq + \frac{1}{j\omega Ceq} \qquad \text{(A.1.1.)}$$

where Meq and Ceq is equivalent mass and compliance (stiffness) respectively.

The Meq for any resonant system is obtained from the expression

$$\text{Kinetic Energy} = \tfrac{1}{2}\, Meq(\dot{w})^2 \qquad \text{(A.1.2.)}$$

and the equivalent compliance Ceq is calculated by equating equation (A.1.1.) to zero. Thus

$$Ceq = \frac{1}{\omega^2} Meq$$

The dynamic deflection curve for a free edge disk with one nodal circle is given by

$$w(r) = I_o(\lambda_n r) + A_1 J_o(\lambda_n r)$$

Where

$$\lambda_n = \frac{3.01}{a}$$

a = radius of disk

$$A_1 = - \frac{I_1(\lambda_n a)}{J_1(\lambda_n a)}$$

The kinetic energy of the disk is given by

$$K.E. = \tfrac{1}{2} \rho_D h \int_0^a (\dot{w})^2 \, 2\pi\gamma d\gamma$$

where ρ_D = density of disk

h = thickness of disk

$$= 2\pi \rho_D a^2 h \left[(A_1)^2 (J_o^2(\lambda_n a) + J_1^2(\lambda_n a) + (I_o^2(\lambda_n a) - I_1^2(\lambda_n a) + 4A_1 \frac{1}{2(\lambda_n a)^2} (\lambda_n a) J_1(\lambda_n a) I_o(\lambda_n a) \right] + (\lambda_n a) J_o(\lambda_n a) I_1(\lambda_n a) \right] \qquad \text{(A.1.3.)}$$

$$(\dot{w})^2_{r=o} = A_1^2 J_o^2(0) + I_o^2(0) + 2A_1 J_o(0) I_o(0)$$

$$= A_1^2 + 3 \qquad \text{(A.1.4.)}$$

Meq at r = 0 is given by

$$(Meq)_{r=o} = \frac{\text{Equation A.1.3}}{\text{Equation A.1.4.}} \qquad \text{(A.1.5.)}$$

$$(Meq)_{r=o} = 0.33 \, M_{ST}$$

where $M_{ST} = \pi a^2 h$

Equivalent campliance is given by

$$Ceq = \frac{1}{\omega^2 \, Meq}$$

The equivalent electrical analogue circuit of the disk is shown in Figure A.1.

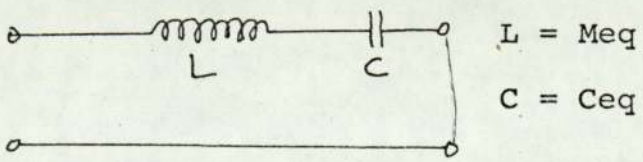

FIGURE A.1.

The equivalent mass at any radial point can easily be computed by determining w at that point and substituting in equation (A.1.5.) This variation of the equivalent mass with distance as shown in Table A.1. and this result is plotted in Figure 3.

$\frac{r}{a}$ =	0.0	0.1	0.2	0.3	0.4	0.5	0.6	0.7	0.8	0.9	1.0
$M_{eq}=(xM_{ST})$	0.33	0.34	0.41	0.55	0.9	2.03	10.0	114.0	3.9	1.19	0.6

TABLE A.1.

BIBLIOGRAPHY

1. Reeve D.A.D. "The Minworth Works of the Upper Tame Main Drainage Authority", Jour. of the Institute of Water Pollution Control No. 5, 1971
2. Reeve D.A.D. "Notes on Sewage Purification and General Description of the Authority's Works", Upper Tame Main Drainage Authority publication, August 1970
3. Reeve D.A.D. "Automation of Sewage Works Operation", Water Pollution Control,p 247-259, 1972
4. Melbourne K.V.,Robertson K.G., Oaten A.B. "Developments in Instruments for Water Pollution Control", Water Pollution Control, p. 278-286, 1972
5. Townend C.B."Recent Middlesex Developments in Mechanisation and Automation of Sewage Plant Operation", Jour. Proc. Inst. Sew. Purif. p. 273-301, 1961
6. Downing A.L., Eden G.E., Briggs R. "Some Recently Developed Instruments:Can they Assist Sewage Work Operation?" The Inst. Sew. Purif. Annual Conference, June 1964 Paper No.3.
7. CIRIA, "Cost-effective Sewage Treatment- the Creation of an Optimising Model", Construction Industry Research and Information Association, Report 46, May 1973
8. Denning R.A. "Calibrating Nuclear Gages" Control Engineering p. 79-81 February 1965
9. Briggs R., Knowles G., "A Photoelectric Sludge-Level Detector" Jour. Proc. Inst. Sew. Purif. 1961

10. Denning R.A. "The Flow of Solids-Water Mixtures in Hydraulic Dredging" Symposium on Rheology - The Amer. Soc. Mech. Eng., 1965

11. Consistency Symposium - Measur. and Control. August 1968

12. Junger M.C. "Vibrations of Elastic Shells in a Fluid Medium and the Associated Radiation of Sound" Jour. of Appl. Mechanics, p 439-445 December, 1952

13. Smirnov Y.K. "Analysis of the Interaction of Viscosity Pickups with a Liquid" Soviet Physics - Acoustics p 104-105, Vol. 12 No. 1. July-September 1966

14. Krutin V.N. and Smirnits I.B. "Measurement of the Viscosity of Newtonian Fluids by Means of Vibratory Probes" Soviet Physics-Acoustics, p 42-45, Vol. 12, No. 1, July-September 1966

15. Kogan I.N. "Tubular Vibrator with Lumped Masses at the Ends as a Viscometer" Soviet Physics-Acoustics p 461-464, Vol.14, No. 4, April-June, 1969

16. Rosin G.S. "Absolute Viscosity Measurements by the Undamped Lengthwise Vibrations of a Plate in Fluid" Soviet Physics-Acoustics p 493-498, Vol. 14, No.4, April-June, 1969

17. Woodward J.G. "A Vibrating-Plate Viscometer" J.A.S.A. p 147-151, Vol.25 No. 1, January 1953

18. McSkimin H.J. "Measurement of Dynamic Shear Viscosity and Stiffness of Viscous Liquids by Means of Travelling Torsional Waves" J.A.S.A. p 355-365 Vol.24, No.4. July 1952

19. Glover G.M., Hall G., Matheson A.J. and Stretton J.L.

"A Magnetostrictive Instrument for Measuring the Viscoelastic Properties of Liquids in the Frequency Range 20-100 KHz" Jour. of Scientific Instruments (Jour. of Phys. Eng.) p 383-388 Vol. 1. Series 2, 1968

20. Roth W. and Rich S.R. "A New Method for Continuous Viscosity Measuremnt. General Theory of the Ultra-Viscosor" Jour. of Appl. Phys. p 940-950, Vol. 24, No. 7, July 1953

21. Zelenev Yu. Z., Melentev P.V. and Elektrovo L.M. "Use of a Quarter-wave Vibrator to Measure the Dynamic Characteristics of Polymers in the Audio Frequency Range" Soviet Physics-Acoustics p 497-498, Vol.19 No. 5, March-April 1974

22. Williams R.C. "Theory of Magnetostrictive Delay Lines for Pulse and Continuous Wave Transmission" IEEE Trans. on Ultrasonic Engineering. Vol. UE-7, February 1959

23. Kikuchi Y. "Magnetostrictive Materials and Applications" IEEE Trans. on Magnetics Vol. Mag-4, No.2 June 1968

24. Morse and Ingard "Theoretical Acoustics" (McGraw-Hill Book Company) 1968

25. Pollard H.F. "Resonant Behaviour of an Acoustical Transmisison Line"

26. Biesterfeldt H.J., Lange J.N. and Skudrgyk E.J. "Vibrations of Rods at Frequencies below their Radial Resonance" J.A.S.A. p 749-764, Vol. 32 No. 6 June, 1960

27. Minnaert M. "Musical Air-Bubbles and Sound of Running Water" Phil. Mag. p 235-248 Vol. 16 1933

28. Davids N. and Thurston E.G. "The Acoustical Impedence of a Bubbly Mixture and its size Distribution Function" J.A.S.A. p 20-30, Vol. 22 1950

29. Mangulis V. "The Effects of a Single Bubble on the Sound Field of a Piston" Jour. Sound Vib. p 42-49 Vol. 5 1967

30. Hourkins S.D. "Measurement of the Resonant Frequency of a Bubble mear a Rigid Boundary" J.A.S.A. p 504-508 Vol 37, 1965

31. Olson H.F. "Acoustical Engineering" (D. Van Nostrand Company) 1967

32. Junger M.C. and Feit D. "Sound, Structures and their Interaction" (MIT Press Combridge) 1972

33. Wiener F.M. "On the Relation between the Sound Fields Radiated and Diffracted by Plane Obstacles" J.A.S.A. p 697-700, Vol. 23 1951

34. Lamb H. "On the Vibrations of and Elastic Plate in Contact with Water" Proc. of Royal Soc. p 205-216, Vol. A98 1920

35. Rayleigh "The Theory of Sound" Vol. 2 (MacMillan and Co. Ltd.) 1896

36. Lax M. "The Effect of Radiation on the Vibrations of a Circular Diaphragm" J.A.S.A. p 5-13, Vol 16 1944

37. Timoshenfo S. "Vibrations of Problems in Engineering" (D. Van Nostrand), second edition, p 427 1937

38. Landau L.D. and Lifshitz E.M. "Fluid Mechanics" (Pergaman Press) 1963

39. Rayleigh Lard "Phil. Mag. " p 697 Vol. 21 1911

40. Havelock T.H. "Phil. Mag." p`620 Vol. 42, 1921

41. Kestin J. and Pilarczyh K. Trans. ASME, p 987 Vol. 76, 1954

42. Wood A.B. "A Textbook of Sound" (G.Bell and Sons) 1960

43. Stephens R.W.B. and Bate A.E. "Acoustics and Vibrational Physics" (Arnold) 1966

44. "The TTL Data Handbook for Design Engineers"(Texas Instruments) 1973

45. Data sheet for operational amplifiers type SN72741

46. Data sheet for voltage follower type LM310

47. Data sheet for voltage comparator type LM306

48. Seth T.N. , Ph.D. Thesis, University of Aston, 1974

49. Lamb H. "Hydrodynamics" Cambridge 1956.

50 Wang C. Y. "The flow field induced by an Oscillating sphere" Jour. of Sound and Vibration p. 257 Vol.2, 1965.

51 Verdin V.G., Semenova, N.G. and Sushkova V. N. "Acoustic streaming in the field of an acoustic dipole". Sov. Phys. Acoust,p.319-321 Vol. 20, No.4, 1975